Targeting BRCA1-BER deficient breast cancer by ATM or DNA-PKcs blockade either alone or in combination with cisplatin for personalized therapy

Nada Albarakati[1], Tarek MA Abdel-Fatah[2], Rachel Doherty[1], Roslin Russell[3], Devika Agarwal[4], Paul Moseley[2], Christina Perry[1] , Arvind Arora[1], Nouf Alsubhi[1], Claire Seedhouse [5], Emad A Rakha[6], Andrew Green[6], Graham Ball[4] , Stephen Chan[2], Carlos Caldas[3], Ian O Ellis[6] and Srinivasan Madhusudan[1,2*]

[1] Academic Unit of Oncology, Division of Cancer and Stem Cells, School of Medicine, University of Nottingham, Nottingham University Hospitals, Nottingham NG51PB, U.K.

[2] Department of Oncology, Nottingham University Hospitals, Nottingham NG51PB, UK.

[3] Cancer Research UK, Cambridge Research Institute, Li Ka Shing Centre, Robinson Way, Cambridge CB2 0RE, UK.

[4] School of Science and Technology, Nottingham Trent University, Clifton campus, Nottingham NG11 8NS, UK.

[5] Academic Haematology, Division of Cancer and Stem Cells, School of Medicine, University of Nottingham, Nottingham University Hospitals, Nottingham NG51PB, U.K.

[6] Department of Pathology, Division of Cancer and Stem Cells, School of Medicine, University of Nottingham, Nottingham University Hospitals, Nottingham NG51PB, U.K.

Running title: Targeting ATM or DNA-PK in BRCA1 deficient cells

Word count: 4989

Figure: 5

Tables: 1

Key words: BRCA1; base excision repair; ATM; DNA-PK; small molecule inhibitors; synthetic lethality, cisplatin; chemopotentiation.

Conflicts of interest: The authors disclose no potential conflicts of interest.

* **Corresponding author:**

Dr Srinivasan Madhusudan

Academic Unit of Oncology

Division of Cancer and Stem Cells

School of Medicine

University of Nottingham

Nottingham University Hospitals

Nottingham NG51PB, U.K

Telephone: +44(0)115 823 1850

Fax: +44(0)115 823 1849

E-Mail: srinivasan.madhusudan@nottingham.ac.uk

ABSTRACT

BRCA1, a key factor in homologous recombination (HR) repair may also regulate base excision repair (BER). Targeting BRCA1-BER deficient cells by blockade of ATM and DNA-PKcs could be a promising strategy in breast cancer. We investigated BRCA1, XRCC1 and pol β protein expression in two cohorts (n=1602 sporadic and n=50 germ-line BRCA1 mutated) and mRNA expression in two cohorts (n=1952 and n=249). Artificial neural network analysis for BRCA1-DNA repair interacting genes was conducted in 249 tumours. Pre-clinically, BRCA1 proficient and deficient cells were DNA repair expression profiled and evaluated for synthetic lethality using ATM and DNA-PKcs inhibitors either alone or in combination with cisplatin. In human tumours, BRCA1 negativity was strongly associated with low XRCC1, and low pol β at mRNA and protein levels ($p<0.0001$). In patients with BRCA1 negative tumours, low XRCC1 or low pol β expression was significantly associated with poor survival in univariate and multivariate analysis compared to high XRCC1 or high pol β expressing BRCA1 negative tumours ($ps<0.05$). Pre-clinically, BRCA1 negative cancer cells exhibit low mRNA and low protein expression of XRCC1 and pol β. BRCA1-BER deficient cells were sensitive to ATM and DNA-PKcs inhibitor treatment either alone or in combination with cisplatin and synthetic lethality was evidenced by DNA double strand breaks accumulation, cell cycle arrest and apoptosis. We conclude that XRCC1 and pol β expression status in BRCA1 negative tumours may have prognostic significance. BRCA1-BER deficient cells could be targeted by ATM or DNA-PKcs inhibitors for personalized therapy.

INTRODUCTION

Breast Cancer Susceptibility Gene 1 (BRCA1) facilitates the efficient resolution of DNA double-strand breaks (DSBs) through HR (Caestecker and Van de Walle, 2013; Huen et al., 2010). Cells lacking functional BRCA1 protein have impaired HR, and thus depend on the more error-prone non-homologous end joining (NHEJ) pathway leading to chromosomal instability that drive breast cancer development (Huen et al., 2010). In women, BRCA1 germ line mutation is associated with a 60%-70% lifetime risk of developing breast cancer (O'Donovan and Livingston, 2010). In the more common sporadic breast cancers, epigenetic silencing of the BRCA1 promoter has been reported in up to 11%-14% of tumours (Turner et al., 2004) and a dysfunctional BRCA pathway may also contribute to a BRCAness phenotype in about 25% of cancers (Turner et al., 2004), where breast cancers do not harbour germ-line BRCA mutations but display similar phenotypes including HR deficiency. BER is critical for processing DNA damage caused by alkylation, oxidation, ring saturation, single strand breaks and base deamination. DNA polymerase β (pol β) and XRCC1 are key BER factors. PARP1 (poly [ADP-ribose] polymerase 1) may play an essential role in single strand break repair (SSBR), a BER-related pathway (Langelier and Pascal, 2013). The DNA repair intermediates generated during BER/SSBR, if unrepaired, may get converted to toxic double strand breaks (DSBs) (Dianov and Hubscher, 2013).

Emerging studies suggest a cross talk between BRCA1 and BER factors. BRCA1 mutated and basal-like breast cancer cells were found to be sensitive to oxidative DNA damage induced by H_2O_2 treatment. The increased sensitivity was associated with defective BER as assessed by cell based BER assay in BRCA1 deficient cells (Alli et al., 2009). In a more recent study, BRCA1 deficient cells were sensitive to methyl methane sulfonate (alkylating

agent) and functional interaction between polβ and BRCA1 was demonstrated in that study (Masaoka et al., 2013) implying a potential role for polβ in BRCA1 mediated DSB repair. In addition, BRCA1 has also been shown to be involved in the transcriptional regulation of BER factor such as OGG1, NTH1 and APE1 (Saha et al., 2010).

Synthetic lethality is a promising strategy for personalized cancer therapy. PARP [poly-(ADP-ribose) polymerase] inhibitors induce synthetic lethality in germ line BRCA1-deficient breast cancers and demonstrate clinical benefit in patients (Lord and Ashworth, 2008). Similarly, we have recently shown that APE1 inhibition is synthetically lethal in BRCA1 deficient breast cancer cells and in PTEN (and DSB repair) deficient melanoma cells. The data provides compelling reasons to investigate other potential synthetic lethal interactions targeting DNA repair for clinical application. Cells that are BRCA1 deficient as well as BER impaired may be reliant upon other back-up repair pathways to maintain genomic integrity and survival. ATM and DNA-PKcs play essential roles in the DNA damage response (DDR) and link DNA damage sensing to DDR effectors that regulate cell cycle progression and DNA repair (Shiloh and Ziv, 2013). ATM, a member of the phosphatidylinositol-3-kinase-like protein kinase (PIKK) family, is a key sensor and transducer of DNA damage signalling during HR (Lee and Paull, 2007; Shiloh and Ziv, 2013). ATM recruitment at sites of DNA damage may be dependent upon functional BRCA1 in cells (Lee et al., 2010). DNA-PKcs is another key member of the PIKK family and a critical component of NHEJ pathway required for repair of DSBs generated throughout the cell cycle (Hill and Lee, 2010). BRCA1 through a role in DNA end-processing may also be involved in the regulation of NHEJ (Durant and Nickoloff, 2005).

Our hypothesis is that impaired BER in BRCA1 deficient tumours may influence prognosis. BRCA1-BER deficient cells may be reliant upon ATM or DNA-PKcs mediated back-up pathways for cellular survival and could be targeted by synthetic lethality using inhibitors of ATM or DNA-PKcs.

MATERIALS AND METHODS

Clinical study

BRCA1 and BER protein expression analysis in Nottingham Tenovus Primary Breast Carcinoma cohort: The study was performed in a consecutive series of 1650 patients with primary invasive breast carcinomas who were diagnosed between 1986 and 1999 and entered into the Nottingham Tenovus Primary Breast Carcinoma series described previously (Sultana et al., 2013). Supplemental Table S1 summarizes patient demographics. Supplemental treatment data 1 summarizes various adjuvant treatments received by patients in this cohort.

BRCA1 and BER protein expression analysis in germ line BRCA1 deficient breast cancer: The demographics of a cohort of 50 germ-line BRCA1 mutated breast cancers confirmed by genetic testing is shown in supplementary table S6. All patients received surgery, adjuvant chemotherapy and radiotherapy according to our institutional policy (supplementary treatment data 1).

Tissue Microarrays (TMAs) and immunohistochemistry (IHC): Tumours were arrayed in tissue microarrays (TMAs) and immunohistochemically profiled for BRCA1, APE1, XRCC1,

Pol β, and other biological markers (Supplementary Table S2) as previously described (Sultana et al., 2013). Supplementary Table S2 summarizes immunohistochemistry protocols for the markers tested using the Bond Max automated staining machine and Leica Bond Refine Detection kit (DS9800) according to manufacturer instructions (Leica Microsystems). We have recently published optimisation and specificity of XRCC1 and pol β antibody used in the current study (Abdel-Fatah et al., 2014b; Sultana et al., 2013). To validate the use of TMAs for immunophenotyping, full-face sections of 40 cases were stained and protein expression levels of the different antibodies were compared. The concordance between TMAs and full-face sections was excellent (k = 0.8). Positive and negative (by omission of the primary antibody and IgG-matched serum) controls were included in each run.

Evaluation of immune staining: The tumour cores were evaluated by specialist pathologists blinded to the clinicopathological characteristics of patients, in two different settings. There was excellent intra and inter-observer agreements ($k > 0.8$; Cohen's $\varkappa$ and multi-rater $\varkappa$ tests, respectively). Whole field inspection of the core was scored and intensities of nuclear staining were grouped as follows: 0 = no staining, 1 = weak staining, 2 = moderate staining, 3 = strong staining. The percentage of each category was estimated (0-100%). H-scores (range 0-300) were calculated by multiplying intensity of staining and percentage staining as previously described (Sultana et al., 2013). Supplementary Table S2 summarizes cut-offs for individual markers.

Statistical analysis: Data analysis was performed using SPSS (SPSS, version 17 Chicago, IL). Where appropriate, Pearson's Chi-square, Fisher's exact, Student's t and ANOVA one way tests were used. Cumulative survival probabilities were estimated using the Kaplan–Meier method, and differences between survival rates were tested for significance using the log-rank test. Multivariate analysis for survival was performed using the Cox proportional

hazard model. A p value < 0.05 considered significant. For multiple comparisons, p values were adjusted according to Holm-Bonferroni correction method.

Transcript levels in the METABRIC (Molecular Taxonomy of Breast Cancer International Consortium) cohort: Investigation of the mRNA expression was performed in METABRIC cohort which refers to a set of 1980 breast cancer samples with a minimum of 5 years of clinical follow up where mRNA expression data was available (Curtis et al.). Patient demographics are summarized in supplementary Table S9. ER positive and/or lymph-node negative patients did not receive adjuvant chemotherapy. ER negative and/or lymph-node positive patients received adjuvant chemotherapy. All the samples were analysed as triplicates. A sliding window analysis was used to identify a cut-off in gene expression values such that the resulting subgroups have significantly different survival courses.

Artificial neural network (ANN) analysis in Uppsala cohort: The demographics of the Uppsala cohort is summarized in supplementary Table S10 and mRNA analysis has been described previously (Bergh et al., 1995). All microarray data are accessible at National Center for Biotechnology Information (NCBI) Gene Expression Omnibus (http://www.ncbi.nlm.nih.gov/geo/, accession number: GSE4922) (Pawitan et al., 2005). All data were normalized using the global mean method (MAS5), and probe set signal intensities were natural log transformed and scaled by adjusting the mean signal to a target value of log 500. The expression levels of the *BRCA1*, for the probe 204531_s_at located on the HG-U133A chip was utilized to generate the ANN based model as described previously (30) (Lancashire et al., 2010) (Lemetre, 2009). A non-linear, ANN modelling based, data mining approach was utilised to identify the best gene probes for sample classification as described previously (30). 47,293 probes were screened for each sample in the test set (n=249). The data mining algorithm comprised a three layer multilayer perception architecture modified with a feed

forward back-propagation algorithm and a sigmoidal transfer function, as previously described (Lancashire et al., 2010). The network momentum and learning rate were respectively set as 0.1 and 0.5. Two hidden nodes were utilised. The output node was coded as 0 if a case was low *BRCA1* expression (<the median) and 1 if high *BRCA1* expression (>median). Inputs were ranked in ascending order based on their classification error. The top 50 predictive genes identified were merged with 150 gene probes involved in the DNA repair process (Supplementary Table S11) and then applied to an ANN based network inference algorithm as described in earlier studies (Lemetre, 2009). This model predicted a weighted link (direction and magnitude) between each of the gene probe markers. This weighting was based on the non-linear correlation between a source gene and a target gene in a multifactorial ANN model. This approach defines a linkage or interaction with a magnitude between every possible pair of genes in the set presented to the algorithm. The approach is data driven and unweighted by biological function. The 100 strongest interactions were then visualised as a map with Cytoscape (Smoot et al., 2011). In a second bioinformatics analysis step, we sought to obtain a robust ranking of genes that are differentially expressed between the mRNA *BRCA1*+ cases and the mRNA *BRCA1*- and have high predictive power, by applying an ensemble sample classification method within a leave-one-out cross-validation scheme. For this purpose, the 249 patient samples were first grouped into 249 different training/test set partitions, using 248 samples for the training sets and the remaining sample as the test set. For each of the 248 training sets differentially expressed genes were selected independently with the "Empirical Bayes moderated t-statistic" (Smyth, 2004) and used to train a machine learning model, which was evaluated based on the left-out sample (a procedure known as "external cross-validation"). To classify the left-out sample, the prediction results of four algorithms (Support Vector Machine, Random Forest, kNN and Prediction Analysis for Microarrays, with all parameters being optimised by using a grid

search within a nested cross-validation) (Tibshirani et al., 2002) were combined to a majority-vote ensemble classifier as to compensate for the inevitable inherent biases and variances that exists amongst each of these machine learning algorithms. In order to rank the genes based on the cross-validation results, their frequency of occurrence in the list of significantly differentially expressed genes (p-value < 0.05) across different cross-validation cycles was recorded, and genes received higher scores the more often they had been selected. All steps of the analysis were conducted using an in-house web-application for microarray analysis, available at www.arraymining.net.

Pre-clinical study

Compounds and reagents: ATM inhibitors (KU55933 and KU60019) and DNA-PKcs inhibitors (NU7441 and NU7026) were purchased from Tocris Bioscience, UK. The compounds were dissolved in 100% DMSO and stored at - 20ºC. Cisplatin was obtained from Nottingham University Hospitals.

Cell lines and culture media: BRCA1 deficient HeLa SilenciX® cells and control BRCA proficient HeLa SilenciX® cells were purchased from Tebu-Bio (www.tebu-bio.com). SilenciX cells were grown in DMEM medium (with L-Glutamine 580mg/L, 4500 mg/L D19 Glucose, with 110mg/L Sodium Pyruvate) supplemented with 10% FBS, 1% penicillin/ streptomycin and 125 µg/ml Hygromycin B. MDA-MB-436 (BRCA1 deficient human breast cancer cells) was grown in DMEM (Sigma, UK) and MCF7 (BRCA1 proficient human breast cancer cells) was grown in RPMI1640 (Sigma, UK). All media used to culture human cancer cell lines were supplemented with 10% FBS (PAA, UK) and 1% penicillin/streptomycin.

Clonogenic survival assay: 200-500 hundred cells per well were seeded in six-well plates. Cells were allowed to adhere for 4 hours. Compounds (ATM inhibitors or DNA-PKcs inhibitors) were added at the indicated concentrations. For cisplatin combination studies, cells

were initially treated with cisplatin for 16 hours and then gently washed twice with 1X phosphate buffered saline and incubated in fresh media with or without ATM or DNA-PK inhibitors at indicated concentration. The plates were left in the incubator for 12-14 days. After incubation, the media was discarded, fixed (with methanol and acetic acid mixture) and stained with crystal violet and counted. Surviving Fraction = [No. of colonies formed/ (No. of cells seeded x Plating efficiency)] x100. All clonogenic assays were done in triplicate.

Evaluation of drug interaction (Combination index): To investigate synergistic and additive activity, combination index was calculated as described previously (Berenbaum, 1981). If D (combination index) is <1 the effect of the combination is synergistic, whereas if D=1 or D is >1 the effect is additive or antagonistic respectively.

γH2AX immunofluorescence microscopy: This assay was performed as described previously(Sultana et al., 2013). Briefly, cells were incubated in medium containing ATM inhibitor or DNA-PKCS inhibitor for 48 hours. For cisplatin combination studies, cells were initially treated with cisplatin for 16 hours and then gently washed twice with 1X phosphate buffered saline and incubated in fresh media with or without ATM or DNA-PK inhibitors at indicated concentration for 48 hours.

Neutral COMET assay: COMET assay reagents were purchased from Trevigen and used according to the manufacturer's neutral COMET protocol (Gaithersburg, MD, USA). Briefly, 1 x 10^5 cells per well were seeded into a 6 well plate and treated with KU55933 (7.5μM) or NU7441 (0.75μM). After 48 hours treatment cells were resuspended in 250 µl PBS. For COMET analysis 25 μl of cell suspension was mixed with 250 μl molten LMAgarose and then 75 μl of the mixture pipetted immediately onto COMET slides. Slides were allowed to set at 4^{o}C for 20 minutes and then immersed in lysis buffer for 60 minutes at 4^{o}C. Slides were

then subjected to electrophoresis at 20 V for 60 minutes in chilled electrophoresis buffer (0.5 M Tris, 1.5 M sodium acetate). Following electrophoresis slides were incubated for 30 minutes in DNA precipitation solution (5 M ammonium acetate in 95% ethanol) at room temperature and subsequently fixed in 70% ethanol for 20 minutes at room temperature. Slides were left to dry overnight at 4^{o}C and then each sample stained with 50 μl Sybr green and scored using COMET ASSAY IV software (Perceptive Instruments Ltd, Bury St Edmonds, UK). Treatments were performed in triplicate and 50 cells counted for each.

Flow cytometric analyses (FACS): Cells grown to sub-confluence were exposed to ATM or DNA-PKcs inhibitors either alone or in combination with cisplatin for 48 hours and collected by trypsinization and centrifugation (1000 rpm for 5 minutes). FACS was performed as described previously (Sultana et al., 2013).

Annexin V flow cytometric analyses: Cells grown to sub-confluence were exposed to ATM or DNA-PKcs inhibitors either alone or in combination with cisplatin for 48 hours and collected by trypsinization and centrifugation (1000 rpm for 5 minutes). The assay was performed as described previously (Sultana et al., 2013).

Quantitative real time PCR: RNA was extracted from cell lines using the RNeasy Mini Kit (Qiagen) and quantified using a microvolume spectrophotometer. cDNA synthesis was performed using the RT^{2} First Strand Kit (Qiagen). Primers used for RT-PCR for BER genes are shown in supplementary table S9. Quantitative PCR was performed on an ABI prism 7700 (Applied Biosystems) using SYBR green detection (Applied Biosystems®, UK). The housekeeping gene GAPDH was used to standardise the samples.

RT² Profiler™ PCR Array for global DNA Repair expression analysis: To evaluate the expression of 84 DNA repair genes simultaneously, real-time PCR was performed using the RT² Profiler™ PCR Array for global DNA Repair expression analysis in technical triplicates (ABI 7500 Fast Block Detection System; Applied Biosystems, Foster City, USA) and the data analysed as per manufacturer's recommendation. GAPDH was used for normalization of the data. A 2 fold change or greater change in expression was considered significant.

RESULTS

Clinical studies

XRCC1, pol β, APE1 and SMUG1 are key BER proteins. Moreover, we have recently shown that XRCC1 (Sultana et al., 2013), pol β (Abdel-Fatah et al., 2014b), APE1 (Abdel-Fatah et al., 2014a) and SMUG1 (Abdel-Fatah et al., 2013b) are promising biomarkers in breast cancer. To evaluate whether they also have prognostic and predictive significance based on BRCA1 status, we proceeded to immunohistochemical evaluation of XRCC1, pol β, APE1 and SMUG1 in BRCA1 positive and BRCA1 negative breast tumours.

BRCA1 negativity is associated with impaired XRCC1 and pol β protein expression in human sporadic breast cancers: A total of 1602 breast tumours were suitable for BRCA1 expression analysis. 1085/1602 (67.7%) of tumours were BRCA1 positive and 517/1602 (32.3%) were negative for BRCA1 expression (Figure 1A). As shown in supplementary Table S3, BRCA1 negative tumours were highly significantly associated with low XRCC1 ($p<0.00001$) and low polβ ($p<0.000001$). In the BRCA1 negative cohort we then evaluated clinicopathological associations of XRCC1 and pol β protein expression (Figure 1A). The data for XRCC1 and polβ are summarized in supplementary tables S4 and S5 respectively. Although no significant associations were seen with stage, tumour grade, tumour types or pleomorphism, BRCA1 negative/ polβ low tumours were more likely to be Bcl2 negative ($p=0.001$) and BRCA1 negative/ XRCC1 low tumours were more likely to be p53 negative ($p= 0.015$).

BRCA1 negative/low XRCC1 or BRCA1 negative/low polβ tumours are associated with poor breast cancer specific survival (BCSS): BRCA1 negativity was significantly associated with poor BCSS compared to BRCA1 positive tumours ($p<0.000001$) (Figure 1B) and is consistent with previous studies showing poor prognostic significance of BRCA1

silencing in sporadic breast tumours (Hsu et al., 2013; Wu et al., 2013). In the BRCA1 negative group we investigated the prognostic influence of XRCC1 and pol β. As shown in Figure 1C1, BRCA1 negative/ low XRCC1 tumours had worse BCSS compared to BRCA1 negative/ high XRCC1 tumours (p=0.001). Similarly, BRCA1 negative/ low polβ tumours had worse BCSS compared to BRCA1 negative/ high polβ tumours (p=0.008) (Figure 1D1). As BRCA1 negativity is likely to be associated with ER negative tumours we conducted further analysis. In the BRCA1 negative/ER negative subgroup, low XRCC1 or low polβ remains associated with poor survival (p=0.033 and p=0.034 respectively, Figure 1C2 and 1D2). In the BRCA1 negative/ER positive subgroup, similarly, low XRCC1 was associated with poor survival (p=0.003, Figure 1C3) and although not significant there was trend with low polβ (p=0.121, Figure1D3). In multivariate cox regression analysis (Table 1), low XRCC1 (p=0.005) and low pol β (p=0.036) were independently associated with poor survival.

In the current study, APE1 and SMUG1 did not influence survival and was not associated with any clinicopathological parameters in BRCA1 negative breast tumours (data not shown).

XRCC1 and pol β expression in germ-line BRCA1 mutated breast cancers: To investigate whether XRCC1 and polβ would also influence outcomes in germ-line BRCA1 deficient breast cancer we investigated a cohort of 50 germ-line BRCA1 mutated breast cancers. Demographics are summarised in supplementary table S6. No significant clinicopathological correlations were observed (supplementary tables S7 and S8). In this small exploratory cohort, low polβ (5/34 tumours) was significantly associated with poor survival (p=0.007) in germ line BRCA1 mutated breast cancers (Figure 2A) compared to high polβ (29/34 tumours). Low XRCC1 expression did not influence survival in this cohort (Supplementary Figure S1A)

Low *XRCC1* and low *pol β* transcript levels have prognostic significance in *BRCA1* mRNA low sporadic breast cancers: To confirm whether the association between BRCA1 and BER also operated at the mRNA level we investigated the Metabric cohort (n=1920, demographics summarized in supplementary table S9) and the Uppsala cohort (n=249, demographics summarized in supplementary table S10) - cohorts where mRNA expression data was available. In ER+ tumours (n=1485, Metabric), low *BRCA1* (n=81) was associated with poor survival compared to high *BRCA1* mRNA expressing tumours (n= 1404) (p= 0.0226, Figure 2B1). In the low *BRCA1*/ER+ group, low polβ (n=66) or low *XRCC1* (n=42) remains associated with poor survival (ps= 0.038 and 0.0321 respectively) compared to high *polβ* (n=14) or high *XRCC1* (n=38) mRNA expressing tumours (Figures 2B2 and 2B3). In the ER- tumours (n=435, metabric), high BRCA1 (n= 385) was associated with poor survival compared to low *BRCA1* mRNA expressing tumours (n=50) (p= 0.0365, Supplementary Figure S2B). In the low *BRCA1*/ER- group, low polβ (n=5) or low *XRCC1* (n=17) remains associated with poor survival compared to high *polβ* (n=43) or high *XRCC1* (n=31) mRNA expressing tumours [ps= 0.0224 and 0.0206 respectively) (Figures 2C1 and 2C2). In the Uppsala cohort, low *polβ* mRNA (36/175 tumours) was associated with poor survival in *BRCA1* low mRNA breast cancers (p=0.03, Supplementary Figure S1C) compared to high *polβ* mRNA tumours (139/175 tumours). *XRCC1* mRNA expression levels did not influence survival in the Uppsala cohort (Supplementary Figure S1D).

Artificial neural network (ANN), ensemble classification and cross-validation analysis for *BRCA1* interacting DNA repair genes: The top 100 strongest are shown in Figure 2D. The biological functions of *BRCA1* interaction genes are summarized in supplementary Table S12. The predominant interactions with genes involved in BER, NER, HR, NHEJ, inter-strand crosslink repair, MMR and transcription is not only consistent with the previously

described functions of *BRCA1* (Caestecker and Van de Walle, 2013; Huen et al., 2010; Silver and Livingston, 2012) but also reveals new BRCA1 interacting genes.

Pre-clinical studies

The clinical and bioinformatics data presented above provides evidence that BRCA1 may influence the expression of multiple DNA repair genes. To provide additional pre-clinical evidence we investigated the expression of DNA repair in BRCA1 deficient and proficient cancer cell lines.

BRCA1 deficient cancer cells exhibit impaired BER expression: BRCA1 deficient HeLa SilenciX cells, control BRCA1 proficient HeLa SilenciX cells, BRCA1 deficient MDA-MB-436 breast cancer cells and BRCA1 proficient MCF7 breast cancer cells were initially examined for the expression of BRCA1, XRCC1 and pol β proteins. BRCA1 deficiency was first confirmed at the protein level in BRCA1 deficient HeLa SilenciX and MDA-MB-436 cells compared to control HeLa SilenciX cells and MCF7 cells (Figures 3A1, 3A2, 3B1, 3B2). The relative expression of XRCC1 and pol β was also found to be low in BRCA1 deficient cells compared to BRCA1 proficient cells at the protein level (Figures 3A1, 3A2, 3B1, 3B2). Low mRNA expression of *BRCA1*, *XRCC1* and *pol β* was confirmed by qRT-PCR in MDA-MB-436 cells compared to MCF-7 cells and BRCA1 deficient HeLa SilenciX compared to control HeLa SilenciX cells (Figure 3A3, 3B3 respectively). The data is also summarized in supplementary Tables S14 and S15. To provide additional evidence that low polβ and low XRCC1 expression confers phenotypic consequence, we investigated MMS sensitivity in MDA-MB-436 and MCF-7 cells. As shown in supplementary Figure S3B, we found that MDA-MB-436 cells are sensitive to MMS. The data concurs with a recent study that showed a similar MMS sensitivity in BRCA1 deficient cells that was associated with impaired functional interaction between polβ and BRCA1(Masaoka et al., 2013).

BRCA1 deficient cells have deregulated gene expression of multiple DNA repair pathways: To investigate whether down regulation of DNA repair is restricted to polβ and XRCC1 or also includes additional DNA repair pathways, we profiled a panel of 84 DNA repair genes in BRCA1 deficient and BRCA1 proficient cells using the RT^2 Profiler DNA Repair PCR array. All experiments were done in triplicates and DNA repair expression was compared between BRCA1 deficient and BRCA1 proficient cells [BRCA1 deficient HeLa SilenciX versus control BRCA1 proficient HeLa SilenciX cells and MDA-MB-436 versus MCF7 cells]. The data is summarized in Figure 3C (BRCA1 deficient and proficient HeLa SilenciX cells), supplementary table S16 (BRCA1 deficient and proficient HeLa SilenciX cells), Figure 3D (MDA-MB-436 and MCF7 cells), and supplementary table S17 (MDA-MB-436 and MCF7 cells). In MDA-MB-436 cells as well as in BRCA1 deficient HeLa SilenciX cells, we observed a consistent down regulation of several BER genes as well as genes involved in other pathways including base excision repair, nucleotide excision repair, homologous recombination, non-homologous end joining, inter-strand crosslink repair and mismatch repair.

BRCA1 deficient cancer cells are sensitive to ATM inhibitors either alone or in combination with cisplatin: KU55933 (2-morpholin-4-yl-6-thianthren-1-yl-pyran-4-one) is an ATP-competitive potent ATM inhibitor with an IC_{50} of 13 nmol/L (Hickson et al., 2004). For additional validation we also tested KU60019 [(2*R*,6*S*-rel)-2,6-Dimethyl-*N*-[5-[6-(4-morpholinyl)-4-oxo-4*H*-pyran-2-yl]-9*H*-thioxanthen-2-yl-4-morpholineacetamide] another ATP-competitive potent ATM inhibitor (Golding et al., 2009). Treatment with KU55933 resulted in reduced survival of BRCA1 deficient HeLa SilenciX cells compared to BRCA1 proficient HeLa SilenciX cells (Figure 4A1). Similarly, MDA-MB-436 cells were sensitive to

KU55933 compared to MCF7 cells respectively (Figures 4B1). As an additional validation we investigated KU60019. As shown in supplementary Figures S3A and S3E, BRCA1 deficient HeLa SilenciX cells and MDA-MB-436 cells were also sensitive to KU60019 compared to BRCA1 proficient cells. 3-aminobenzamide, a PARP inhibitor (Shekh et al., 2014) was used as a positive control. As shown in supplementary Figure S2A and S2B, BRCA1 deficient cells, as expected, are sensitive to PARP inhibitor.

To provide mechanistic evidence that ATM inhibition leads to a synthetic lethality effect in BRCA1 deficient cells, we investigated the functional consequence of ATM inhibition in BRCA1 proficient and BRCA1 deficient cells. Double strand breaks (DSBs) induce phosphorylation of H2AX at serine 139 (γH2AX), and accumulation of γH2AX foci in the nucleus is a marker of DSBs. Therefore, γH2AX immunocytochemistry was performed in BRCA1 deficient HeLa SilenciX cells and MDA-MB-436 cells and compared to BRCA1 proficient control SilenciX or MCF7 cells (Supplementary Figure S3A). Nuclei containing more than six γH2AX foci were considered positive. Cells were treated with KU55933 (10μM) for 48 hours. The percentage of cells with more than six γH2AX foci was significantly higher in BRCA1 deficient cells in comparison to BRCA1 proficient cells (Figures 4A2, 4B2). Similar results were observed with KU60019 (Supplementary Figures S4B and S4F). The data provides evidence that BRCA1 deficient cells accumulate DSBs at an increased rate after treatment with an ATM inhibitor relative to BRCA1proficient cells. As an additional validation we performed neutral COMET assays after ATM or DNA-PKcs inhibitor treatment in cells. As shown in supplementary Figure S3C, BRCA1 deficient cells accumulated significantly more DSBs compared to BRCA1 proficient cells. Accumulation of DSBs may delay cell cycle progression. In BRCA1 deficient and BRCA1 proficient cells, cell cycle progression was monitored after 48 hours of treatment with KU55933 (10μM) (Supplementary Figure S4B). BRCA1 deficient cells were shown to be significantly arrested

in G2/M phase of the cell cycle compared to BRCA1 proficient cells (Figures 4A3, 4B3). Similar results were observed with KU60019 (Supplementary Figures S5C and S5G). Accumulation of DSBs may result in eventual induction of apoptosis. Apoptosis detection by FITC-annexin V flow cytometric analysis was therefore performed in cells treated with KU55933 (10μM) for 48 hours (Supplementary Figure S4C). The percentage of cells undergoing apoptosis following ATM inhibitor treatment was significantly higher in BRCA1 deficient cells in comparison to BRCA1 proficient cells (Figures 4A4, 4B4). Similar results were observed with KU60019 (Supplementary Figures S5D and S5H). The functional studies together provide evidence that ATM inhibition can induce synthetic lethality in BRCA1 deficient cells by causing accumulation of DSBs, G2M cell cycle arrest and induction of apoptosis. However the level of synthetic lethality effect seen with ATM inhibitor was modest compared that demonstrated previously using PARP inhibitors in BRCA1 deficient cells (Lord and Ashworth, 2008).

Cisplatin hypersensitivity has been well established in BRCA1 deficient cells (Tassone et al., 2009). We investigated whether low dose cisplatin could potentiate synthetic lethality induced by KU55933. Cells were treated with a combination of low dose cisplatin (0.00001μM – 0.1 μM) and KU55933 (5μM). As shown in Figure 4C1 and 4D1, KU55933 treatment increased cytotoxicity of cisplatin in BRCA1 deficient HeLa SilenciX as well in MDA-MB-436 compared to BRCA1 proficient control SilenciX and MCF7 cells. The interaction was synergistic [combination index= 0.6 (BRCA1 deficient HeLa SilneciX) and 0.7 (MDA-MB-436), supplementary Figure S7A]. In BRCA1 deficient cells treated with a combination of cisplatin and KU55933, the observed increased cytotoxicity was associated with accumulation of DSBs (Figure 4C2 and 4D2), G2/M cell cycle arrest (Figure 4C3 and 4D3) and increased apoptosis (Figure 4C4 and 4D4).

BRCA1 deficient cancer cells are sensitive to DNA-PKcs inhibitors either alone or in combination with cisplatin: NU7441 (2-N-morpholino-8-dibenzothiophenyl-chromen-4-one) is a potent and a specific inhibitor of DNA-PKcs with an IC_{50} of 14 nmol/L for DNA-PK inhibition (Tavecchio et al., 2012). NU7026 (2-(morpholin-4-yl)-benzo[h]chromen-4-one) is another DNA-PKcs inhibitor (Nutley et al., 2005).

Treatment with NU7441 resulted in reduced survival of BRCA1 deficient HeLa SilenciX cells compared to BRCA1 deficient HeLa SilenciX cells (Figure 5A1). MDA-MB-436 cells were modestly sensitive to NU7441 compared to MCF7 cells respectively (Figures 5B1). As an additional validation we investigated NU7026. As shown in supplementary Figures S6A and S6E, BRCA1 deficient HeLa SilenciX cells and MDA-MB-436 cells were also sensitive to NU7026 compared to BRCA1 proficient cells. To provide mechanistic evidence that DNA-PKcs inhibition leads to a synthetic lethality effect in BRCA1 deficient cells, we investigated the functional consequence of DNA-PKcs inhibition in BRCA1 proficient and BRCA1 deficient cells. Cells were treated with NU7441 (1.5μM) for 48 hours. The percentage of cells with more than six γH2AX foci was significantly higher in BRCA1 deficient cells in comparison to BRCA1 proficient cells (Figures 5A2, 5B2). Similar results were observed with NU7026 (supplementary Figures S6B and S6F). In BRCA1 deficient and BRCA1 proficient cells, cell cycle progression was monitored after 48 hours of treatment with NU7441 (1.5μM). BRCA1 deficient cells were shown to be significantly arrested in G1 phase of the cell cycle compared to BRCA1 proficient cells (Figures 5A3, 5B3). Similar results were observed with NU7026 (supplementary Figures S6C and S6G). Apoptosis detection by FITC-annexin V flow cytometric analysis was therefore performed in cells treated with NU7441 (1.5μM) for 48 hours. The percentage of cells undergoing apoptosis following DNA-PKcs inhibitor treatment was significantly higher in BRCA1 deficient cells in comparison to BRCA1 proficient cells (Figures 5A4, 5B4). Similar results were observed

with NU7026 (Supplementary Figures S6D and S6H). The functional studies together provide evidence that DNA-PKcs inhibition can induce synthetic lethality in BRCA1 deficient cells by causing accumulation of DSBs, G1 cell cycle arrest and induction of apoptosis. We then investigated whether low dose cisplatin could potentiate synthetic lethality induced by NU7441. Cells were treated with a combination of cisplatin (0.00001μM – 0.1 μM) and NU7441 (0.75μM). As shown in Figure 5C1 and 5D1, NU7441 treatment substantially increased cytotoxicity of low dose cisplatin in BRCA1 deficient HeLa SilenciX as well as in MDA-MB-436 compared to BRCA1 proficient control SilenciX and MCF7 cells. The interaction was synergistic [combination index= 0.5 (BRCA1 deficient HeLa SilneciX) and 0.6 (MDA-MB-436), supplementary figure S7B]. Increased cytotoxicity was associated with accumulation of DSBs (Figure 5C2 and 5D2), G2/M cell cycle arrest (Figure 5C3 and 5D3) and increased apoptosis (Figure 5C4 and 5D4).

DISCUSSION

We have shown, for the first time, that BRCA1 negative tumours have significantly lower expression of XRCC1 and Polβ, a feature that was also seen in BRCA1 deficient cancer cell lines. Patients with BRCA1 negative/ low XRCC1 or BRCA1 negative /low Polβ breast tumours also have worse breast cancer specific survival including in ER+ and ER- sub-groups. These new observations suggest that polβ/XRCC1 based sub-stratification may refine prognostication in BRCA1 deficient phenotypes. In addition, poor prognostic significance of pol β in a small cohort of germ-line BRCA1 mutated tumours is also consistent with a recent preclinical study linking BRCA1 and pol β in cancer cell line models (Masaoka et al., 2013). Additionally, at the mRNA level we conducted neural network analysis and demonstrated that the predominant *BRCA1* interactions were with genes involved in BER, NHEJ, NER and MMR inter-strand crosslink repair and transcription. To compliment clinical observations we DNA repair profiled BRCA1 proficient and deficient cell lines and also demonstrated impairment in BER, NHEJ, NER and MMR. A surprising finding in the current study was that several genes involved in DDR were down regulated in BRCA1 deficient HeLa as well as in breast cancer cells as one would anticipate that this would reduce survival in the absence of exogenous DNA damage. Moreover, as inhibition of BER (via PARP inhibition) is synthetically lethal in association with BRCA defects, we expected BRCA deficient cells to have compensatory up-regulation of BER pathway. In contrast we observed consistent down regulation of BER implying a complex regulation, including transcriptional regulation of BER by BRCA1. Although in BRCA deficient cells PARP1 may be up-regulated as a compensatory mechanism, in our cell line models we actually observed low expression of *PARP1* mRNA, *PARP2* mRNA and *PARP3* mRNA in BRCA1 deficient HeLa cells and low expression of *PARP1* mRNA and *PARP2* mRNA in MDA-MB-436 cells. Although these new

observations are intriguing, mechanism for down-regulation is currently unknown. However, we speculate that genomic instability in BRCA1 null cells may over a period of time, in the cell lines used in the current study, eventually lead to acquisition of new defects in other DNA repair pathways along with compensatory up-regulation of pro-survival pathways. In addition, recent studies implicating a role for BRCA1 in transcriptional regulation of BER (Saha et al., 2010) and NER(Hartman and Ford, 2002) suggests additional mechanisms may also operate for the observed genomic instability in BRCA1 deficient cells. The altered expression of XRCC1 and polβ shown here also concurs to a large extent with a recent study by De Summa et al. who investigated the expression of APE1, NTHL1, OGG1, PARP1, XRCC1 and miR17 in BRCA1/2 mutated and sporadic breast cancers (De Summa et al., 2014). Down-regulation of XRCC1, APE1 and NTHL1 was evident in that study. Interestingly overexpression of PARP1 and miR17 were observed in BRCA1 mutated tumours implying that they could be investigated as biomarker of BRCAness phenotype. In contrast, we observed PARP1 down regulation in BRCA1 deficient HeLa as well as in MDA-MB-436 breast cancer cell line in our study. Larger studies in human breast tumours are required to confirm these findings.

Although from preclinical studies we would expect DNA repair deficiency to be associated with chemosensitivity and improved survival in patient who received adjuvant chemotherapy, in the current clinical study we found that low BRCA1 or low BRCA1/low XRCC1 or low BRCA1/low Pol β was associated with poor survival. Our recent studies of DNA repair in breast cancer suggest that the relationship may be complex. In previous studies we found that low XRCC1 (Sultana et al., 2013) and low DNA pol β (Abdel-Fatah et al., 2014b) to be associated with poor survival. As BER deficiency could lead to accelerated accumulation of mutations resulting in a mutator phenotype (Bielas et al., 2006) that is associated with an aggressive biology, we speculate that the observed effect for XRCC1 and pol β may reflect

this phenomenon. On the other hand, high SMUG1 (Abdel-Fatah et al., 2013b) and high FEN1 (Abdel-Fatah et al., 2014c) was associated with poor survival in patients who have received adjuvant chemotherapy implying a DNA repair influenced predictive significance for SMUG1 and FEN1 in breast cancer.

We have demonstrated that a potential synthetic lethality relationship also exists between BRCA1 deficiency and blockade of ATM or DNA-PKcs in cells. A model for synthetic lethality is shown in supplementary figure S8. We have concluded synthetic lethality for the following reasons: a) BRCA1 deficient cells have increased sensitivity to ATM or DNA-PKcs inhibitors; b) upon ATM inhibitor treatment, BRCA1 deficient cells accumulate DSBs, exhibit G2/M cell cycle arrest and induction of apoptosis; and c) upon DNA-PKcs inhibitor treatment, BRCA1 deficient cells accumulate DSBs, exhibit G1 cell cycle arrest and induction of apoptosis. Interestingly, BRCA1 deficient cells also exhibit low mRNA levels of ATM and DNA-PKcs but are sensitive to ATM and DNA-PKcs inhibitors. The data suggest a dose dependent effect where although ATM and DNA levels are low the cells are able to tolerate genomic instability and survive. However, with additional functional inhibition through small molecule inhibition, pronounced accumulation of DSBs could lead to a synthetic lethality effect. Although phosphorylation of H2AX is ATM and DNA-Pkcs dependent, we observed accumulation of γH2AX foci in BRCA1 deficient cells incubated in medium containing ATM inhibitor or DNA-PKcs inhibitor for 48 hours. Whether reflects a timing issue are whether H2AX phosphorylation may be contributed by other factors such as activated ATR is unclear. To confirm DSB accumulation we also performed neutral COMET assay and have demonstrated DSB accumulation in BRCA1 deficient cells treated with ATM or DNA-PKcs inhibitor. Moreover the effects on cell cycle progression, although significant, appear to be modest. In the current study, the magnitude of synthetic lethality seen in BRCA1 deficient cells treated with ATM or DNA-PKcs inhibitor alone was not as

pronounced as that demonstrated for PARP inhibitors (Lord and Ashworth, 2008), we found that low dose cisplatin combination significantly enhanced synthetic lethality. Of note, the dose of cisplatin used in our study was 1/10th the dose used in previous preclinical studies investigating cisplatin sensitivity *in vitro* in BRCA1 deficient cells (Husain et al., 1998). At higher doses of cisplatin similar to the doses used by Husain et al, BRCA1 deficient cells remain highly sensitive to platinum therapy (data not shown). We speculate that low dose cisplatin treatment generates low levels of DSBs. In cells with proficient BRCA1 and BER, despite ATM or DNA-PKcs blockade, DSBs may be rapidly repaired in back-up DNA repair pathways and cells continue to survive. The back-up repair could operate at multiple levels including the complex interactions/overlap between HR, NHEJ, alternative NHEJ (B-NHEJ) (Chapman et al., 2012; Schipler and Iliakis, 2013), components of NER and ICL repair pathways. On the other hand, in cells with deficient BRCA1 and low BER, the associated pharmacological blockade with ATM or DNA-PKcs inhibitors may lead to DSB accumulation which beyond a threshold, may severely compromise back-up DNA repair machinery leading to DSB accumulation, cell cycle arrest and apoptosis. We have recently shown that XRCC1 deficient cells are cisplatin sensitive (Abdel-Fatah et al., 2013a) and ATM or DNA-PKcs inhibitors are also synthetically lethal in XRCC1 deficient cells (Sultana et al., 2013). Given the potential role of XRCC1 in B-NHEJ (Mladenov and Iliakis, 2011) we speculate that BRCA1 deficient cells that have low XRCC1 could also have compromised B-NHEJ in addition to BER resulting in increased genomic instability and enhanced synthetic lethality with cisplatin treatment seen in the current study. Moreover, ATM or DNA-PKcs modulation has previously been shown to enhance cisplatin cytotoxicity (Dejmek et al., 2009; Yoshida et al., 2008). Taken together, the data suggests that cisplatin combination may be more successful than ATM or DNA-PK monotherapy in BRCA1 negative tumours and would be consistent with a recent study showing enhancement of synthetic lethality with ABT-888

(PARP inhibitor) in combination with platinum chemotherapy in BRCA deficient cells (Clark et al., 2012).

REFERENCE

Abdel-Fatah, T., Sultana, R., Abbotts, R., Hawkes, C., Seedhouse, C., Chan, S.,Madhusudan, S., 2013a. Clinicopathological and functional significance of XRCC1 expression in ovarian cancer. International journal of cancer. Journal international du cancer 132, 2778-2786.

Abdel-Fatah, T. M., Albarakati, N., Bowell, L., Agarwal, D., Moseley, P., Hawkes, C., Ball, G., Chan, S., Ellis, I. O.,Madhusudan, S., 2013b. Single-strand selective monofunctional uracil-DNA glycosylase (SMUG1) deficiency is linked to aggressive breast cancer and predicts response to adjuvant therapy. Breast cancer research and treatment 142, 515-527.

Abdel-Fatah, T. M., Perry, C., Moseley, P., Johnson, K., Arora, A., Chan, S., Ellis, I. O.,Madhusudan, S., 2014a. Clinicopathological significance of human apurinic/apyrimidinic endonuclease 1 (APE1) expression in oestrogen-receptor-positive breast cancer. Breast cancer research and treatment 143, 411-421.

Abdel-Fatah, T. M., Russell, R., Agarwal, D., Moseley, P., Abayomi, M. A., Perry, C., Albarakati, N., Ball, G., Chan, S., Caldas, C., Ellis, I. O.,Madhusudan, S., 2014b. DNA polymerase beta deficiency is linked to aggressive breast cancer: A comprehensive analysis of gene copy number, mRNA and protein expression in multiple cohorts. Mol Oncol.

Abdel-Fatah, T. M., Russell, R., Albarakati, N., Maloney, D. J., Dorjsuren, D., Rueda, O. M., Moseley, P., Mohan, V., Sun, H., Abbotts, R., Mukherjee, A., Agarwal, D., Illuzzi, J. L., Jadhav, A., Simeonov, A., Ball, G., Chan, S., Caldas, C., Ellis, I. O., Wilson, D. M., 3rd,Madhusudan, S., 2014c. Genomic and protein expression analysis reveals flap endonuclease 1 (FEN1) as a key biomarker in breast and ovarian cancer. Mol Oncol.

Alli, E., Sharma, V. B., Sunderesakumar, P.,Ford, J. M., 2009. Defective repair of oxidative dna damage in triple-negative breast cancer confers sensitivity to inhibition of poly(ADP-ribose) polymerase. Cancer Res 69, 3589-3596.

Berenbaum, M. C., 1981. Criteria for analyzing interactions between biologically active agents. Adv Cancer Res 35, 269-335.

Bergh, J., Norberg, T., Sjogren, S., Lindgren, A.,Holmberg, L., 1995. Complete sequencing of the p53 gene provides prognostic information in breast cancer patients, particularly in relation to adjuvant systemic therapy and radiotherapy. Nature medicine 1, 1029-1034.

Bielas, J. H., Loeb, K. R., Rubin, B. P., True, L. D.,Loeb, L. A., 2006. Human cancers express a mutator phenotype. Proc Natl Acad Sci U S A 103, 18238-18242.

Caestecker, K. W.,Van de Walle, G. R., 2013. The role of BRCA1 in DNA double-strand repair: past and present. Experimental cell research 319, 575-587.

Chapman, J. R., Taylor, M. R.,Boulton, S. J., 2012. Playing the end game: DNA double-strand break repair pathway choice. Molecular cell 47, 497-510.

Clark, C. C., Weitzel, J. N.,O'Connor, T. R., 2012. Enhancement of synthetic lethality via combinations of ABT-888, a PARP inhibitor, and carboplatin in vitro and in vivo using BRCA1 and BRCA2 isogenic models. Molecular cancer therapeutics 11, 1948-1958.

Curtis, C., Shah, S. P., Chin, S. F., Turashvili, G., Rueda, O. M., Dunning, M. J., Speed, D., Lynch, A. G., Samarajiwa, S., Yuan, Y., Graf, S., Ha, G., Haffari, G., Bashashati, A., Russell, R., McKinney, S., Langerod, A., Green, A., Provenzano, E., Wishart, G., Pinder, S., Watson, P., Markowetz, F., Murphy, L.,

Ellis, I., Purushotham, A., Borresen-Dale, A. L., Brenton, J. D., Tavare, S., Caldas, C.,Aparicio, S., The genomic and transcriptomic architecture of 2,000 breast tumours reveals novel subgroups. Nature 486, 346-352.

De Summa, S., Pinto, R., Pilato, B., Sambiasi, D., Porcelli, L., Guida, G., Mattioli, E., Paradiso, A., Merla, G., Micale, L., De Nittis, P.,Tommasi, S., 2014. Expression of base excision repair key factors and miR17 in familial and sporadic breast cancer. Cell Death Dis 5, e1076.

Dejmek, J., Iglehart, J. D.,Lazaro, J. B., 2009. DNA-dependent protein kinase (DNA-PK)-dependent cisplatin-induced loss of nucleolar facilitator of chromatin transcription (FACT) and regulation of cisplatin sensitivity by DNA-PK and FACT. Molecular cancer research : MCR 7, 581-591.

Dianov, G. L.,Hubscher, U., 2013. Mammalian base excision repair: the forgotten archangel. Nucleic acids research 41, 3483-3490.

Durant, S. T.,Nickoloff, J. A., 2005. Good timing in the cell cycle for precise DNA repair by BRCA1. Cell cycle 4, 1216-1222.

Golding, S. E., Rosenberg, E., Valerie, N., Hussaini, I., Frigerio, M., Cockcroft, X. F., Chong, W. Y., Hummersone, M., Rigoreau, L., Menear, K. A., O'Connor, M. J., Povirk, L. F., van Meter, T.,Valerie, K., 2009. Improved ATM kinase inhibitor KU-60019 radiosensitizes glioma cells, compromises insulin, AKT and ERK prosurvival signaling, and inhibits migration and invasion. Molecular cancer therapeutics 8, 2894-2902.

Hartman, A. R.,Ford, J. M., 2002. BRCA1 induces DNA damage recognition factors and enhances nucleotide excision repair. Nature genetics 32, 180-184.

Hickson, I., Zhao, Y., Richardson, C. J., Green, S. J., Martin, N. M., Orr, A. I., Reaper, P. M., Jackson, S. P., Curtin, N. J.,Smith, G. C., 2004. Identification and characterization of a novel and specific inhibitor of the ataxia-telangiectasia mutated kinase ATM. Cancer Res 64, 9152-9159.

Hill, R.,Lee, P. W., 2010. The DNA-dependent protein kinase (DNA-PK): More than just a case of making ends meet? Cell cycle 9, 3460-3469.

Hsu, N. C., Huang, Y. F., Yokoyama, K. K., Chu, P. Y., Chen, F. M.,Hou, M. F., 2013. Methylation of BRCA1 promoter region is associated with unfavorable prognosis in women with early-stage breast cancer. PloS one 8, e56256.

Huen, M. S., Sy, S. M.,Chen, J., 2010. BRCA1 and its toolbox for the maintenance of genome integrity. Nature reviews. Molecular cell biology 11, 138-148.

Husain, A., He, G., Venkatraman, E. S.,Spriggs, D. R., 1998. BRCA1 up-regulation is associated with repair-mediated resistance to cis-diamminedichloroplatinum(II). Cancer Res 58, 1120-1123.

Lancashire, L. J., Powe, D. G., Reis-Filho, J. S., Rakha, E., Lemetre, C., Weigelt, B., Abdel-Fatah, T. M., Green, A. R., Mukta, R., Blamey, R., Paish, E. C., Rees, R. C., Ellis, I. O.,Ball, G. R., 2010. A validated gene expression profile for detecting clinical outcome in breast cancer using artificial neural networks. Breast cancer research and treatment 120, 83-93.

Langelier, M. F.,Pascal, J. M., 2013. PARP-1 mechanism for coupling DNA damage detection to poly(ADP-ribose) synthesis. Current opinion in structural biology 23, 134-143.

Lee, J. H., Goodarzi, A. A., Jeggo, P. A.,Paull, T. T., 2010. 53BP1 promotes ATM activity through direct interactions with the MRN complex. The EMBO journal 29, 574-585.

Lee, J. H.,Paull, T. T., 2007. Activation and regulation of ATM kinase activity in response to DNA double-strand breaks. Oncogene 26, 7741-7748.

Lemetre, C., . et al, 2009. Artificial Neural Network Based algorithm for Biomolecular Interaction Modeling. "Bio-Inspired Systems: Computational and Ambient Intellegence. Lecture Notes in Computer Science 5517, 877-885.

Lord, C. J.,Ashworth, A., 2008. Targeted therapy for cancer using PARP inhibitors. Current opinion in pharmacology 8, 363-369.

Masaoka, A., Gassman, N. R., Horton, J. K., Kedar, P. S., Witt, K. L., Hobbs, C. A., Kissling, G. E., Tano, K., Asagoshi, K.,Wilson, S. H., 2013. Interaction between DNA Polymerase beta and BRCA1. PloS one 8, e66801.

Mladenov, E.,Iliakis, G., 2011. Induction and repair of DNA double strand breaks: the increasing spectrum of non-homologous end joining pathways. Mutat Res 711, 61-72.

Nutley, B. P., Smith, N. F., Hayes, A., Kelland, L. R., Brunton, L., Golding, B. T., Smith, G. C., Martin, N. M., Workman, P.,Raynaud, F. I., 2005. Preclinical pharmacokinetics and metabolism of a novel prototype DNA-PK inhibitor NU7026. British journal of cancer 93, 1011-1018.

O'Donovan, P. J.,Livingston, D. M., 2010. BRCA1 and BRCA2: breast/ovarian cancer susceptibility gene products and participants in DNA double-strand break repair. Carcinogenesis 31, 961-967.

Pawitan, Y., Bjohle, J., Amler, L., Borg, A. L., Egyhazi, S., Hall, P., Han, X., Holmberg, L., Huang, F., Klaar, S., Liu, E. T., Miller, L., Nordgren, H., Ploner, A., Sandelin, K., Shaw, P. M., Smeds, J., Skoog, L., Wedren, S.,Bergh, J., 2005. Gene expression profiling spares early breast cancer patients from adjuvant therapy: derived and validated in two population-based cohorts. Breast cancer research : BCR 7, R953-964.

Saha, T., Rih, J. K., Roy, R., Ballal, R.,Rosen, E. M., 2010. Transcriptional regulation of the base excision repair pathway by BRCA1. The Journal of biological chemistry 285, 19092-19105.

Schipler, A.,Iliakis, G., 2013. DNA double-strand-break complexity levels and their possible contributions to the probability for error-prone processing and repair pathway choice. Nucleic acids research 41, 7589-7605.

Shekh, K., Khan, S., Jena, G., Kansara, B. R.,Kushwaha, S., 2014. 3-Aminobenzamide--a PARP inhibitor enhances the sensitivity of peripheral blood micronucleus and comet assays in mice. Toxicol Mech Methods 24, 332-341.

Shiloh, Y.,Ziv, Y., 2013. The ATM protein kinase: regulating the cellular response to genotoxic stress, and more. Nature reviews. Molecular cell biology 14, 197-210.

Silver, D. P.,Livingston, D. M., 2012. Mechanisms of BRCA1 tumor suppression. Cancer discovery 2, 679-684.

Smoot, M. E., Ono, K., Ruscheinski, J., Wang, P. L.,Ideker, T., 2011. Cytoscape 2.8: new features for data integration and network visualization. Bioinformatics 27, 431-432.

Smyth, G. K., 2004. Linear models and empirical bayes methods for assessing differential expression in microarray experiments. Statistical applications in genetics and molecular biology 3, Article3.
Sultana, R., Abdel-Fatah, T., Abbotts, R., Hawkes, C., Albarakati, N., Seedhouse, C., Ball, G., Chan, S., Rakha, E. A., Ellis, I. O.,Madhusudan, S., 2013. Targeting XRCC1 deficiency in breast cancer for personalized therapy. Cancer Res 73, 1621-1634.

Tassone, P., Di Martino, M. T., Ventura, M., Pietragalla, A., Cucinotto, I., Calimeri, T., Bulotta, A., Neri, P., Caraglia, M.,Tagliaferri, P., 2009. Loss of BRCA1 function increases the antitumor activity of cisplatin against human breast cancer xenografts in vivo. Cancer biology & therapy 8, 648-653.

Tavecchio, M., Munck, J. M., Cano, C., Newell, D. R.,Curtin, N. J., 2012. Further characterisation of the cellular activity of the DNA-PK inhibitor, NU7441, reveals potential cross-talk with homologous recombination. Cancer chemotherapy and pharmacology 69, 155-164.

Tibshirani, R., Hastie, T., Narasimhan, B.,Chu, G., 2002. Diagnosis of multiple cancer types by shrunken centroids of gene expression. Proc Natl Acad Sci U S A 99, 6567-6572.

Turner, N., Tutt, A.,Ashworth, A., 2004. Hallmarks of 'BRCAness' in sporadic cancers. Nature reviews. Cancer 4, 814-819.

Wu, L., Wang, F., Xu, R., Zhang, S., Peng, X., Feng, Y., Wang, J.,Lu, C., 2013. Promoter methylation of BRCA1 in the prognosis of breast cancer: a meta-analysis. Breast cancer research and treatment 142, 619-627.

Yoshida, K., Ozaki, T., Furuya, K., Nakanishi, M., Kikuchi, H., Yamamoto, H., Ono, S., Koda, T., Omura, K.,Nakagawara, A., 2008. ATM-dependent nuclear accumulation of IKK-alpha plays an important role in the regulation of p73-mediated apoptosis in response to cisplatin. Oncogene 27, 1183-1188.

Table 1. Multivariate analysis in BRCA1 negative sporadic breast cancers (Nottingham cohort).

Variables	Multivariate Model		
	Exp (B)	**CI 95%**	**P Value**
Pol beta expression	0.810	0.666-0.986	**0.036**
XRCC1 expression	0.831	0.731-0.945	**0.005**
Tumour stage	3.088	2.414-3.950	**<0.0001**
ER receptor status	0.522	0.328-0.833	**0.006**
Chemotherapy status	0.522	0.356-0.764	**0.001**

FIGURE LEGENDS

Figure 1. BRCA1 and BER protein expression in human breast cancer. **A.** Microphotographs of BRCA1 negative, BRCA1 positive, polβ positive and XRCC1 positive breast cancers. **B.** Kaplan Meier curves showing breast cancer specific survival (BCSS) in patients based on BRCA1 expression status. **C1.** Kaplan Meier curves showing breast cancer specific survival (BCSS) in patients with BRCA1 negative tumours based on XRCC1 expression status. **C2.** Kaplan Meier curves showing breast cancer specific survival (BCSS) in patients with BRCA1 negative/ER negative tumours based on XRCC1 expression status. **C3.** Kaplan Meier curves showing breast cancer specific survival (BCSS) in patients with BRCA1 negative/ER positive tumours based on XRCC1 expression status. **D1.** Kaplan Meier curves showing breast cancer specific survival (BCSS) in patients with BRCA1 negative tumours based on polβ expression status. **D2.** Kaplan Meier curves showing breast cancer specific survival (BCSS) in patients with BRCA1 negative/ER negative tumours based on polβ expression status. **D3.** Kaplan Meier curves showing breast cancer specific survival (BCSS) in patients with BRCA1 negative/ER positive tumours based on polβ expression status.

Figure 2. A. Kaplan Meier curves showing overall survival in patients with germ-line BRCA1mutated tumours based on polβ protein expression status. **B1.** Kaplan Meier curves showing breast cancer specific survival (BCSS) in patients based on BRCA1 mRNA expression status in ER+ breast cancer (METABRIC cohort). **B2.** Kaplan Meier curves showing breast cancer specific survival (BCSS) in patients with BRCA1 mRNA low/ER+ who received adjuvant endocrine therapy based on polβ mRNA status (METABRIC cohort). **B3.** Kaplan Meier curves showing breast cancer specific survival (BCSS) in patients with BRCA1 mRNA low/ER+ who received adjuvant endocrine therapy based on XRCC1 mRNA

status (METABRIC cohort). **C1.** Kaplan Meier curves showing breast cancer specific survival (BCSS) in patients with BRCA1 mRNA low/ER- who received adjuvant chemotherapy based on polβ mRNA status (METABRIC cohort). **C2.** Kaplan Meier curves showing breast cancer specific survival (BCSS) in patients with BRCA1 mRNA low/ER- who received adjuvant chemotherapy based on XRCC1 mRNA status (METABRIC cohort). **D.** The neural network illustrates the top genes that interact with BRCA1 and other DNA repair genes. In addition, the artificial neural network also reveals how these top genes interact with each other. Top pair-wise interactions for gene probe markers associated with BRCA1 expression and the DNA repair process in 249 breast cancers is shown here. Each gene probe is represented by a node and the interaction weight between them as an edge, the width being defined by the magnitude of the weight. Interactions are directed from a source gene to a target gene as indicated by arrows. Red interactions indicate an excitatory interaction and blue indicates an inhibitory interaction. Highly linked genes represent hubs that are indicated to be highly influential or highly regulated in the BRCA1-DNA repair system. See supplementary data x for the biological functions of individual genes.

Figure 3. DNA repair expression in BRCA1 deficient and BRCA1 proficient cells **A1.** Representative Western blots of BRCA1, XRCC1 and polβ in BRCA1 deficient HeLa SilenciX cells and control BRCA1 proficient HeLa SilenciX cells. **A2.** Protein quantification in BRCA1 deficient HeLa SilenciX cells and control BRCA1 proficient HeLa SilenciX cells are shown here. The Figure shows fold change in BRCA1 deficient cells in comparison to BRCA1 proficient cells. **A3.** mRNA expression in BRCA1 deficient HeLa SilenciX cells and control BRCA1 proficient HeLa SilenciX cells are shown here. The Figure shows fold change in BRCA1 deficient cells in comparison to BRCA1 proficient cells. **B1.** Representative Western blots of BRCA1, XRCC1 and polβ in BRCA1 deficient MDA-MB-436 cells and BRCA1 proficient MCF7 cells. **B2.** Protein quantification in MDA-

MB-436 cells and MCF7 cells are shown here. The Figure shows fold change in BRCA1 deficient cells in comparison to BRCA1 proficient cells. **B3.** mRNA expression in MDA-MB-436 cells and MCF7 cells are shown here. The Figure shows fold change in BRCA1 deficient cells in comparison to BRCA proficient cells. **C.** Scatter plots indicate up- and down-regulation of DNA repair mRNA expression in BRCA1 deficient HeLa SilenciX cells compared to BRCA1 proficient HeLa SilenciX cells. **D.** Scatter plots indicate up- and down-regulation of DNA repair mRNA expression in MDA-MB-436 cells compared to MCF7 cells are shown here. Green circles show genes that are two-fold or more down-regulated. See also results section and supplementary table S16 and S17.

Figure 4. ATM inhibitors in BRCA1 deficient and BRCA1 proficient cells. **A1.** Clonogenic survival assays in BRCA1 deficient HeLa SilenciX cells and control BRCA1 proficient HeLa SilenciX cells treated with KU55933. **A2.** yH2AX immunohistochemistry in BRCA1 deficient HeLa SilenciX cells and control BRCA1 proficient HeLa SilenciX cells treated with KU55933. **A3.** FACS analysis in BRCA1 deficient HeLa SilenciX cells and control BRCA1 proficient HeLa SilenciX cells treated with KU55933. **A4.** Annexin V flow cytometric analysis in BRCA1 deficient HeLa SilenciX cells and control BRCA1 proficient HeLa SilenciX cells treated with KU55933.**B1.** Clonogenic survival assays in MDA-MB-436 and MCF7 cells treated with KU55933. **B2.** yH2AX immunohistochemistry in MDA-MB-436 and MCF7 cells treated with KU55933. **B3.** FACS analysis in MDA-MB-436 and MCF7 cells treated with KU55933. **B4.** Annexin V flow cytometric analysis in MDA-MB-436 and MCF7 cells treated with KU55933. Inhibitors were added at the indicated concentrations (see methods for details). **C1.** Clonogenic survival assays in BRCA1 deficient HeLa SilenciX cells and control BRCA1 proficient HeLa SilenciX cells treated with cisplatin alone or in combination with KU55933. **C2.** yH2AX immunohistochemistry in BRCA1 deficient HeLa SilenciX cells and control BRCA1 proficient HeLa SilenciX cells treated with cisplatin alone

or in combination with KU55933. **C3.** FACS analysis in BRCA1 deficient HeLa SilenciX cells and control BRCA1 proficient HeLa SilenciX cells treated with cisplatin alone or in combination with KU55933. **C4.** Annexin V flow cytometric analysis in BRCA1 deficient HeLa SilenciX cells and control BRCA1 proficient HeLa SilenciX cells treated with cisplatin alone or in combination with KU55933. **D1.** Clonogenic survival assays in MDA-MB-436 and MCF7 cells treated with cisplatin alone or in combination with KU55933. **D2.** yH2AX immunohistochemistry in MDA-MB-436 and MCF7 cells treated with cisplatin alone or in combination with KU55933. **D3.** FACS analysis in MDA-MB-436 and MCF7 cells treated with cisplatin alone or in combination with KU55933. **D4.** Annexin V flow cytometric analysis in MDA-MB-436 and MCF7 cells treated with cisplatin alone or in combination with KU55933. * $p<0.05$, ** $p<0.01$.

Figure 5. DNA-PKcs inhibitors in BRCA1 deficient and BRCA1 proficient cells. **A1.** Clonogenic survival assays in BRCA1 deficient HeLa SilenciX cells and control BRCA1 proficient HeLa SilenciX cells treated with NU7441. **A2.** yH2AX immunohistochemistry in BRCA1 deficient HeLa SilenciX cells and control BRCA1 proficient HeLa SilenciX cells treated with NU7441. **A3.** FACS analysis in BRCA1 deficient HeLa SilenciX cells and control BRCA1 proficient HeLa SilenciX cells treated with NU7441. **A4.** Annexin V flow cytometric analysis in BRCA1 deficient HeLa SilenciX cells and control BRCA1 proficient HeLa SilenciX cells treated with NU7441.**B1.** Clonogenic survival assays in MDA-MB-436 and MCF7 cells treated with NU7441. **B2.** yH2AX immunohistochemistry in MDA-MB-436 and MCF7 cells treated with NU7441. **B3.** FACS analysis in MDA-MB-436 and MCF7 cells treated with NU7441. **B4.** Annexin V flow cytometric analysis in MDA-MB-436 and MCF7 cells treated with NU7441. Inhibitors were added at the indicated concentrations (see methods for details). **C1.** Clonogenic survival assays in BRCA1 deficient HeLa SilenciX cells and control BRCA1 proficient HeLa SilenciX cells treated with cisplatin alone or in

combination with NU7441. **C2.** yH2AX immunohistochemistry in BRCA1 deficient HeLa SilenciX cells and control BRCA1 proficient HeLa SilenciX cells treated with cisplatin alone or in combination with NU7441. **C3.** FACS analysis in BRCA1 deficient HeLa SilenciX cells and control BRCA1 proficient HeLa SilenciX cells treated with cisplatin alone or in combination with NU7441. **C4.** Annexin V flow cytometric analysis in BRCA1 deficient HeLa SilenciX cells and control BRCA1 proficient HeLa SilenciX cells treated with cisplatin alone or in combination with NU7441. **D1.** Clonogenic survival assays in MDA-MB-436 and MCF7 cells treated with cisplatin alone or in combination with NU7441. **D2.** yH2AX immunohistochemistry in MDA-MB-436 and MCF7 cells treated with cisplatin alone or in combination with NU7441. **D3.** FACS analysis in MDA-MB-436 and MCF7 cells treated with cisplatin alone or in combination with NU7441. **D4.** Annexin V flow cytometric analysis in MDA-MB-436 and MCF7 cells treated with cisplatin alone or in combination with NU7441. * $p<0.05$, ** $p<0.01$.

Targeting BRCA1-BER deficient breast cancer by ATM or DNA-PKcs blockade either alone or in combination with cisplatin for personalized therapy

Nada Albarakati[1], Tarek MA Abdel-Fatah[2], Rachel Doherty[1], Roslin Russell[3], Devika Agarwal[4], Paul Moseley[2], Christina Perry[1] , Arvind Arora[1], Nouf Alsubhi[1], Claire Seedhouse [5], Emad A Rakha[6], Andrew Green[6], Graham Ball[4] , Stephen Chan[2], Carlos Caldas[3], Ian O Ellis[6] and Srinivasan Madhusudan[1,2*]

[1] Academic Unit of Oncology, Division of Cancer and Stem Cells, School of Medicine, University of Nottingham, Nottingham University Hospitals, Nottingham NG51PB, U.K.

[2] Department of Oncology, Nottingham University Hospitals, Nottingham NG51PB, UK.

[3] Cancer Research UK, Cambridge Research Institute, Li Ka Shing Centre, Robinson Way, Cambridge CB2 0RE, UK.

[4] School of Science and Technology, Nottingham Trent University, Clifton campus, Nottingham NG11 8NS, UK.

[5] Academic Haematology, Division of Cancer and Stem Cells, School of Medicine, University of Nottingham, Nottingham University Hospitals, Nottingham NG51PB, U.K.

[6] Department of Pathology, Division of Cancer and Stem Cells, School of Medicine, University of Nottingham, Nottingham University Hospitals, Nottingham NG51PB, U.K.

Running title: Targeting ATM or DNA-PK in BRCA1 deficient cells

Word count: 4989

Figure: 5

Tables: 1

Key words: BRCA1; base excision repair; ATM; DNA-PK; small molecule inhibitors; synthetic lethality, cisplatin; chemopotentiation.

Conflicts of interest: The authors disclose no potential conflicts of interest.

* **Corresponding author:**

Dr Srinivasan Madhusudan

Academic Unit of Oncology

Division of Cancer and Stem Cells

School of Medicine

University of Nottingham

Nottingham University Hospitals

Nottingham NG51PB, U.K

Telephone: +44(0)115 823 1850

Fax: +44(0)115 823 1849

E-Mail: srinivasan.madhusudan@nottingham.ac.uk

ABSTRACT

BRCA1, a key factor in homologous recombination (HR) repair may also regulate base excision repair (BER). Targeting BRCA1-BER deficient cells by blockade of ATM and DNA-PKcs could be a promising strategy in breast cancer. We investigated BRCA1, XRCC1 and pol β protein expression in two cohorts (n=1602 sporadic and n=50 germ-line BRCA1 mutated) and mRNA expression in two cohorts (n=1952 and n=249). Artificial neural network analysis for BRCA1-DNA repair interacting genes was conducted in 249 tumours. Pre-clinically, BRCA1 proficient and deficient cells were DNA repair expression profiled and evaluated for synthetic lethality using ATM and DNA-PKcs inhibitors either alone or in combination with cisplatin. In human tumours, BRCA1 negativity was strongly associated with low XRCC1, and low pol β at mRNA and protein levels ($p<0.0001$). In patients with BRCA1 negative tumours, low XRCC1 or low pol β expression was significantly associated with poor survival in univariate and multivariate analysis compared to high XRCC1 or high pol β expressing BRCA1 negative tumours ($ps<0.05$). Pre-clinically, BRCA1 negative cancer cells exhibit low mRNA and low protein expression of XRCC1 and pol β. BRCA1-BER deficient cells were sensitive to ATM and DNA-PKcs inhibitor treatment either alone or in combination with cisplatin and synthetic lethality was evidenced by DNA double strand breaks accumulation, cell cycle arrest and apoptosis. We conclude that XRCC1 and pol β expression status in BRCA1 negative tumours may have prognostic significance. BRCA1-BER deficient cells could be targeted by ATM or DNA-PKcs inhibitors for personalized therapy.

INTRODUCTION

Breast Cancer Susceptibility Gene 1 (BRCA1) facilitates the efficient resolution of DNA double-strand breaks (DSBs) through HR (Caestecker and Van de Walle, 2013; Huen et al., 2010). Cells lacking functional BRCA1 protein have impaired HR, and thus depend on the more error-prone non-homologous end joining (NHEJ) pathway leading to chromosomal instability that drive breast cancer development (Huen et al., 2010). In women, BRCA1 germ line mutation is associated with a 60%-70% lifetime risk of developing breast cancer (O'Donovan and Livingston, 2010). In the more common sporadic breast cancers, epigenetic silencing of the BRCA1 promoter has been reported in up to 11%-14% of tumours (Turner et al., 2004) and a dysfunctional BRCA pathway may also contribute to a BRCAness phenotype in about 25% of cancers (Turner et al., 2004), where breast cancers do not harbour germ-line BRCA mutations but display similar phenotypes including HR deficiency. BER is critical for processing DNA damage caused by alkylation, oxidation, ring saturation, single strand breaks and base deamination. DNA polymerase β (pol β) and XRCC1 are key BER factors. PARP1 (poly [ADP-ribose] polymerase 1) may play an essential role in single strand break repair (SSBR), a BER-related pathway (Langelier and Pascal, 2013). The DNA repair intermediates generated during BER/SSBR, if unrepaired, may get converted to toxic double strand breaks (DSBs) (Dianov and Hubscher, 2013).

Emerging studies suggest a cross talk between BRCA1 and BER factors. BRCA1 mutated and basal-like breast cancer cells were found to be sensitive to oxidative DNA damage induced by H_2O_2 treatment. The increased sensitivity was associated with defective BER as assessed by cell based BER assay in BRCA1 deficient cells (Alli et al., 2009). In a more recent study, BRCA1 deficient cells were sensitive to methyl methane sulfonate (alkylating

agent) and functional interaction between polβ and BRCA1 was demonstrated in that study (Masaoka et al., 2013) implying a potential role for polβ in BRCA1 mediated DSB repair. In addition, BRCA1 has also been shown to be involved in the transcriptional regulation of BER factor such as OGG1, NTH1 and APE1 (Saha et al., 2010).

Synthetic lethality is a promising strategy for personalized cancer therapy. PARP [poly-(ADP-ribose) polymerase] inhibitors induce synthetic lethality in germ line BRCA1-deficient breast cancers and demonstrate clinical benefit in patients (Lord and Ashworth, 2008). Similarly, we have recently shown that APE1 inhibition is synthetically lethal in BRCA1 deficient breast cancer cells and in PTEN (and DSB repair) deficient melanoma cells. The data provides compelling reasons to investigate other potential synthetic lethal interactions targeting DNA repair for clinical application. Cells that are BRCA1 deficient as well as BER impaired may be reliant upon other back-up repair pathways to maintain genomic integrity and survival. ATM and DNA-PKcs play essential roles in the DNA damage response (DDR) and link DNA damage sensing to DDR effectors that regulate cell cycle progression and DNA repair (Shiloh and Ziv, 2013). ATM, a member of the phosphatidylinositol-3-kinase-like protein kinase (PIKK) family, is a key sensor and transducer of DNA damage signalling during HR (Lee and Paull, 2007; Shiloh and Ziv, 2013). ATM recruitment at sites of DNA damage may be dependent upon functional BRCA1 in cells (Lee et al., 2010). DNA-PKcs is another key member of the PIKK family and a critical component of NHEJ pathway required for repair of DSBs generated throughout the cell cycle (Hill and Lee, 2010). BRCA1 through a role in DNA end-processing may also be involved in the regulation of NHEJ (Durant and Nickoloff, 2005).

Our hypothesis is that impaired BER in BRCA1 deficient tumours may influence prognosis. BRCA1-BER deficient cells may be reliant upon ATM or DNA-PKcs mediated back-up pathways for cellular survival and could be targeted by synthetic lethality using inhibitors of ATM or DNA-PKcs.

MATERIALS AND METHODS

Clinical study

BRCA1 and BER protein expression analysis in Nottingham Tenovus Primary Breast Carcinoma cohort: The study was performed in a consecutive series of 1650 patients with primary invasive breast carcinomas who were diagnosed between 1986 and 1999 and entered into the Nottingham Tenovus Primary Breast Carcinoma series described previously (Sultana et al., 2013). Supplemental Table S1 summarizes patient demographics. Supplemental treatment data 1 summarizes various adjuvant treatments received by patients in this cohort.

BRCA1 and BER protein expression analysis in germ line BRCA1 deficient breast cancer: The demographics of a cohort of 50 germ-line BRCA1 mutated breast cancers confirmed by genetic testing is shown in supplementary table S6. All patients received surgery, adjuvant chemotherapy and radiotherapy according to our institutional policy (supplementary treatment data 1).

Tissue Microarrays (TMAs) and immunohistochemistry (IHC): Tumours were arrayed in tissue microarrays (TMAs) and immunohistochemically profiled for BRCA1, APE1, XRCC1,

Pol β, and other biological markers (Supplementary Table S2) as previously described (Sultana et al., 2013). Supplementary Table S2 summarizes immunohistochemistry protocols for the markers tested using the Bond Max automated staining machine and Leica Bond Refine Detection kit (DS9800) according to manufacturer instructions (Leica Microsystems). We have recently published optimisation and specificity of XRCC1 and pol β antibody used in the current study (Abdel-Fatah et al., 2014b; Sultana et al., 2013). To validate the use of TMAs for immunophenotyping, full-face sections of 40 cases were stained and protein expression levels of the different antibodies were compared. The concordance between TMAs and full-face sections was excellent (k = 0.8). Positive and negative (by omission of the primary antibody and IgG-matched serum) controls were included in each run.

Evaluation of immune staining: The tumour cores were evaluated by specialist pathologists blinded to the clinicopathological characteristics of patients, in two different settings. There was excellent intra and inter-observer agreements ($k > 0.8$; Cohen's $\varkappa$ and multi-rater $\varkappa$ tests, respectively). Whole field inspection of the core was scored and intensities of nuclear staining were grouped as follows: 0 = no staining, 1 = weak staining, 2 = moderate staining, 3 = strong staining. The percentage of each category was estimated (0-100%). H-scores (range 0-300) were calculated by multiplying intensity of staining and percentage staining as previously described (Sultana et al., 2013). Supplementary Table S2 summarizes cut-offs for individual markers.

Statistical analysis: Data analysis was performed using SPSS (SPSS, version 17 Chicago, IL). Where appropriate, Pearson's Chi-square, Fisher's exact, Student's t and ANOVA one way tests were used. Cumulative survival probabilities were estimated using the Kaplan–Meier method, and differences between survival rates were tested for significance using the log-rank test. Multivariate analysis for survival was performed using the Cox proportional

hazard model. A p value < 0.05 considered significant. For multiple comparisons, p values were adjusted according to Holm-Bonferroni correction method.

Transcript levels in the METABRIC (Molecular Taxonomy of Breast Cancer International Consortium) cohort: Investigation of the mRNA expression was performed in METABRIC cohort which refers to a set of 1980 breast cancer samples with a minimum of 5 years of clinical follow up where mRNA expression data was available (Curtis et al.). Patient demographics are summarized in supplementary Table S9. ER positive and/or lymph-node negative patients did not receive adjuvant chemotherapy. ER negative and/or lymph-node positive patients received adjuvant chemotherapy. All the samples were analysed as triplicates. A sliding window analysis was used to identify a cut-off in gene expression values such that the resulting subgroups have significantly different survival courses.

Artificial neural network (ANN) analysis in Uppsala cohort: The demographics of the Uppsala cohort is summarized in supplementary Table S10 and mRNA analysis has been described previously (Bergh et al., 1995). All microarray data are accessible at National Center for Biotechnology Information (NCBI) Gene Expression Omnibus (http://www.ncbi.nlm.nih.gov/geo/, accession number: GSE4922) (Pawitan et al., 2005). All data were normalized using the global mean method (MAS5), and probe set signal intensities were natural log transformed and scaled by adjusting the mean signal to a target value of log 500. The expression levels of the *BRCA1*, for the probe 204531_s_at located on the HG-U133A chip was utilized to generate the ANN based model as described previously (30) (Lancashire et al., 2010) (Lemetre, 2009). A non-linear, ANN modelling based, data mining approach was utilised to identify the best gene probes for sample classification as described previously (30). 47,293 probes were screened for each sample in the test set (n=249). The data mining algorithm comprised a three layer multilayer perception architecture modified with a feed

forward back-propagation algorithm and a sigmoidal transfer function, as previously described (Lancashire et al., 2010). The network momentum and learning rate were respectively set as 0.1 and 0.5. Two hidden nodes were utilised. The output node was coded as 0 if a case was low *BRCA1* expression (<the median) and 1 if high *BRCA1* expression (>median). Inputs were ranked in ascending order based on their classification error. The top 50 predictive genes identified were merged with 150 gene probes involved in the DNA repair process (Supplementary Table S11) and then applied to an ANN based network inference algorithm as described in earlier studies (Lemetre, 2009). This model predicted a weighted link (direction and magnitude) between each of the gene probe markers. This weighting was based on the non-linear correlation between a source gene and a target gene in a multifactorial ANN model. This approach defines a linkage or interaction with a magnitude between every possible pair of genes in the set presented to the algorithm. The approach is data driven and unweighted by biological function. The 100 strongest interactions were then visualised as a map with Cytoscape (Smoot et al., 2011). In a second bioinformatics analysis step, we sought to obtain a robust ranking of genes that are differentially expressed between the mRNA *BRCA1*+ cases and the mRNA *BRCA1*- and have high predictive power, by applying an ensemble sample classification method within a leave-one-out cross-validation scheme. For this purpose, the 249 patient samples were first grouped into 249 different training/test set partitions, using 248 samples for the training sets and the remaining sample as the test set. For each of the 248 training sets differentially expressed genes were selected independently with the "Empirical Bayes moderated t-statistic" (Smyth, 2004) and used to train a machine learning model, which was evaluated based on the left-out sample (a procedure known as "external cross-validation"). To classify the left-out sample, the prediction results of four algorithms (Support Vector Machine, Random Forest, kNN and Prediction Analysis for Microarrays, with all parameters being optimised by using a grid

search within a nested cross-validation) (Tibshirani et al., 2002) were combined to a majority-vote ensemble classifier as to compensate for the inevitable inherent biases and variances that exists amongst each of these machine learning algorithms. In order to rank the genes based on the cross-validation results, their frequency of occurrence in the list of significantly differentially expressed genes (p-value < 0.05) across different cross-validation cycles was recorded, and genes received higher scores the more often they had been selected. All steps of the analysis were conducted using an in-house web-application for microarray analysis, available at www.arraymining.net.

Pre-clinical study

Compounds and reagents: ATM inhibitors (KU55933 and KU60019) and DNA-PKcs inhibitors (NU7441 and NU7026) were purchased from Tocris Bioscience, UK. The compounds were dissolved in 100% DMSO and stored at - 20ºC. Cisplatin was obtained from Nottingham University Hospitals.

Cell lines and culture media: BRCA1 deficient HeLa SilenciX® cells and control BRCA proficient HeLa SilenciX® cells were purchased from Tebu-Bio (www.tebu-bio.com). SilenciX cells were grown in DMEM medium (with L-Glutamine 580mg/L, 4500 mg/L D19 Glucose, with 110mg/L Sodium Pyruvate) supplemented with 10% FBS, 1% penicillin/ streptomycin and 125 µg/ml Hygromycin B. MDA-MB-436 (BRCA1 deficient human breast cancer cells) was grown in DMEM (Sigma, UK) and MCF7 (BRCA1 proficient human breast cancer cells) was grown in RPMI1640 (Sigma, UK). All media used to culture human cancer cell lines were supplemented with 10% FBS (PAA, UK) and 1% penicillin/streptomycin.

Clonogenic survival assay: 200-500 hundred cells per well were seeded in six-well plates. Cells were allowed to adhere for 4 hours. Compounds (ATM inhibitors or DNA-PKcs inhibitors) were added at the indicated concentrations. For cisplatin combination studies, cells

were initially treated with cisplatin for 16 hours and then gently washed twice with 1X phosphate buffered saline and incubated in fresh media with or without ATM or DNA-PK inhibitors at indicated concentration. The plates were left in the incubator for 12-14 days. After incubation, the media was discarded, fixed (with methanol and acetic acid mixture) and stained with crystal violet and counted. Surviving Fraction = [No. of colonies formed/ (No. of cells seeded x Plating efficiency)] x100. All clonogenic assays were done in triplicate.

Evaluation of drug interaction (Combination index): To investigate synergistic and additive activity, combination index was calculated as described previously (Berenbaum, 1981). If D (combination index) is <1 the effect of the combination is synergistic, whereas if D=1 or D is >1 the effect is additive or antagonistic respectively.

γH2AX immunofluorescence microscopy: This assay was performed as described previously(Sultana et al., 2013). Briefly, cells were incubated in medium containing ATM inhibitor or DNA-PKCS inhibitor for 48 hours. For cisplatin combination studies, cells were initially treated with cisplatin for 16 hours and then gently washed twice with 1X phosphate buffered saline and incubated in fresh media with or without ATM or DNA-PK inhibitors at indicated concentration for 48 hours.

Neutral COMET assay: COMET assay reagents were purchased from Trevigen and used according to the manufacturer's neutral COMET protocol (Gaithersburg, MD, USA). Briefly, 1 x 10^5 cells per well were seeded into a 6 well plate and treated with KU55933 (7.5μM) or NU7441 (0.75μM). After 48 hours treatment cells were resuspended in 250 µl PBS. For COMET analysis 25 μl of cell suspension was mixed with 250 μl molten LMAgarose and then 75 μl of the mixture pipetted immediately onto COMET slides. Slides were allowed to set at 4^{o}C for 20 minutes and then immersed in lysis buffer for 60 minutes at 4^{o}C. Slides were

then subjected to electrophoresis at 20 V for 60 minutes in chilled electrophoresis buffer (0.5 M Tris, 1.5 M sodium acetate). Following electrophoresis slides were incubated for 30 minutes in DNA precipitation solution (5 M ammonium acetate in 95% ethanol) at room temperature and subsequently fixed in 70% ethanol for 20 minutes at room temperature. Slides were left to dry overnight at 4^{o}C and then each sample stained with 50 μl Sybr green and scored using COMET ASSAY IV software (Perceptive Instruments Ltd, Bury St Edmonds, UK). Treatments were performed in triplicate and 50 cells counted for each.

Flow cytometric analyses (FACS): Cells grown to sub-confluence were exposed to ATM or DNA-PKcs inhibitors either alone or in combination with cisplatin for 48 hours and collected by trypsinization and centrifugation (1000 rpm for 5 minutes). FACS was performed as described previously (Sultana et al., 2013).

Annexin V flow cytometric analyses: Cells grown to sub-confluence were exposed to ATM or DNA-PKcs inhibitors either alone or in combination with cisplatin for 48 hours and collected by trypsinization and centrifugation (1000 rpm for 5 minutes). The assay was performed as described previously (Sultana et al., 2013).

Quantitative real time PCR: RNA was extracted from cell lines using the RNeasy Mini Kit (Qiagen) and quantified using a microvolume spectrophotometer. cDNA synthesis was performed using the RT^{2} First Strand Kit (Qiagen). Primers used for RT-PCR for BER genes are shown in supplementary table S9. Quantitative PCR was performed on an ABI prism 7700 (Applied Biosystems) using SYBR green detection (Applied Biosystems®, UK). The housekeeping gene GAPDH was used to standardise the samples.

RT² Profiler™ PCR Array for global DNA Repair expression analysis: To evaluate the expression of 84 DNA repair genes simultaneously, real-time PCR was performed using the RT² Profiler™ PCR Array for global DNA Repair expression analysis in technical triplicates (ABI 7500 Fast Block Detection System; Applied Biosystems, Foster City, USA) and the data analysed as per manufacturer's recommendation. GAPDH was used for normalization of the data. A 2 fold change or greater change in expression was considered significant.

RESULTS

Clinical studies

XRCC1, pol β, APE1 and SMUG1 are key BER proteins. Moreover, we have recently shown that XRCC1 (Sultana et al., 2013), pol β (Abdel-Fatah et al., 2014b), APE1 (Abdel-Fatah et al., 2014a) and SMUG1 (Abdel-Fatah et al., 2013b) are promising biomarkers in breast cancer. To evaluate whether they also have prognostic and predictive significance based on BRCA1 status, we proceeded to immunohistochemical evaluation of XRCC1, pol β, APE1 and SMUG1 in BRCA1 positive and BRCA1 negative breast tumours.

BRCA1 negativity is associated with impaired XRCC1 and pol β protein expression in human sporadic breast cancers: A total of 1602 breast tumours were suitable for BRCA1 expression analysis. 1085/1602 (67.7%) of tumours were BRCA1 positive and 517/1602 (32.3%) were negative for BRCA1 expression (Figure 1A). As shown in supplementary Table S3, BRCA1 negative tumours were highly significantly associated with low XRCC1 ($p<0.00001$) and low polβ ($p<0.000001$). In the BRCA1 negative cohort we then evaluated clinicopathological associations of XRCC1 and pol β protein expression (Figure 1A). The data for XRCC1 and polβ are summarized in supplementary tables S4 and S5 respectively. Although no significant associations were seen with stage, tumour grade, tumour types or pleomorphism, BRCA1 negative/ polβ low tumours were more likely to be Bcl2 negative ($p=0.001$) and BRCA1 negative/ XRCC1 low tumours were more likely to be p53 negative ($p= 0.015$).

BRCA1 negative/low XRCC1 or BRCA1 negative/low polβ tumours are associated with poor breast cancer specific survival (BCSS): BRCA1 negativity was significantly associated with poor BCSS compared to BRCA1 positive tumours ($p<0.000001$) (Figure 1B) and is consistent with previous studies showing poor prognostic significance of BRCA1

silencing in sporadic breast tumours (Hsu et al., 2013; Wu et al., 2013). In the BRCA1 negative group we investigated the prognostic influence of XRCC1 and pol β. As shown in Figure 1C1, BRCA1 negative/ low XRCC1 tumours had worse BCSS compared to BRCA1 negative/ high XRCC1 tumours (p=0.001). Similarly, BRCA1 negative/ low polβ tumours had worse BCSS compared to BRCA1 negative/ high polβ tumours (p=0.008) (Figure 1D1). As BRCA1 negativity is likely to be associated with ER negative tumours we conducted further analysis. In the BRCA1 negative/ER negative subgroup, low XRCC1 or low polβ remains associated with poor survival (p=0.033 and p=0.034 respectively, Figure 1C2 and 1D2). In the BRCA1 negative/ER positive subgroup, similarly, low XRCC1 was associated with poor survival (p=0.003, Figure 1C3) and although not significant there was trend with low polβ (p=0.121, Figure1D3). In multivariate cox regression analysis (Table 1), low XRCC1 (p=0.005) and low pol β (p=0.036) were independently associated with poor survival.

In the current study, APE1 and SMUG1 did not influence survival and was not associated with any clinicopathological parameters in BRCA1 negative breast tumours (data not shown).

XRCC1 and pol β expression in germ-line BRCA1 mutated breast cancers: To investigate whether XRCC1 and polβ would also influence outcomes in germ-line BRCA1 deficient breast cancer we investigated a cohort of 50 germ-line BRCA1 mutated breast cancers. Demographics are summarised in supplementary table S6. No significant clinicopathological correlations were observed (supplementary tables S7 and S8). In this small exploratory cohort, low polβ (5/34 tumours) was significantly associated with poor survival (p=0.007) in germ line BRCA1 mutated breast cancers (Figure 2A) compared to high polβ (29/34 tumours). Low XRCC1 expression did not influence survival in this cohort (Supplementary Figure S1A)

Low *XRCC1* and low *pol β* transcript levels have prognostic significance in *BRCA1* mRNA low sporadic breast cancers: To confirm whether the association between BRCA1 and BER also operated at the mRNA level we investigated the Metabric cohort (n=1920, demographics summarized in supplementary table S9) and the Uppsala cohort (n=249, demographics summarized in supplementary table S10) - cohorts where mRNA expression data was available. In ER+ tumours (n=1485, Metabric), low *BRCA1* (n=81) was associated with poor survival compared to high *BRCA1* mRNA expressing tumours (n= 1404) (p= 0.0226, Figure 2B1). In the low *BRCA1*/ER+ group, low polβ (n=66) or low *XRCC1* (n=42) remains associated with poor survival (ps= 0.038 and 0.0321 respectively) compared to high *polβ* (n=14) or high *XRCC1* (n=38) mRNA expressing tumours (Figures 2B2 and 2B3). In the ER- tumours (n=435, metabric), high BRCA1 (n= 385) was associated with poor survival compared to low *BRCA1* mRNA expressing tumours (n=50) (p= 0.0365, Supplementary Figure S2B). In the low *BRCA1*/ER- group, low polβ (n=5) or low *XRCC1* (n=17) remains associated with poor survival compared to high *polβ* (n=43) or high *XRCC1* (n=31) mRNA expressing tumours [ps= 0.0224 and 0.0206 respectively) (Figures 2C1 and 2C2). In the Uppsala cohort, low *polβ* mRNA (36/175 tumours) was associated with poor survival in *BRCA1* low mRNA breast cancers (p=0.03, Supplementary Figure S1C) compared to high *polβ* mRNA tumours (139/175 tumours). *XRCC1* mRNA expression levels did not influence survival in the Uppsala cohort (Supplementary Figure S1D).

Artificial neural network (ANN), ensemble classification and cross-validation analysis for *BRCA1* interacting DNA repair genes: The top 100 strongest are shown in Figure 2D. The biological functions of *BRCA1* interaction genes are summarized in supplementary Table S12. The predominant interactions with genes involved in BER, NER, HR, NHEJ, inter-strand crosslink repair, MMR and transcription is not only consistent with the previously

described functions of *BRCA1* (Caestecker and Van de Walle, 2013; Huen et al., 2010; Silver and Livingston, 2012) but also reveals new BRCA1 interacting genes.

Pre-clinical studies

The clinical and bioinformatics data presented above provides evidence that BRCA1 may influence the expression of multiple DNA repair genes. To provide additional pre-clinical evidence we investigated the expression of DNA repair in BRCA1 deficient and proficient cancer cell lines.

BRCA1 deficient cancer cells exhibit impaired BER expression: BRCA1 deficient HeLa SilenciX cells, control BRCA1 proficient HeLa SilenciX cells, BRCA1 deficient MDA-MB-436 breast cancer cells and BRCA1 proficient MCF7 breast cancer cells were initially examined for the expression of BRCA1, XRCC1 and pol β proteins. BRCA1 deficiency was first confirmed at the protein level in BRCA1 deficient HeLa SilenciX and MDA-MB-436 cells compared to control HeLa SilenciX cells and MCF7 cells (Figures 3A1, 3A2, 3B1, 3B2). The relative expression of XRCC1 and pol β was also found to be low in BRCA1 deficient cells compared to BRCA1 proficient cells at the protein level (Figures 3A1, 3A2, 3B1, 3B2). Low mRNA expression of *BRCA1*, *XRCC1* and *pol β* was confirmed by qRT-PCR in MDA-MB-436 cells compared to MCF-7 cells and BRCA1 deficient HeLa SilenciX compared to control HeLa SilenciX cells (Figure 3A3, 3B3 respectively). The data is also summarized in supplementary Tables S14 and S15. To provide additional evidence that low polβ and low XRCC1 expression confers phenotypic consequence, we investigated MMS sensitivity in MDA-MB-436 and MCF-7 cells. As shown in supplementary Figure S3B, we found that MDA-MB-436 cells are sensitive to MMS. The data concurs with a recent study that showed a similar MMS sensitivity in BRCA1 deficient cells that was associated with impaired functional interaction between polβ and BRCA1(Masaoka et al., 2013).

BRCA1 deficient cells have deregulated gene expression of multiple DNA repair pathways: To investigate whether down regulation of DNA repair is restricted to polβ and XRCC1 or also includes additional DNA repair pathways, we profiled a panel of 84 DNA repair genes in BRCA1 deficient and BRCA1 proficient cells using the RT^2 Profiler DNA Repair PCR array. All experiments were done in triplicates and DNA repair expression was compared between BRCA1 deficient and BRCA1 proficient cells [BRCA1 deficient HeLa SilenciX versus control BRCA1 proficient HeLa SilenciX cells and MDA-MB-436 versus MCF7 cells]. The data is summarized in Figure 3C (BRCA1 deficient and proficient HeLa SilenciX cells), supplementary table S16 (BRCA1 deficient and proficient HeLa SilenciX cells), Figure 3D (MDA-MB-436 and MCF7 cells), and supplementary table S17 (MDA-MB-436 and MCF7 cells). In MDA-MB-436 cells as well as in BRCA1 deficient HeLa SilenciX cells, we observed a consistent down regulation of several BER genes as well as genes involved in other pathways including base excision repair, nucleotide excision repair, homologous recombination, non-homologous end joining, inter-strand crosslink repair and mismatch repair.

BRCA1 deficient cancer cells are sensitive to ATM inhibitors either alone or in combination with cisplatin: KU55933 (2-morpholin-4-yl-6-thianthren-1-yl-pyran-4-one) is an ATP-competitive potent ATM inhibitor with an IC_{50} of 13 nmol/L (Hickson et al., 2004). For additional validation we also tested KU60019 [(2*R*,6*S*-rel)-2,6-Dimethyl-*N*-[5-[6-(4-morpholinyl)-4-oxo-4*H*-pyran-2-yl]-9*H*-thioxanthen-2-yl-4-morpholineacetamide] another ATP-competitive potent ATM inhibitor (Golding et al., 2009). Treatment with KU55933 resulted in reduced survival of BRCA1 deficient HeLa SilenciX cells compared to BRCA1 proficient HeLa SilenciX cells (Figure 4A1). Similarly, MDA-MB-436 cells were sensitive to

KU55933 compared to MCF7 cells respectively (Figures 4B1). As an additional validation we investigated KU60019. As shown in supplementary Figures S3A and S3E, BRCA1 deficient HeLa SilenciX cells and MDA-MB-436 cells were also sensitive to KU60019 compared to BRCA1 proficient cells. 3-aminobenzamide, a PARP inhibitor (Shekh et al., 2014) was used as a positive control. As shown in supplementary Figure S2A and S2B, BRCA1 deficient cells, as expected, are sensitive to PARP inhibitor.

To provide mechanistic evidence that ATM inhibition leads to a synthetic lethality effect in BRCA1 deficient cells, we investigated the functional consequence of ATM inhibition in BRCA1 proficient and BRCA1 deficient cells. Double strand breaks (DSBs) induce phosphorylation of H2AX at serine 139 (γH2AX), and accumulation of γH2AX foci in the nucleus is a marker of DSBs. Therefore, γH2AX immunocytochemistry was performed in BRCA1 deficient HeLa SilenciX cells and MDA-MB-436 cells and compared to BRCA1 proficient control SilenciX or MCF7 cells (Supplementary Figure S3A). Nuclei containing more than six γH2AX foci were considered positive. Cells were treated with KU55933 (10μM) for 48 hours. The percentage of cells with more than six γH2AX foci was significantly higher in BRCA1 deficient cells in comparison to BRCA1 proficient cells (Figures 4A2, 4B2). Similar results were observed with KU60019 (Supplementary Figures S4B and S4F). The data provides evidence that BRCA1 deficient cells accumulate DSBs at an increased rate after treatment with an ATM inhibitor relative to BRCA1proficient cells. As an additional validation we performed neutral COMET assays after ATM or DNA-PKcs inhibitor treatment in cells. As shown in supplementary Figure S3C, BRCA1 deficient cells accumulated significantly more DSBs compared to BRCA1 proficient cells. Accumulation of DSBs may delay cell cycle progression. In BRCA1 deficient and BRCA1 proficient cells, cell cycle progression was monitored after 48 hours of treatment with KU55933 (10μM) (Supplementary Figure S4B). BRCA1 deficient cells were shown to be significantly arrested

in G2/M phase of the cell cycle compared to BRCA1 proficient cells (Figures 4A3, 4B3). Similar results were observed with KU60019 (Supplementary Figures S5C and S5G). Accumulation of DSBs may result in eventual induction of apoptosis. Apoptosis detection by FITC-annexin V flow cytometric analysis was therefore performed in cells treated with KU55933 (10μM) for 48 hours (Supplementary Figure S4C). The percentage of cells undergoing apoptosis following ATM inhibitor treatment was significantly higher in BRCA1 deficient cells in comparison to BRCA1 proficient cells (Figures 4A4, 4B4). Similar results were observed with KU60019 (Supplementary Figures S5D and S5H). The functional studies together provide evidence that ATM inhibition can induce synthetic lethality in BRCA1 deficient cells by causing accumulation of DSBs, G2M cell cycle arrest and induction of apoptosis. However the level of synthetic lethality effect seen with ATM inhibitor was modest compared that demonstrated previously using PARP inhibitors in BRCA1 deficient cells (Lord and Ashworth, 2008).

Cisplatin hypersensitivity has been well established in BRCA1 deficient cells (Tassone et al., 2009). We investigated whether low dose cisplatin could potentiate synthetic lethality induced by KU55933. Cells were treated with a combination of low dose cisplatin (0.00001μM – 0.1 μM) and KU55933 (5μM). As shown in Figure 4C1 and 4D1, KU55933 treatment increased cytotoxicity of cisplatin in BRCA1 deficient HeLa SilenciX as well in MDA-MB-436 compared to BRCA1 proficient control SilenciX and MCF7 cells. The interaction was synergistic [combination index= 0.6 (BRCA1 deficient HeLa SilneciX) and 0.7 (MDA-MB-436), supplementary Figure S7A]. In BRCA1 deficient cells treated with a combination of cisplatin and KU55933, the observed increased cytotoxicity was associated with accumulation of DSBs (Figure 4C2 and 4D2), G2/M cell cycle arrest (Figure 4C3 and 4D3) and increased apoptosis (Figure 4C4 and 4D4).

BRCA1 deficient cancer cells are sensitive to DNA-PKcs inhibitors either alone or in combination with cisplatin: NU7441 (2-N-morpholino-8-dibenzothiophenyl-chromen-4-one) is a potent and a specific inhibitor of DNA-PKcs with an IC_{50} of 14 nmol/L for DNA-PK inhibition (Tavecchio et al., 2012). NU7026 (2-(morpholin-4-yl)-benzo[h]chromen-4-one) is another DNA-PKcs inhibitor (Nutley et al., 2005).

Treatment with NU7441 resulted in reduced survival of BRCA1 deficient HeLa SilenciX cells compared to BRCA1 deficient HeLa SilenciX cells (Figure 5A1). MDA-MB-436 cells were modestly sensitive to NU7441 compared to MCF7 cells respectively (Figures 5B1). As an additional validation we investigated NU7026. As shown in supplementary Figures S6A and S6E, BRCA1 deficient HeLa SilenciX cells and MDA-MB-436 cells were also sensitive to NU7026 compared to BRCA1 proficient cells. To provide mechanistic evidence that DNA-PKcs inhibition leads to a synthetic lethality effect in BRCA1 deficient cells, we investigated the functional consequence of DNA-PKcs inhibition in BRCA1 proficient and BRCA1 deficient cells. Cells were treated with NU7441 (1.5μM) for 48 hours. The percentage of cells with more than six γH2AX foci was significantly higher in BRCA1 deficient cells in comparison to BRCA1 proficient cells (Figures 5A2, 5B2). Similar results were observed with NU7026 (supplementary Figures S6B and S6F). In BRCA1 deficient and BRCA1 proficient cells, cell cycle progression was monitored after 48 hours of treatment with NU7441 (1.5μM). BRCA1 deficient cells were shown to be significantly arrested in G1 phase of the cell cycle compared to BRCA1 proficient cells (Figures 5A3, 5B3). Similar results were observed with NU7026 (supplementary Figures S6C and S6G). Apoptosis detection by FITC-annexin V flow cytometric analysis was therefore performed in cells treated with NU7441 (1.5μM) for 48 hours. The percentage of cells undergoing apoptosis following DNA-PKcs inhibitor treatment was significantly higher in BRCA1 deficient cells in comparison to BRCA1 proficient cells (Figures 5A4, 5B4). Similar results were observed

with NU7026 (Supplementary Figures S6D and S6H). The functional studies together provide evidence that DNA-PKcs inhibition can induce synthetic lethality in BRCA1 deficient cells by causing accumulation of DSBs, G1 cell cycle arrest and induction of apoptosis. We then investigated whether low dose cisplatin could potentiate synthetic lethality induced by NU7441. Cells were treated with a combination of cisplatin (0.00001μM – 0.1 μM) and NU7441 (0.75μM). As shown in Figure 5C1 and 5D1, NU7441 treatment substantially increased cytotoxicity of low dose cisplatin in BRCA1 deficient HeLa SilenciX as well as in MDA-MB-436 compared to BRCA1 proficient control SilenciX and MCF7 cells. The interaction was synergistic [combination index= 0.5 (BRCA1 deficient HeLa SilneciX) and 0.6 (MDA-MB-436), supplementary figure S7B]. Increased cytotoxicity was associated with accumulation of DSBs (Figure 5C2 and 5D2), G2/M cell cycle arrest (Figure 5C3 and 5D3) and increased apoptosis (Figure 5C4 and 5D4).

DISCUSSION

We have shown, for the first time, that BRCA1 negative tumours have significantly lower expression of XRCC1 and Polβ, a feature that was also seen in BRCA1 deficient cancer cell lines. Patients with BRCA1 negative/ low XRCC1 or BRCA1 negative /low Polβ breast tumours also have worse breast cancer specific survival including in ER+ and ER- sub-groups. These new observations suggest that polβ/XRCC1 based sub-stratification may refine prognostication in BRCA1 deficient phenotypes. In addition, poor prognostic significance of pol β in a small cohort of germ-line BRCA1 mutated tumours is also consistent with a recent preclinical study linking BRCA1 and pol β in cancer cell line models (Masaoka et al., 2013). Additionally, at the mRNA level we conducted neural network analysis and demonstrated that the predominant *BRCA1* interactions were with genes involved in BER, NHEJ, NER and MMR inter-strand crosslink repair and transcription. To compliment clinical observations we DNA repair profiled BRCA1 proficient and deficient cell lines and also demonstrated impairment in BER, NHEJ, NER and MMR. A surprising finding in the current study was that several genes involved in DDR were down regulated in BRCA1 deficient HeLa as well as in breast cancer cells as one would anticipate that this would reduce survival in the absence of exogenous DNA damage. Moreover, as inhibition of BER (via PARP inhibition) is synthetically lethal in association with BRCA defects, we expected BRCA deficient cells to have compensatory up-regulation of BER pathway. In contrast we observed consistent down regulation of BER implying a complex regulation, including transcriptional regulation of BER by BRCA1. Although in BRCA deficient cells PARP1 may be up-regulated as a compensatory mechanism, in our cell line models we actually observed low expression of *PARP1* mRNA, *PARP2* mRNA and *PARP3* mRNA in BRCA1 deficient HeLa cells and low expression of *PARP1* mRNA and *PARP2* mRNA in MDA-MB-436 cells. Although these new

observations are intriguing, mechanism for down-regulation is currently unknown. However, we speculate that genomic instability in BRCA1 null cells may over a period of time, in the cell lines used in the current study, eventually lead to acquisition of new defects in other DNA repair pathways along with compensatory up-regulation of pro-survival pathways. In addition, recent studies implicating a role for BRCA1 in transcriptional regulation of BER (Saha et al., 2010) and NER(Hartman and Ford, 2002) suggests additional mechanisms may also operate for the observed genomic instability in BRCA1 deficient cells. The altered expression of XRCC1 and polβ shown here also concurs to a large extent with a recent study by De Summa et al. who investigated the expression of APE1, NTHL1, OGG1, PARP1, XRCC1 and miR17 in BRCA1/2 mutated and sporadic breast cancers (De Summa et al., 2014). Down-regulation of XRCC1, APE1 and NTHL1 was evident in that study. Interestingly overexpression of PARP1 and miR17 were observed in BRCA1 mutated tumours implying that they could be investigated as biomarker of BRCAness phenotype. In contrast, we observed PARP1 down regulation in BRCA1 deficient HeLa as well as in MDA-MB-436 breast cancer cell line in our study. Larger studies in human breast tumours are required to confirm these findings.

Although from preclinical studies we would expect DNA repair deficiency to be associated with chemosensitivity and improved survival in patient who received adjuvant chemotherapy, in the current clinical study we found that low BRCA1 or low BRCA1/low XRCC1 or low BRCA1/low Pol β was associated with poor survival. Our recent studies of DNA repair in breast cancer suggest that the relationship may be complex. In previous studies we found that low XRCC1 (Sultana et al., 2013) and low DNA pol β (Abdel-Fatah et al., 2014b) to be associated with poor survival. As BER deficiency could lead to accelerated accumulation of mutations resulting in a mutator phenotype (Bielas et al., 2006) that is associated with an aggressive biology, we speculate that the observed effect for XRCC1 and pol β may reflect

this phenomenon. On the other hand, high SMUG1 (Abdel-Fatah et al., 2013b) and high FEN1 (Abdel-Fatah et al., 2014c) was associated with poor survival in patients who have received adjuvant chemotherapy implying a DNA repair influenced predictive significance for SMUG1 and FEN1 in breast cancer.

We have demonstrated that a potential synthetic lethality relationship also exists between BRCA1 deficiency and blockade of ATM or DNA-PKcs in cells. A model for synthetic lethality is shown in supplementary figure S8. We have concluded synthetic lethality for the following reasons: a) BRCA1 deficient cells have increased sensitivity to ATM or DNA-PKcs inhibitors; b) upon ATM inhibitor treatment, BRCA1 deficient cells accumulate DSBs, exhibit G2/M cell cycle arrest and induction of apoptosis; and c) upon DNA-PKcs inhibitor treatment, BRCA1 deficient cells accumulate DSBs, exhibit G1 cell cycle arrest and induction of apoptosis. Interestingly, BRCA1 deficient cells also exhibit low mRNA levels of ATM and DNA-PKcs but are sensitive to ATM and DNA-PKcs inhibitors. The data suggest a dose dependent effect where although ATM and DNA levels are low the cells are able to tolerate genomic instability and survive. However, with additional functional inhibition through small molecule inhibition, pronounced accumulation of DSBs could lead to a synthetic lethality effect. Although phosphorylation of H2AX is ATM and DNA-Pkcs dependent, we observed accumulation of γH2AX foci in BRCA1 deficient cells incubated in medium containing ATM inhibitor or DNA-PKcs inhibitor for 48 hours. Whether reflects a timing issue are whether H2AX phosphorylation may be contributed by other factors such as activated ATR is unclear. To confirm DSB accumulation we also performed neutral COMET assay and have demonstrated DSB accumulation in BRCA1 deficient cells treated with ATM or DNA-PKcs inhibitor. Moreover the effects on cell cycle progression, although significant, appear to be modest. In the current study, the magnitude of synthetic lethality seen in BRCA1 deficient cells treated with ATM or DNA-PKcs inhibitor alone was not as

pronounced as that demonstrated for PARP inhibitors (Lord and Ashworth, 2008), we found that low dose cisplatin combination significantly enhanced synthetic lethality. Of note, the dose of cisplatin used in our study was 1/10th the dose used in previous preclinical studies investigating cisplatin sensitivity *in vitro* in BRCA1 deficient cells (Husain et al., 1998). At higher doses of cisplatin similar to the doses used by Husain et al, BRCA1 deficient cells remain highly sensitive to platinum therapy (data not shown). We speculate that low dose cisplatin treatment generates low levels of DSBs. In cells with proficient BRCA1 and BER, despite ATM or DNA-PKcs blockade, DSBs may be rapidly repaired in back-up DNA repair pathways and cells continue to survive. The back-up repair could operate at multiple levels including the complex interactions/overlap between HR, NHEJ, alternative NHEJ (B-NHEJ) (Chapman et al., 2012; Schipler and Iliakis, 2013), components of NER and ICL repair pathways. On the other hand, in cells with deficient BRCA1 and low BER, the associated pharmacological blockade with ATM or DNA-PKcs inhibitors may lead to DSB accumulation which beyond a threshold, may severely compromise back-up DNA repair machinery leading to DSB accumulation, cell cycle arrest and apoptosis. We have recently shown that XRCC1 deficient cells are cisplatin sensitive (Abdel-Fatah et al., 2013a) and ATM or DNA-PKcs inhibitors are also synthetically lethal in XRCC1 deficient cells (Sultana et al., 2013). Given the potential role of XRCC1 in B-NHEJ (Mladenov and Iliakis, 2011) we speculate that BRCA1 deficient cells that have low XRCC1 could also have compromised B-NHEJ in addition to BER resulting in increased genomic instability and enhanced synthetic lethality with cisplatin treatment seen in the current study. Moreover, ATM or DNA-PKcs modulation has previously been shown to enhance cisplatin cytotoxicity (Dejmek et al., 2009; Yoshida et al., 2008). Taken together, the data suggests that cisplatin combination may be more successful than ATM or DNA-PK monotherapy in BRCA1 negative tumours and would be consistent with a recent study showing enhancement of synthetic lethality with ABT-888

(PARP inhibitor) in combination with platinum chemotherapy in BRCA deficient cells (Clark et al., 2012).

REFERENCE

Abdel-Fatah, T., Sultana, R., Abbotts, R., Hawkes, C., Seedhouse, C., Chan, S.,Madhusudan, S., 2013a. Clinicopathological and functional significance of XRCC1 expression in ovarian cancer. International journal of cancer. Journal international du cancer 132, 2778-2786.

Abdel-Fatah, T. M., Albarakati, N., Bowell, L., Agarwal, D., Moseley, P., Hawkes, C., Ball, G., Chan, S., Ellis, I. O.,Madhusudan, S., 2013b. Single-strand selective monofunctional uracil-DNA glycosylase (SMUG1) deficiency is linked to aggressive breast cancer and predicts response to adjuvant therapy. Breast cancer research and treatment 142, 515-527.

Abdel-Fatah, T. M., Perry, C., Moseley, P., Johnson, K., Arora, A., Chan, S., Ellis, I. O.,Madhusudan, S., 2014a. Clinicopathological significance of human apurinic/apyrimidinic endonuclease 1 (APE1) expression in oestrogen-receptor-positive breast cancer. Breast cancer research and treatment 143, 411-421.

Abdel-Fatah, T. M., Russell, R., Agarwal, D., Moseley, P., Abayomi, M. A., Perry, C., Albarakati, N., Ball, G., Chan, S., Caldas, C., Ellis, I. O.,Madhusudan, S., 2014b. DNA polymerase beta deficiency is linked to aggressive breast cancer: A comprehensive analysis of gene copy number, mRNA and protein expression in multiple cohorts. Mol Oncol.

Abdel-Fatah, T. M., Russell, R., Albarakati, N., Maloney, D. J., Dorjsuren, D., Rueda, O. M., Moseley, P., Mohan, V., Sun, H., Abbotts, R., Mukherjee, A., Agarwal, D., Illuzzi, J. L., Jadhav, A., Simeonov, A., Ball, G., Chan, S., Caldas, C., Ellis, I. O., Wilson, D. M., 3rd,Madhusudan, S., 2014c. Genomic and protein expression analysis reveals flap endonuclease 1 (FEN1) as a key biomarker in breast and ovarian cancer. Mol Oncol.

Alli, E., Sharma, V. B., Sunderesakumar, P.,Ford, J. M., 2009. Defective repair of oxidative dna damage in triple-negative breast cancer confers sensitivity to inhibition of poly(ADP-ribose) polymerase. Cancer Res 69, 3589-3596.

Berenbaum, M. C., 1981. Criteria for analyzing interactions between biologically active agents. Adv Cancer Res 35, 269-335.

Bergh, J., Norberg, T., Sjogren, S., Lindgren, A.,Holmberg, L., 1995. Complete sequencing of the p53 gene provides prognostic information in breast cancer patients, particularly in relation to adjuvant systemic therapy and radiotherapy. Nature medicine 1, 1029-1034.

Bielas, J. H., Loeb, K. R., Rubin, B. P., True, L. D.,Loeb, L. A., 2006. Human cancers express a mutator phenotype. Proc Natl Acad Sci U S A 103, 18238-18242.

Caestecker, K. W.,Van de Walle, G. R., 2013. The role of BRCA1 in DNA double-strand repair: past and present. Experimental cell research 319, 575-587.

Chapman, J. R., Taylor, M. R.,Boulton, S. J., 2012. Playing the end game: DNA double-strand break repair pathway choice. Molecular cell 47, 497-510.

Clark, C. C., Weitzel, J. N.,O'Connor, T. R., 2012. Enhancement of synthetic lethality via combinations of ABT-888, a PARP inhibitor, and carboplatin in vitro and in vivo using BRCA1 and BRCA2 isogenic models. Molecular cancer therapeutics 11, 1948-1958.

Curtis, C., Shah, S. P., Chin, S. F., Turashvili, G., Rueda, O. M., Dunning, M. J., Speed, D., Lynch, A. G., Samarajiwa, S., Yuan, Y., Graf, S., Ha, G., Haffari, G., Bashashati, A., Russell, R., McKinney, S., Langerod, A., Green, A., Provenzano, E., Wishart, G., Pinder, S., Watson, P., Markowetz, F., Murphy, L.,

Ellis, I., Purushotham, A., Borresen-Dale, A. L., Brenton, J. D., Tavare, S., Caldas, C.,Aparicio, S., The genomic and transcriptomic architecture of 2,000 breast tumours reveals novel subgroups. Nature 486, 346-352.

De Summa, S., Pinto, R., Pilato, B., Sambiasi, D., Porcelli, L., Guida, G., Mattioli, E., Paradiso, A., Merla, G., Micale, L., De Nittis, P.,Tommasi, S., 2014. Expression of base excision repair key factors and miR17 in familial and sporadic breast cancer. Cell Death Dis 5, e1076.

Dejmek, J., Iglehart, J. D.,Lazaro, J. B., 2009. DNA-dependent protein kinase (DNA-PK)-dependent cisplatin-induced loss of nucleolar facilitator of chromatin transcription (FACT) and regulation of cisplatin sensitivity by DNA-PK and FACT. Molecular cancer research : MCR 7, 581-591.

Dianov, G. L.,Hubscher, U., 2013. Mammalian base excision repair: the forgotten archangel. Nucleic acids research 41, 3483-3490.

Durant, S. T.,Nickoloff, J. A., 2005. Good timing in the cell cycle for precise DNA repair by BRCA1. Cell cycle 4, 1216-1222.

Golding, S. E., Rosenberg, E., Valerie, N., Hussaini, I., Frigerio, M., Cockcroft, X. F., Chong, W. Y., Hummersone, M., Rigoreau, L., Menear, K. A., O'Connor, M. J., Povirk, L. F., van Meter, T.,Valerie, K., 2009. Improved ATM kinase inhibitor KU-60019 radiosensitizes glioma cells, compromises insulin, AKT and ERK prosurvival signaling, and inhibits migration and invasion. Molecular cancer therapeutics 8, 2894-2902.

Hartman, A. R.,Ford, J. M., 2002. BRCA1 induces DNA damage recognition factors and enhances nucleotide excision repair. Nature genetics 32, 180-184.

Hickson, I., Zhao, Y., Richardson, C. J., Green, S. J., Martin, N. M., Orr, A. I., Reaper, P. M., Jackson, S. P., Curtin, N. J.,Smith, G. C., 2004. Identification and characterization of a novel and specific inhibitor of the ataxia-telangiectasia mutated kinase ATM. Cancer Res 64, 9152-9159.

Hill, R.,Lee, P. W., 2010. The DNA-dependent protein kinase (DNA-PK): More than just a case of making ends meet? Cell cycle 9, 3460-3469.

Hsu, N. C., Huang, Y. F., Yokoyama, K. K., Chu, P. Y., Chen, F. M.,Hou, M. F., 2013. Methylation of BRCA1 promoter region is associated with unfavorable prognosis in women with early-stage breast cancer. PloS one 8, e56256.

Huen, M. S., Sy, S. M.,Chen, J., 2010. BRCA1 and its toolbox for the maintenance of genome integrity. Nature reviews. Molecular cell biology 11, 138-148.

Husain, A., He, G., Venkatraman, E. S.,Spriggs, D. R., 1998. BRCA1 up-regulation is associated with repair-mediated resistance to cis-diamminedichloroplatinum(II). Cancer Res 58, 1120-1123.

Lancashire, L. J., Powe, D. G., Reis-Filho, J. S., Rakha, E., Lemetre, C., Weigelt, B., Abdel-Fatah, T. M., Green, A. R., Mukta, R., Blamey, R., Paish, E. C., Rees, R. C., Ellis, I. O.,Ball, G. R., 2010. A validated gene expression profile for detecting clinical outcome in breast cancer using artificial neural networks. Breast cancer research and treatment 120, 83-93.

Langelier, M. F.,Pascal, J. M., 2013. PARP-1 mechanism for coupling DNA damage detection to poly(ADP-ribose) synthesis. Current opinion in structural biology 23, 134-143.

Lee, J. H., Goodarzi, A. A., Jeggo, P. A.,Paull, T. T., 2010. 53BP1 promotes ATM activity through direct interactions with the MRN complex. The EMBO journal 29, 574-585.

Lee, J. H.,Paull, T. T., 2007. Activation and regulation of ATM kinase activity in response to DNA double-strand breaks. Oncogene 26, 7741-7748.

Lemetre, C., . et al, 2009. Artificial Neural Network Based algorithm for Biomolecular Interaction Modeling. "Bio-Inspired Systems: Computational and Ambient Intellegence. Lecture Notes in Computer Science 5517, 877-885.

Lord, C. J.,Ashworth, A., 2008. Targeted therapy for cancer using PARP inhibitors. Current opinion in pharmacology 8, 363-369.

Masaoka, A., Gassman, N. R., Horton, J. K., Kedar, P. S., Witt, K. L., Hobbs, C. A., Kissling, G. E., Tano, K., Asagoshi, K.,Wilson, S. H., 2013. Interaction between DNA Polymerase beta and BRCA1. PloS one 8, e66801.

Mladenov, E.,Iliakis, G., 2011. Induction and repair of DNA double strand breaks: the increasing spectrum of non-homologous end joining pathways. Mutat Res 711, 61-72.

Nutley, B. P., Smith, N. F., Hayes, A., Kelland, L. R., Brunton, L., Golding, B. T., Smith, G. C., Martin, N. M., Workman, P.,Raynaud, F. I., 2005. Preclinical pharmacokinetics and metabolism of a novel prototype DNA-PK inhibitor NU7026. British journal of cancer 93, 1011-1018.

O'Donovan, P. J.,Livingston, D. M., 2010. BRCA1 and BRCA2: breast/ovarian cancer susceptibility gene products and participants in DNA double-strand break repair. Carcinogenesis 31, 961-967.

Pawitan, Y., Bjohle, J., Amler, L., Borg, A. L., Egyhazi, S., Hall, P., Han, X., Holmberg, L., Huang, F., Klaar, S., Liu, E. T., Miller, L., Nordgren, H., Ploner, A., Sandelin, K., Shaw, P. M., Smeds, J., Skoog, L., Wedren, S.,Bergh, J., 2005. Gene expression profiling spares early breast cancer patients from adjuvant therapy: derived and validated in two population-based cohorts. Breast cancer research : BCR 7, R953-964.

Saha, T., Rih, J. K., Roy, R., Ballal, R.,Rosen, E. M., 2010. Transcriptional regulation of the base excision repair pathway by BRCA1. The Journal of biological chemistry 285, 19092-19105.

Schipler, A.,Iliakis, G., 2013. DNA double-strand-break complexity levels and their possible contributions to the probability for error-prone processing and repair pathway choice. Nucleic acids research 41, 7589-7605.

Shekh, K., Khan, S., Jena, G., Kansara, B. R.,Kushwaha, S., 2014. 3-Aminobenzamide--a PARP inhibitor enhances the sensitivity of peripheral blood micronucleus and comet assays in mice. Toxicol Mech Methods 24, 332-341.

Shiloh, Y.,Ziv, Y., 2013. The ATM protein kinase: regulating the cellular response to genotoxic stress, and more. Nature reviews. Molecular cell biology 14, 197-210.

Silver, D. P.,Livingston, D. M., 2012. Mechanisms of BRCA1 tumor suppression. Cancer discovery 2, 679-684.

Smoot, M. E., Ono, K., Ruscheinski, J., Wang, P. L.,Ideker, T., 2011. Cytoscape 2.8: new features for data integration and network visualization. Bioinformatics 27, 431-432.

Smyth, G. K., 2004. Linear models and empirical bayes methods for assessing differential expression in microarray experiments. Statistical applications in genetics and molecular biology 3, Article3.
Sultana, R., Abdel-Fatah, T., Abbotts, R., Hawkes, C., Albarakati, N., Seedhouse, C., Ball, G., Chan, S., Rakha, E. A., Ellis, I. O.,Madhusudan, S., 2013. Targeting XRCC1 deficiency in breast cancer for personalized therapy. Cancer Res 73, 1621-1634.

Tassone, P., Di Martino, M. T., Ventura, M., Pietragalla, A., Cucinotto, I., Calimeri, T., Bulotta, A., Neri, P., Caraglia, M.,Tagliaferri, P., 2009. Loss of BRCA1 function increases the antitumor activity of cisplatin against human breast cancer xenografts in vivo. Cancer biology & therapy 8, 648-653.

Tavecchio, M., Munck, J. M., Cano, C., Newell, D. R.,Curtin, N. J., 2012. Further characterisation of the cellular activity of the DNA-PK inhibitor, NU7441, reveals potential cross-talk with homologous recombination. Cancer chemotherapy and pharmacology 69, 155-164.

Tibshirani, R., Hastie, T., Narasimhan, B.,Chu, G., 2002. Diagnosis of multiple cancer types by shrunken centroids of gene expression. Proc Natl Acad Sci U S A 99, 6567-6572.

Turner, N., Tutt, A.,Ashworth, A., 2004. Hallmarks of 'BRCAness' in sporadic cancers. Nature reviews. Cancer 4, 814-819.

Wu, L., Wang, F., Xu, R., Zhang, S., Peng, X., Feng, Y., Wang, J.,Lu, C., 2013. Promoter methylation of BRCA1 in the prognosis of breast cancer: a meta-analysis. Breast cancer research and treatment 142, 619-627.

Yoshida, K., Ozaki, T., Furuya, K., Nakanishi, M., Kikuchi, H., Yamamoto, H., Ono, S., Koda, T., Omura, K.,Nakagawara, A., 2008. ATM-dependent nuclear accumulation of IKK-alpha plays an important role in the regulation of p73-mediated apoptosis in response to cisplatin. Oncogene 27, 1183-1188.

Table 1. Multivariate analysis in BRCA1 negative sporadic breast cancers (Nottingham cohort).

Variables	Multivariate Model		
	Exp (B)	**CI 95%**	**P Value**
Pol beta expression	0.810	0.666-0.986	**0.036**
XRCC1 expression	0.831	0.731-0.945	**0.005**
Tumour stage	3.088	2.414-3.950	**<0.0001**
ER receptor status	0.522	0.328-0.833	**0.006**
Chemotherapy status	0.522	0.356-0.764	**0.001**

FIGURE LEGENDS

Figure 1. BRCA1 and BER protein expression in human breast cancer. **A.** Microphotographs of BRCA1 negative, BRCA1 positive, polβ positive and XRCC1 positive breast cancers. **B.** Kaplan Meier curves showing breast cancer specific survival (BCSS) in patients based on BRCA1 expression status. **C1.** Kaplan Meier curves showing breast cancer specific survival (BCSS) in patients with BRCA1 negative tumours based on XRCC1 expression status. **C2.** Kaplan Meier curves showing breast cancer specific survival (BCSS) in patients with BRCA1 negative/ER negative tumours based on XRCC1 expression status. **C3.** Kaplan Meier curves showing breast cancer specific survival (BCSS) in patients with BRCA1 negative/ER positive tumours based on XRCC1 expression status. **D1.** Kaplan Meier curves showing breast cancer specific survival (BCSS) in patients with BRCA1 negative tumours based on polβ expression status. **D2.** Kaplan Meier curves showing breast cancer specific survival (BCSS) in patients with BRCA1 negative/ER negative tumours based on polβ expression status. **D3.** Kaplan Meier curves showing breast cancer specific survival (BCSS) in patients with BRCA1 negative/ER positive tumours based on polβ expression status.

Figure 2. A. Kaplan Meier curves showing overall survival in patients with germ-line BRCA1mutated tumours based on polβ protein expression status. **B1.** Kaplan Meier curves showing breast cancer specific survival (BCSS) in patients based on BRCA1 mRNA expression status in ER+ breast cancer (METABRIC cohort). **B2.** Kaplan Meier curves showing breast cancer specific survival (BCSS) in patients with BRCA1 mRNA low/ER+ who received adjuvant endocrine therapy based on polβ mRNA status (METABRIC cohort). **B3.** Kaplan Meier curves showing breast cancer specific survival (BCSS) in patients with BRCA1 mRNA low/ER+ who received adjuvant endocrine therapy based on XRCC1 mRNA

status (METABRIC cohort). **C1.** Kaplan Meier curves showing breast cancer specific survival (BCSS) in patients with BRCA1 mRNA low/ER- who received adjuvant chemotherapy based on polβ mRNA status (METABRIC cohort). **C2.** Kaplan Meier curves showing breast cancer specific survival (BCSS) in patients with BRCA1 mRNA low/ER- who received adjuvant chemotherapy based on XRCC1 mRNA status (METABRIC cohort). **D.** The neural network illustrates the top genes that interact with BRCA1 and other DNA repair genes. In addition, the artificial neural network also reveals how these top genes interact with each other. Top pair-wise interactions for gene probe markers associated with BRCA1 expression and the DNA repair process in 249 breast cancers is shown here. Each gene probe is represented by a node and the interaction weight between them as an edge, the width being defined by the magnitude of the weight. Interactions are directed from a source gene to a target gene as indicated by arrows. Red interactions indicate an excitatory interaction and blue indicates an inhibitory interaction. Highly linked genes represent hubs that are indicated to be highly influential or highly regulated in the BRCA1-DNA repair system. See supplementary data x for the biological functions of individual genes.

Figure 3. DNA repair expression in BRCA1 deficient and BRCA1 proficient cells **A1.** Representative Western blots of BRCA1, XRCC1 and polβ in BRCA1 deficient HeLa SilenciX cells and control BRCA1 proficient HeLa SilenciX cells. **A2.** Protein quantification in BRCA1 deficient HeLa SilenciX cells and control BRCA1 proficient HeLa SilenciX cells are shown here. The Figure shows fold change in BRCA1 deficient cells in comparison to BRCA1 proficient cells. **A3.** mRNA expression in BRCA1 deficient HeLa SilenciX cells and control BRCA1 proficient HeLa SilenciX cells are shown here. The Figure shows fold change in BRCA1 deficient cells in comparison to BRCA1 proficient cells. **B1.** Representative Western blots of BRCA1, XRCC1 and polβ in BRCA1 deficient MDA-MB-436 cells and BRCA1 proficient MCF7 cells. **B2.** Protein quantification in MDA-

MB-436 cells and MCF7 cells are shown here. The Figure shows fold change in BRCA1 deficient cells in comparison to BRCA1 proficient cells. **B3.** mRNA expression in MDA-MB-436 cells and MCF7 cells are shown here. The Figure shows fold change in BRCA1 deficient cells in comparison to BRCA proficient cells. **C.** Scatter plots indicate up- and down-regulation of DNA repair mRNA expression in BRCA1 deficient HeLa SilenciX cells compared to BRCA1 proficient HeLa SilenciX cells. **D.** Scatter plots indicate up- and down-regulation of DNA repair mRNA expression in MDA-MB-436 cells compared to MCF7 cells are shown here. Green circles show genes that are two-fold or more down-regulated. See also results section and supplementary table S16 and S17.

Figure 4. ATM inhibitors in BRCA1 deficient and BRCA1 proficient cells. **A1.** Clonogenic survival assays in BRCA1 deficient HeLa SilenciX cells and control BRCA1 proficient HeLa SilenciX cells treated with KU55933. **A2.** yH2AX immunohistochemistry in BRCA1 deficient HeLa SilenciX cells and control BRCA1 proficient HeLa SilenciX cells treated with KU55933. **A3.** FACS analysis in BRCA1 deficient HeLa SilenciX cells and control BRCA1 proficient HeLa SilenciX cells treated with KU55933. **A4.** Annexin V flow cytometric analysis in BRCA1 deficient HeLa SilenciX cells and control BRCA1 proficient HeLa SilenciX cells treated with KU55933.**B1.** Clonogenic survival assays in MDA-MB-436 and MCF7 cells treated with KU55933. **B2.** yH2AX immunohistochemistry in MDA-MB-436 and MCF7 cells treated with KU55933. **B3.** FACS analysis in MDA-MB-436 and MCF7 cells treated with KU55933. **B4.** Annexin V flow cytometric analysis in MDA-MB-436 and MCF7 cells treated with KU55933. Inhibitors were added at the indicated concentrations (see methods for details). **C1.** Clonogenic survival assays in BRCA1 deficient HeLa SilenciX cells and control BRCA1 proficient HeLa SilenciX cells treated with cisplatin alone or in combination with KU55933. **C2.** yH2AX immunohistochemistry in BRCA1 deficient HeLa SilenciX cells and control BRCA1 proficient HeLa SilenciX cells treated with cisplatin alone

or in combination with KU55933. **C3.** FACS analysis in BRCA1 deficient HeLa SilenciX cells and control BRCA1 proficient HeLa SilenciX cells treated with cisplatin alone or in combination with KU55933. **C4.** Annexin V flow cytometric analysis in BRCA1 deficient HeLa SilenciX cells and control BRCA1 proficient HeLa SilenciX cells treated with cisplatin alone or in combination with KU55933. **D1.** Clonogenic survival assays in MDA-MB-436 and MCF7 cells treated with cisplatin alone or in combination with KU55933. **D2.** yH2AX immunohistochemistry in MDA-MB-436 and MCF7 cells treated with cisplatin alone or in combination with KU55933. **D3.** FACS analysis in MDA-MB-436 and MCF7 cells treated with cisplatin alone or in combination with KU55933. **D4.** Annexin V flow cytometric analysis in MDA-MB-436 and MCF7 cells treated with cisplatin alone or in combination with KU55933. * $p<0.05$, ** $p<0.01$.

Figure 5. DNA-PKcs inhibitors in BRCA1 deficient and BRCA1 proficient cells. **A1.** Clonogenic survival assays in BRCA1 deficient HeLa SilenciX cells and control BRCA1 proficient HeLa SilenciX cells treated with NU7441. **A2.** yH2AX immunohistochemistry in BRCA1 deficient HeLa SilenciX cells and control BRCA1 proficient HeLa SilenciX cells treated with NU7441. **A3.** FACS analysis in BRCA1 deficient HeLa SilenciX cells and control BRCA1 proficient HeLa SilenciX cells treated with NU7441. **A4.** Annexin V flow cytometric analysis in BRCA1 deficient HeLa SilenciX cells and control BRCA1 proficient HeLa SilenciX cells treated with NU7441.**B1.** Clonogenic survival assays in MDA-MB-436 and MCF7 cells treated with NU7441. **B2.** yH2AX immunohistochemistry in MDA-MB-436 and MCF7 cells treated with NU7441. **B3.** FACS analysis in MDA-MB-436 and MCF7 cells treated with NU7441. **B4.** Annexin V flow cytometric analysis in MDA-MB-436 and MCF7 cells treated with NU7441. Inhibitors were added at the indicated concentrations (see methods for details). **C1.** Clonogenic survival assays in BRCA1 deficient HeLa SilenciX cells and control BRCA1 proficient HeLa SilenciX cells treated with cisplatin alone or in

combination with NU7441. **C2.** yH2AX immunohistochemistry in BRCA1 deficient HeLa SilenciX cells and control BRCA1 proficient HeLa SilenciX cells treated with cisplatin alone or in combination with NU7441. **C3.** FACS analysis in BRCA1 deficient HeLa SilenciX cells and control BRCA1 proficient HeLa SilenciX cells treated with cisplatin alone or in combination with NU7441. **C4.** Annexin V flow cytometric analysis in BRCA1 deficient HeLa SilenciX cells and control BRCA1 proficient HeLa SilenciX cells treated with cisplatin alone or in combination with NU7441. **D1.** Clonogenic survival assays in MDA-MB-436 and MCF7 cells treated with cisplatin alone or in combination with NU7441. **D2.** yH2AX immunohistochemistry in MDA-MB-436 and MCF7 cells treated with cisplatin alone or in combination with NU7441. **D3.** FACS analysis in MDA-MB-436 and MCF7 cells treated with cisplatin alone or in combination with NU7441. **D4.** Annexin V flow cytometric analysis in MDA-MB-436 and MCF7 cells treated with cisplatin alone or in combination with NU7441. * $p<0.05$, ** $p<0.01$.

Figure 1

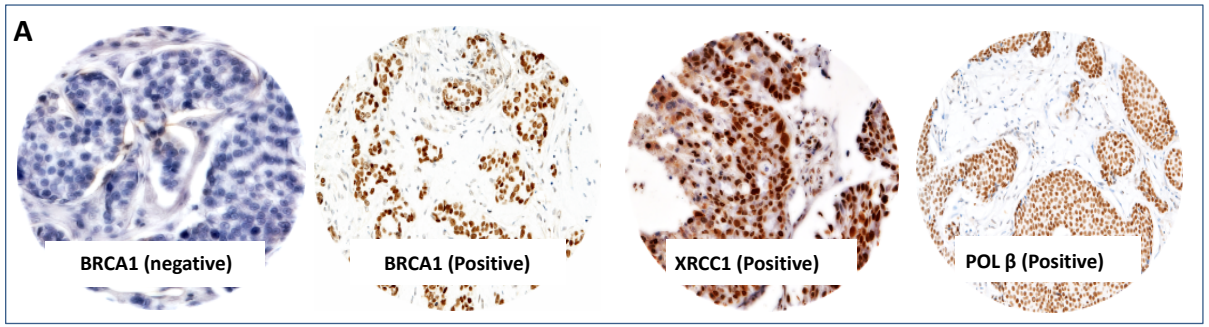
A
BRCA1 (negative)
BRCA1 (Positive)
XRCC1 (Positive)
POL β (Positive)

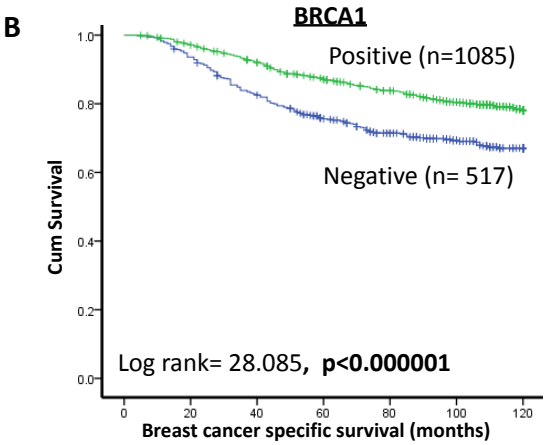
B
BRCA1
Positive (n=1085)
Negative (n= 517)
Cum Survival
Log rank= 28.085, p<0.000001
Breast cancer specific survival (months)

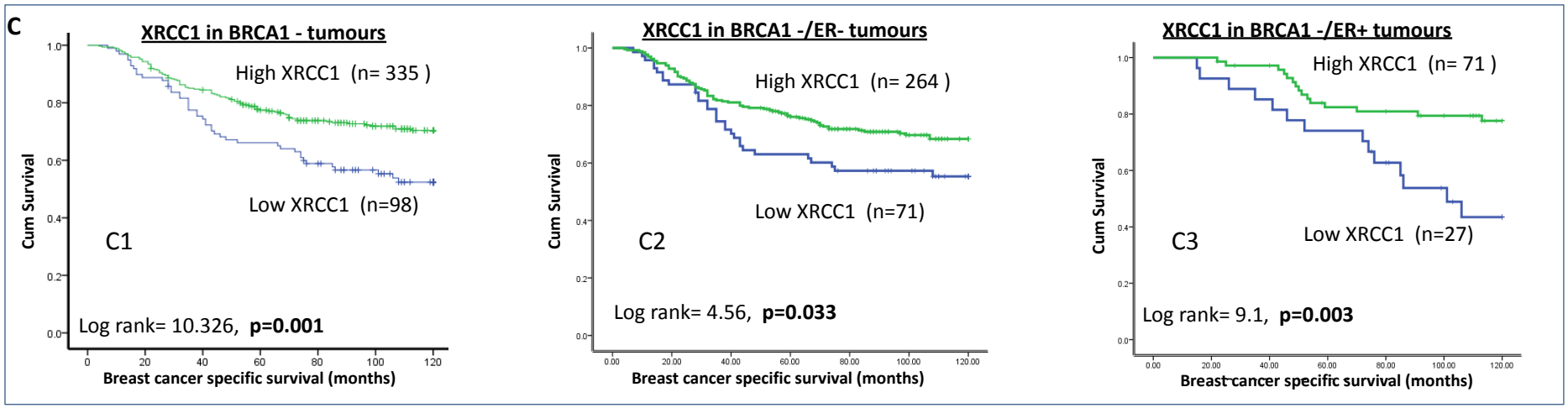
C
XRCC1 in BRCA1 - tumours
High XRCC1 (n= 335)
Low XRCC1 (n=98)
C1
Log rank= 10.326, p=0.001
XRCC1 in BRCA1 -/ER- tumours
High XRCC1 (n= 264)
Low XRCC1 (n=71)
C2
Log rank= 4.56, p=0.033
XRCC1 in BRCA1 -/ER+ tumours
High XRCC1 (n= 71)
Low XRCC1 (n=27)
C3
Log rank= 9.1, p=0.003
Cum Survival
Breast cancer specific survival (months)

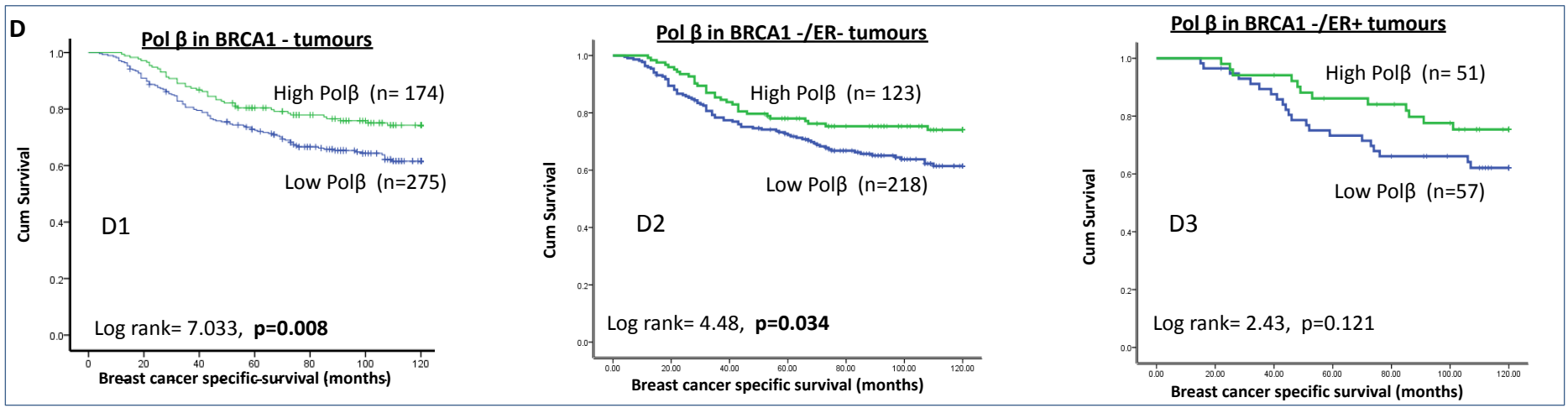
D
Pol β in BRCA1 - tumours
High Polβ (n= 174)
Low Polβ (n=275)
D1
Log rank= 7.033, p=0.008
Pol β in BRCA1 -/ER- tumours
High Polβ (n= 123)
Low Polβ (n=218)
D2
Log rank= 4.48, p=0.034
Pol β in BRCA1 -/ER+ tumours
High Polβ (n= 51)
Low Polβ (n=57)
D3
Log rank= 2.43, p=0.121
Cum Survival
Breast cancer specific survival (months)

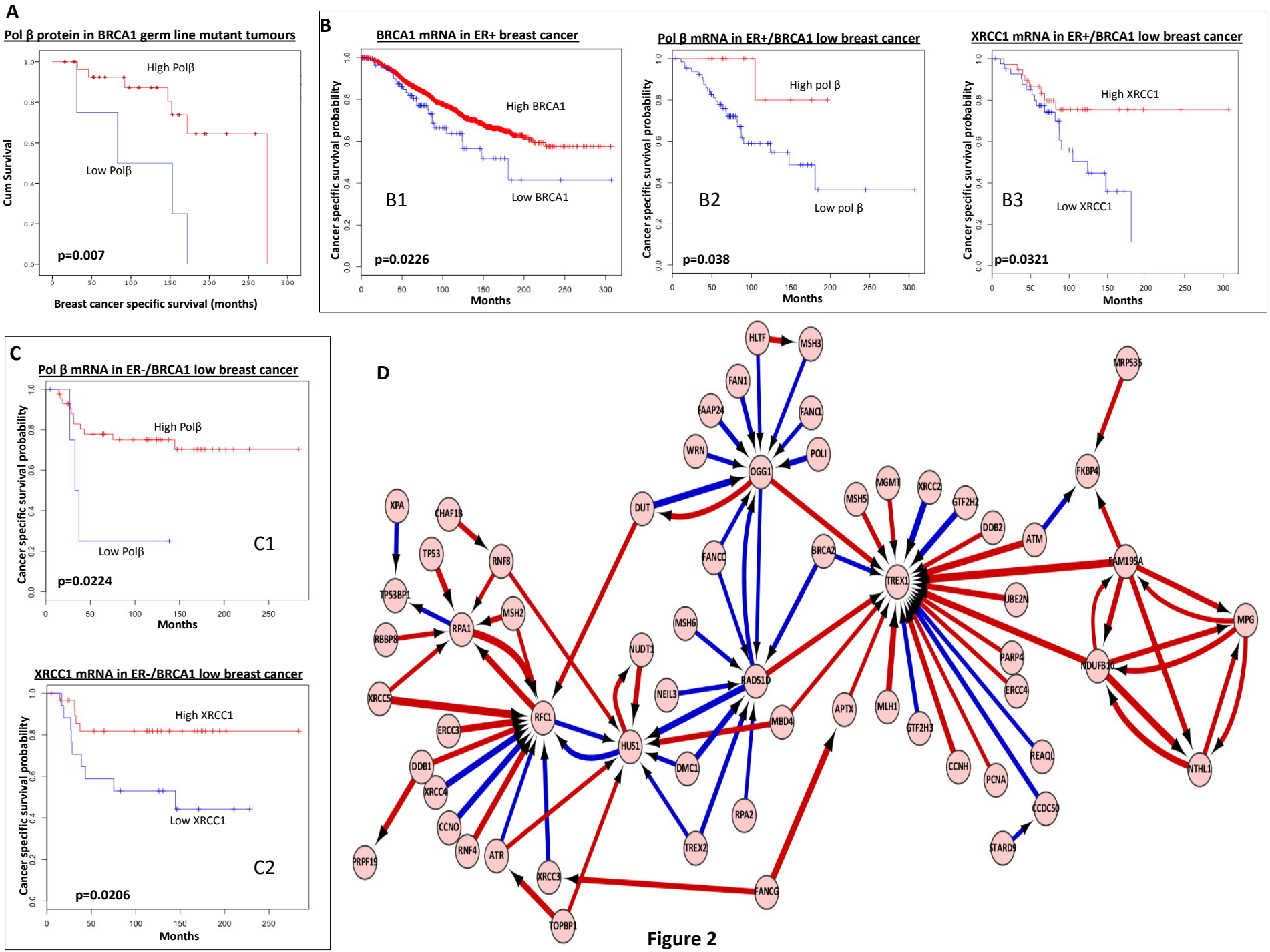
A
Pol β protein in BRCA1 germ line mutant tumours
High Polβ
Low Polβ
p=0.007
Cum Survival
Breast cancer specific survival (months)
B
BRCA1 mRNA in ER+ breast cancer
High BRCA1
Low BRCA1
B1
p=0.0226
Pol β mRNA in ER+/BRCA1 low breast cancer
High pol β
Low pol β
B2
p=0.038
XRCC1 mRNA in ER+/BRCA1 low breast cancer
High XRCC1
Low XRCC1
B3
p=0.0321
Cancer specific survival probability
Months
C
Pol β mRNA in ER-/BRCA1 low breast cancer
High Polβ
Low Polβ
C1
p=0.0224
XRCC1 mRNA in ER-/BRCA1 low breast cancer
High XRCC1
Low XRCC1
C2
p=0.0206
D
HLTF
MSH3
FAN1
FAAP24
FANCL
WRN
POLI
OGG1
DUT
XPA
CHAF1B
TP53
RNF8
TP53BP1
RPA1
MSH2
RBBP8
XRCC5
RFC1
ERCC3
DDB1
XRCC4
CCNO
RNF4
ATR
PRPF19
XRCC3
TOPBP1
NUDT1
HUS1
NEIL3
MSH6
RAD51D
MBD4
DMC1
RPA2
TREX2
FANCG
FANCC
BRCA2
MSH5
MGMT
XRCC2
GTF2H2
DDB2
ATM
TREX1
UBE2N
PARP4
ERCC4
APTX
MLH1
GTF2H3
CCNH
PCNA
REAQL
CCDC50
STARD9
MRPS35
FKBP4
FAM195A
MPG
NDUFB10
NTHL1

Figure 2

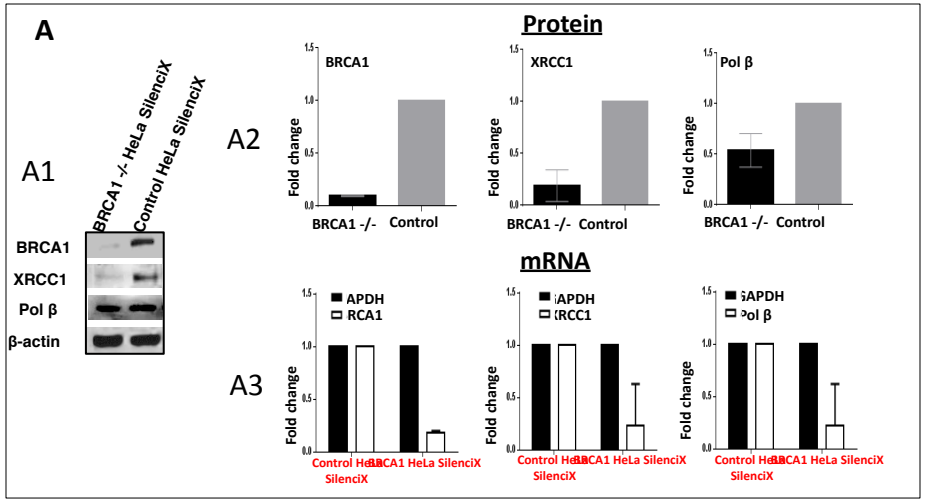
A
A1
BRCA1 -/- HeLa SilenciX
Control HeLa SilenciX
BRCA1
XRCC1
Pol β
β-actin
A2
Protein
BRCA1
XRCC1
Pol β
Fold change
BRCA1 -/- Control
A3
mRNA
APDH
RCA1
RRCC1
Pol β
Control HeLa SilenciX
BRCA1 HeLa SilenciX

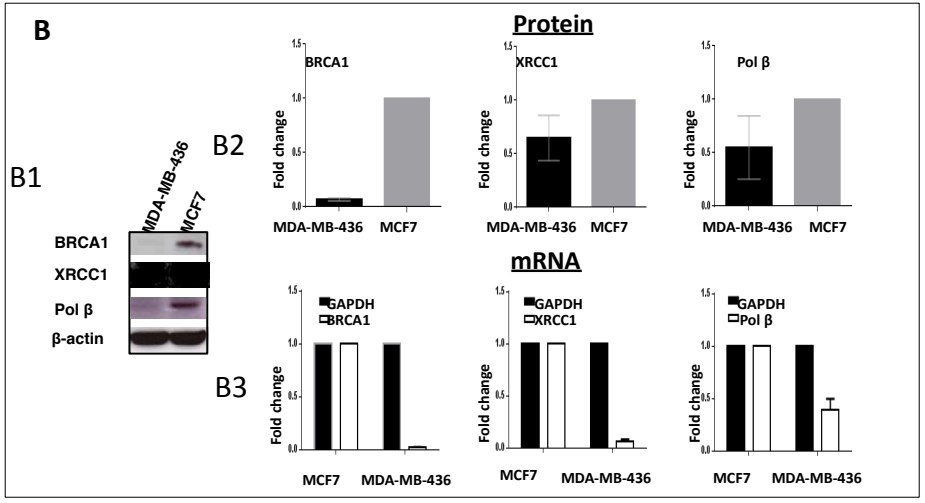
B
B1
MDA-MB-436
MCF7
BRCA1
XRCC1
Pol β
β-actin
B2
Protein
BRCA1
XRCC1
Pol β
Fold change
MDA-MB-436
MCF7
B3
mRNA
GAPDH
BRCA1
XRCC1
Pol β
MCF7
MDA-MB-436

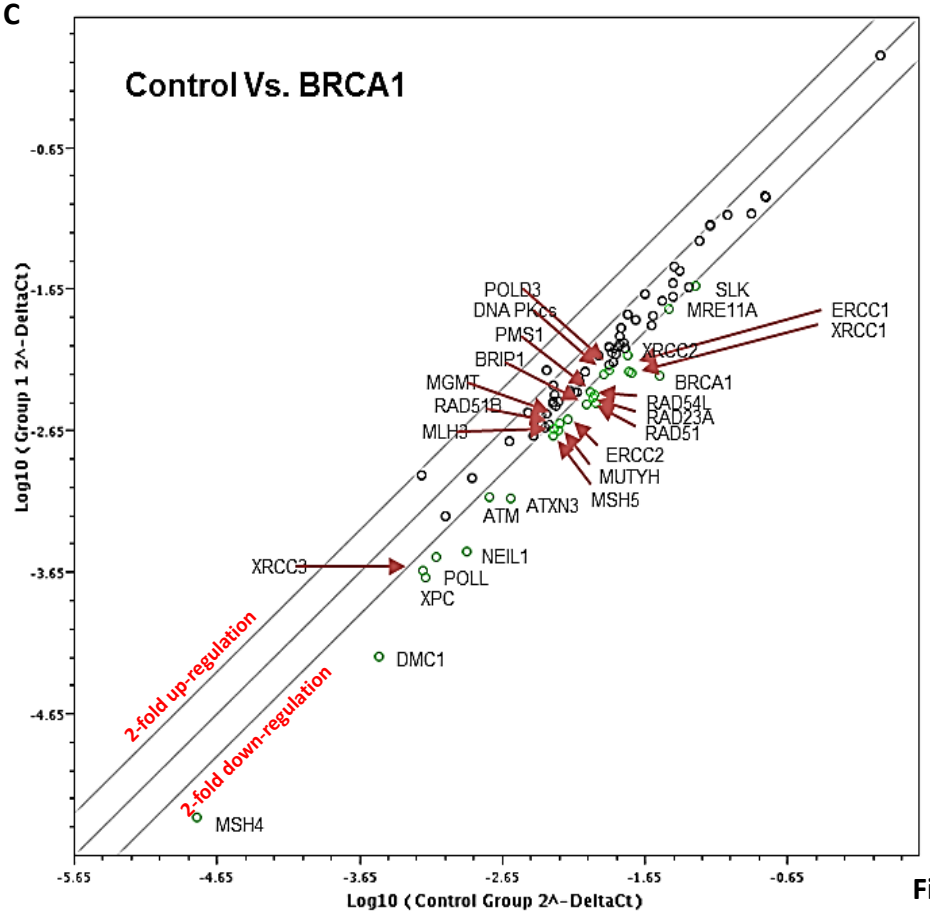
C
Control Vs. BRCA1
Log10 (Group 1 2^-DeltaCt)
Log10 (Control Group 2^-DeltaCt)
-0.65
-1.65
-2.65
-3.65
-4.65
-5.65
POLD3
DNA PKcs
PMS1
BRIP1
MGMT
RAD51B
MLH3
SLK
MRE11A
ERCC1
XRCC1
XRCC2
BRCA1
RAD54L
RAD23A
RAD51
ERCC2
MUTYH
MSH5
ATM
ATXN3
XRCC3
NEIL1
POLL
XPC
DMC1
MSH4
2-fold up-regulation
2-fold down-regulation

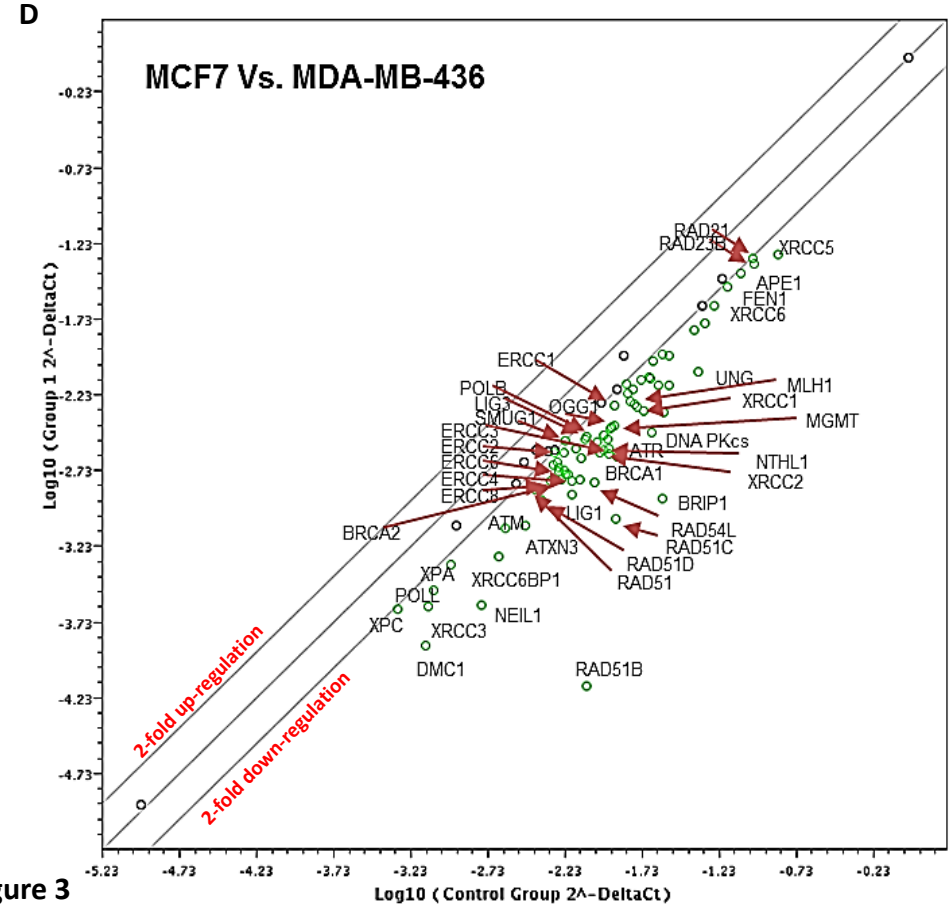
D
MCF7 Vs. MDA-MB-436
Log10 (Group 1 2^-DeltaCt)
Log10 (Control Group 2^-DeltaCt)
-0.23
-0.73
-1.23
-1.73
-2.23
-2.73
-3.23
-3.73
-4.23
-4.73
-5.23
RAD21
RAD23B
XRCC5
APE1
FEN1
XRCC6
ERCC1
POLB
LIG3
SMUG1
OGG1
UNG
MLH1
XRCC1
MGMT
DNA PKcs
ATR
BRCA1
NTHL1
XRCC2
BRIP1
LIG1
ATM
ATXN3
BRCA2
RAD54L
RAD51C
RAD51D
RAD51
XPA
XRCC6BP1
POLL
XPC
NEIL1
XRCC3
DMC1
RAD51B
2-fold up-regulation
2-fold down-regulation

Figure 3

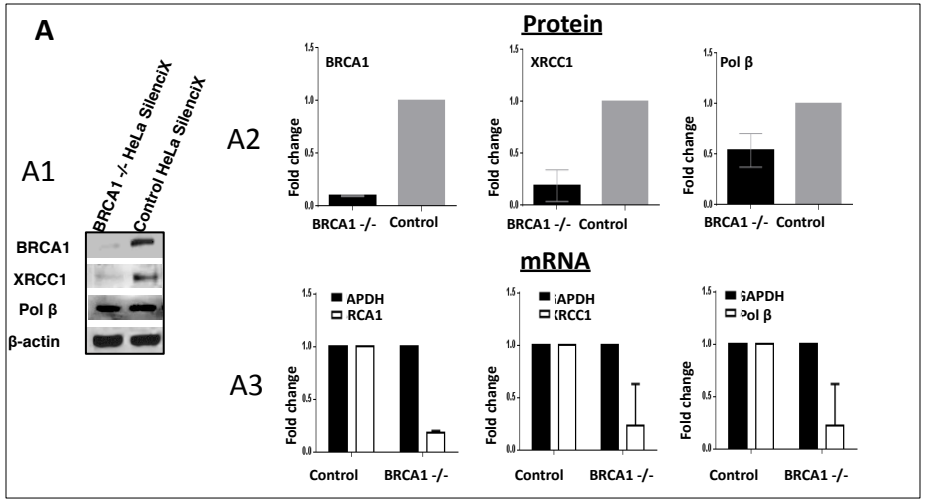
A
A1
BRCA1 -/- HeLa SilenciX
Control HeLa SilenciX
BRCA1
XRCC1
Pol β
β-actin
A2
Protein
BRCA1
XRCC1
Pol β
Fold change
BRCA1 -/- Control
A3
mRNA
APDH
RCA1
RRCC1
Pol β
Control BRCA1 -/-

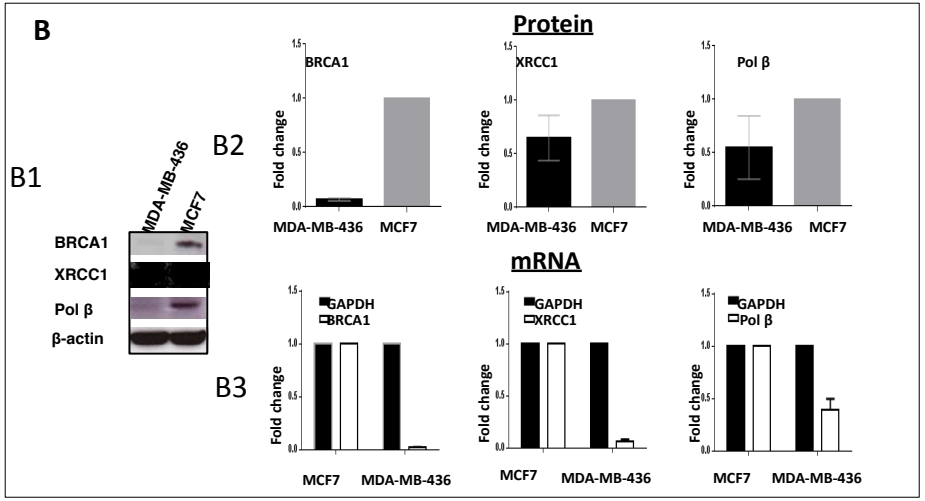
B
B1
MDA-MB-436
MCF7
BRCA1
XRCC1
Pol β
β-actin
B2
Protein
BRCA1
XRCC1
Pol β
Fold change
MDA-MB-436 MCF7
B3
mRNA
GAPDH
BRCA1
XRCC1
Pol β
MCF7 MDA-MB-436

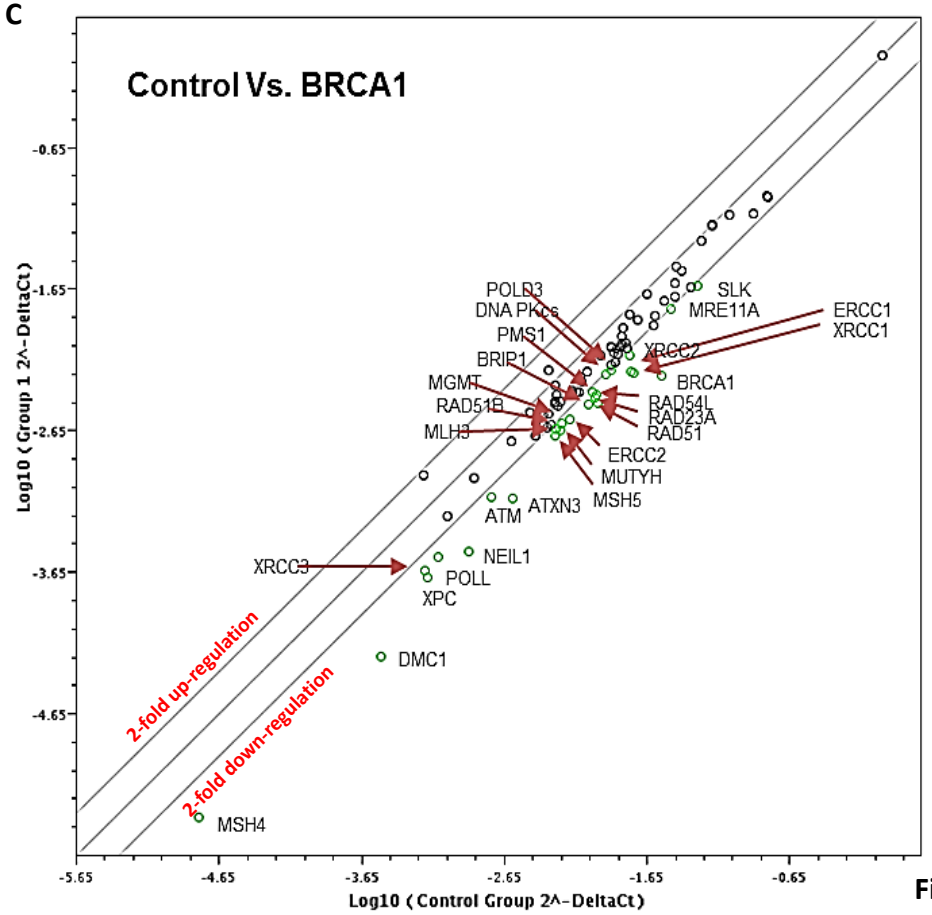
C
Control Vs. BRCA1
Log10 (Group 1 2^-DeltaCt)
Log10 (Control Group 2^-DeltaCt)
-0.65
-1.65
-2.65
-3.65
-4.65
-5.65
POLD3
DNA PKcs
PMS1
BRIP1
MGMT
RAD51B
MLH3
SLK
MRE11A
ERCC1
XRCC1
XRCC2
BRCA1
RAD54L
RAD23A
RAD51
ERCC2
MUTYH
MSH5
ATM
ATXN3
NEIL1
POLL
XPC
XRCC3
DMC1
MSH4
2-fold up-regulation
2-fold down-regulation

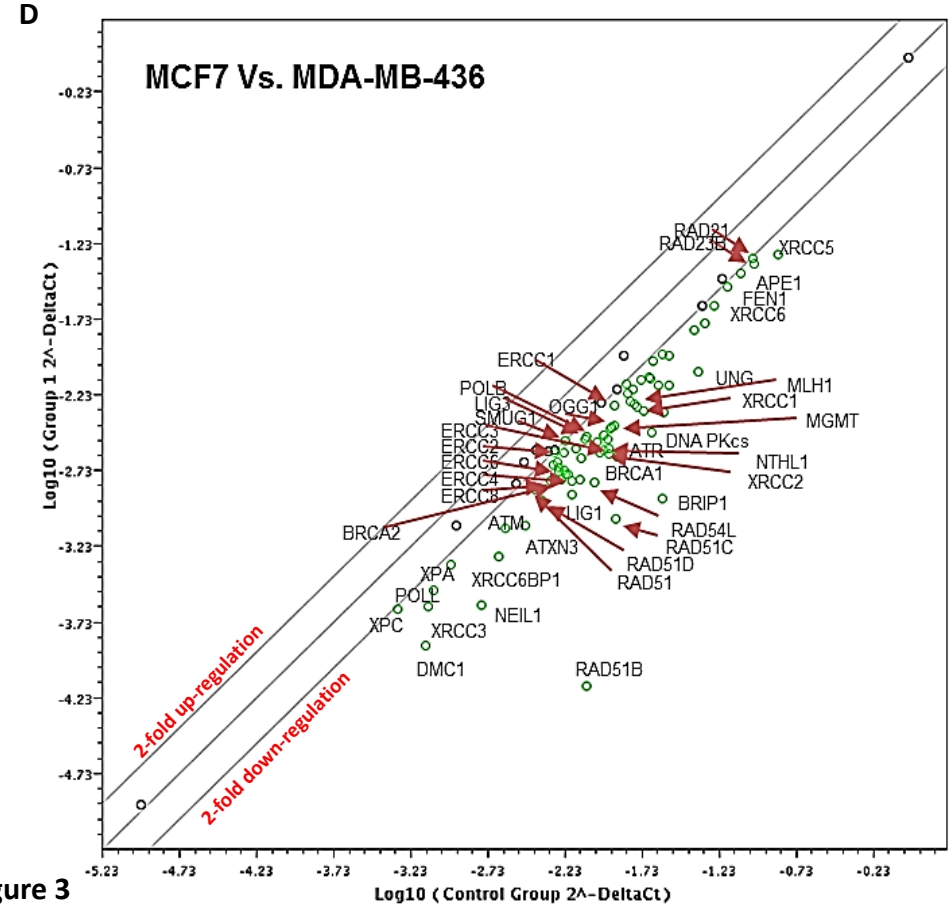
D
MCF7 Vs. MDA-MB-436
Log10 (Group 1 2^-DeltaCt)
Log10 (Control Group 2^-DeltaCt)
-0.23
-0.73
-1.23
-1.73
-2.23
-2.73
-3.23
-3.73
-4.23
-4.73
-5.23
RAD21
RAD23B
XRCC5
APE1
FEN1
XRCC6
ERCC1
POLB
LIG3
SMUG1
OGG1
UNG
MLH1
XRCC1
MGMT
DNA PKcs
ATR
BRCA1
NTHL1
XRCC2
BRIP1
LIG1
ATM
ATXN3
BRCA2
RAD54L
RAD51C
RAD51D
RAD51
XPA
XRCC6BP1
POLL
XPC
NEIL1
XRCC3
DMC1
RAD51B
2-fold up-regulation
2-fold down-regulation

Figure 3

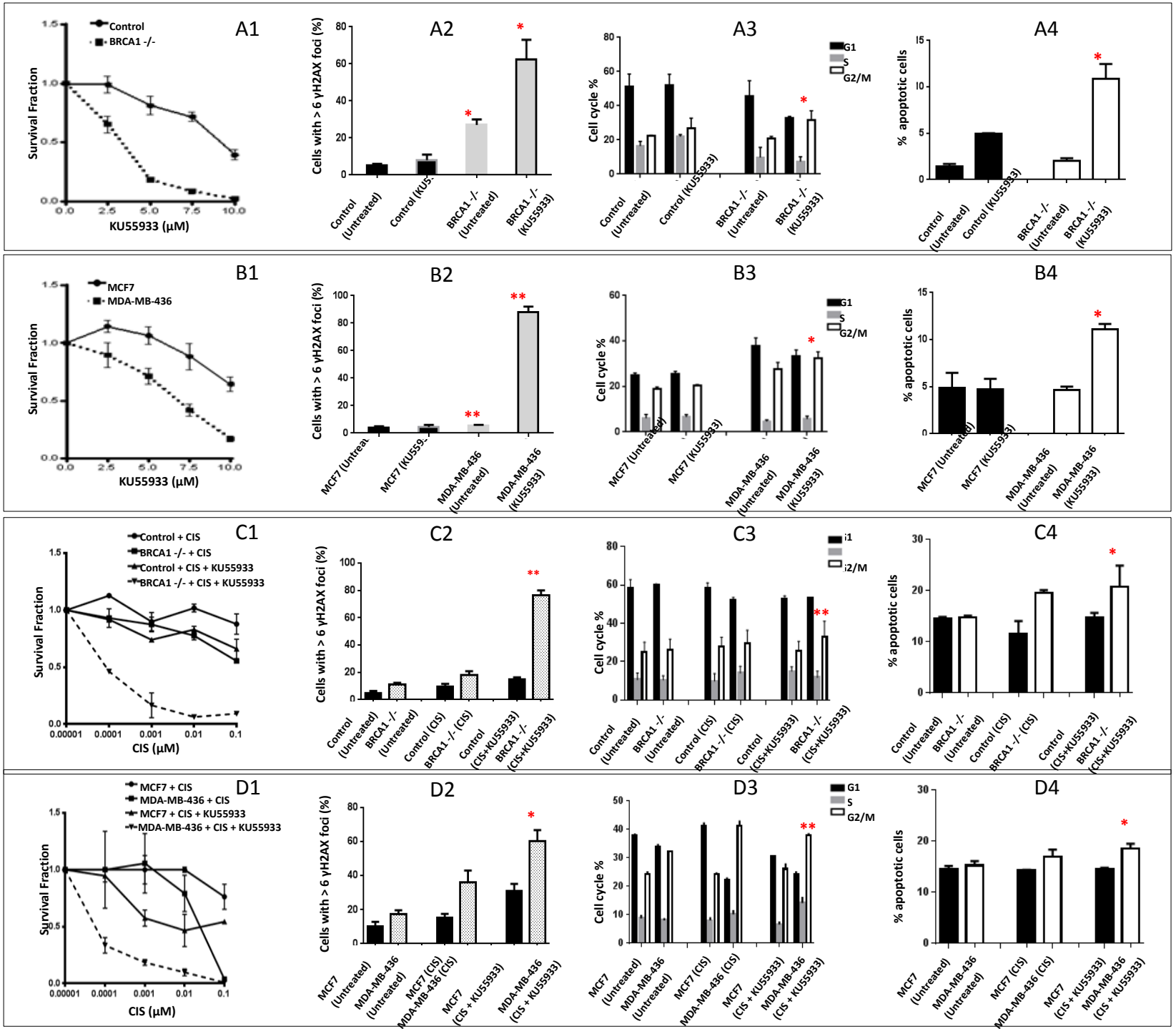
A
A1
Control
BRCA1 -/-
Survival Fraction
KU55933 (μM)
A2
Cells with > 6 γH2AX foci (%)
Control (Untreated)
Control (KU55933)
BRCA1 -/- (Untreated)
BRCA1 -/- (KU55933)
A3
Cell cycle %
G1
S
G2/M
A4
% apoptotic cells
B
B1
MCF7
MDA-MB-436
B2
B3
B4
C
C1
Control + CIS
BRCA1 -/- + CIS
Control + CIS + KU55933
BRCA1 -/- + CIS + KU55933
CIS (μM)
C2
C3
C4
D
D1
MCF7 + CIS
MDA-MB-436 + CIS
MCF7 + CIS + KU55933
MDA-MB-436 + CIS + KU55933
D2
D3
D4

Figure 4

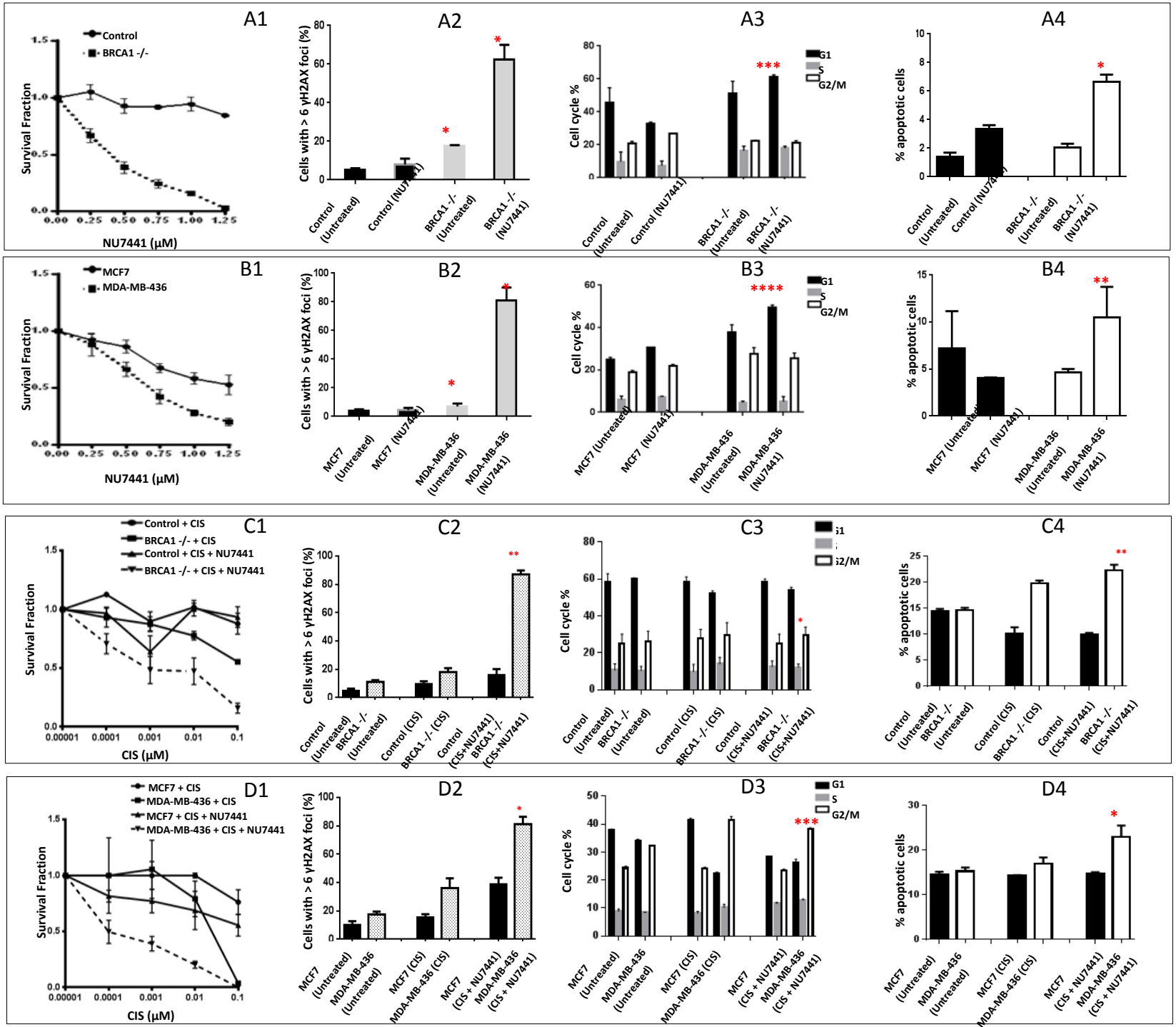
A
A1
Control
BRCA1 -/-
Survival Fraction
NU7441 (μM)
A2
Cells with > 6 γH2AX foci (%)
Control (Untreated)
Control (NU7441)
BRCA1 -/- (Untreated)
BRCA1 -/- (NU7441)
A3
Cell cycle %
G1
S
G2/M
A4
% apoptotic cells
B
B1
MCF7
MDA-MB-436
B2
B3
B4
C
C1
Control + CIS
BRCA1 -/- + CIS
Control + CIS + NU7441
BRCA1 -/- + CIS + NU7441
CIS (μM)
C2
C3
C4
D
D1
MCF7 + CIS
MDA-MB-436 + CIS
MCF7 + CIS + NU7441
MDA-MB-436 + CIS + NU7441
D2
D3
D4

Figure 5

Highlights:

- BRCA1 may regulate base excision repair (BER).
- BRCA1-BER deficient cells may be sensitive to blockade of ATM and DNA-PKcs.
- We show that low XRCC1/low polβ have prognostic significance in BRCA1$^{-/-}$ tumours.
- ATM or DNA-PKcs inhibitors are synthetically lethal in BRCA1-BER deficient cells.
- Synthetic lethality is enhanced in combination with cisplatin.

Supplementary figure legends

Supplementary Figure S1: A. Kaplan Meier curves showing breast cancer specific survival (BCSS) in patients with germ-line BRCA1 mutant tumours based on XRCC1 expression status. **B.** Kaplan Meier curves showing breast cancer specific survival (BCSS) in patients with ER- negative tumours based on BRCA1 mRNA expression status. **C.** Kaplan Meier curves showing breast cancer specific survival (BCSS) in patients with BRCA1 low mRNA tumours based on pol β mRNA expression status. **D.** Kaplan Meier curves showing breast cancer specific survival (BCSS) in patients with BRCA1 low mRNA tumours based on XRCC1 mRNA expression status.

Supplementary Figure S2: A. Clonogenic survival assays in BRCA1 deficient HeLa SilenciX cells and control BRCA1 proficient HeLa SilenciX cells treated with 3-aminobenzamide. **B.** Clonogenic survival assays in MCF-7 cells and MDA-MB-436 cells treated with 3-aminobenzamide.

Supplementary Figure S3: A. Survival assay in MCF-7 and MDA-MB-436 cells treated with cisplatin. **B.** Survival assays in MCF-7 and MDA-MB-436 cells treated with MMS. **C.** Neutral COMET assay in MCF-7 and MDA-MB-436 cells treated with NU7441 or KU55933.

Supplementary Figure S4: Functional analysis in cells (see methods section for more details). **A.** yH2AX immunohistochemistry in BRCA1 deficient HeLa SilenciX cells and control BRCA1 proficient HeLa SilenciX cells treated with KU55933. **B.** FACS analysis in BRCA1 deficient HeLa SilenciX cells and control BRCA1 proficient HeLa SilenciX cells treated with KU55933. **C.** Annexin V flow cytometric analysis in BRCA1 deficient HeLa SilenciX cells and control BRCA1 proficient HeLa SilenciX cells treated with KU55933.

Supplementary Figure S5: A. Clonogenic survival assays in BRCA1 deficient HeLa SilenciX cells and control BRCA1 proficient HeLa SilenciX cells treated with KU60019. **B.** yH2AX immunohistochemistry in BRCA1 deficient HeLa SilenciX cells and control BRCA1 proficient HeLa SilenciX cells treated with KU60019. **C.** FACS analysis in BRCA1 deficient HeLa SilenciX cells and control BRCA1 proficient HeLa SilenciX cells treated with KU60019. **D.** Annexin V flow cytometric analysis in BRCA1 deficient HeLa SilenciX cells and control BRCA1 proficient HeLa SilenciX cells treated with KU60019. **E.** Clonogenic survival assays in MDA-MB-436 and MCF7 cells treated with KU60019. **F.** yH2AX immunohistochemistry in MDA-MB-436 and MCF7 cells treated with KU60019. **G.** FACS analysis in MDA-MB-436 and MCF7 cells treated with KU60019. H**.** Annexin V flow cytometric analysis in MDA-MB-436 and MCF7 cells treated with KU60019. * $p<0.05$, ** $p<0.01$.

Supplementary Figure S6: A. Clonogenic survival assays in BRCA1 deficient HeLa SilenciX cells and control BRCA1 proficient HeLa SilenciX cells treated with NU7026. **B.** yH2AX immunohistochemistry in BRCA1 deficient HeLa SilenciX cells and control BRCA1 proficient HeLa SilenciX cells treated with NU7026. **C.** FACS analysis in BRCA1 deficient HeLa SilenciX cells and control BRCA1 proficient HeLa SilenciX cells treated with NU7026. **D.** Annexin V flow cytometric analysis in BRCA1 deficient HeLa SilenciX cells and control BRCA1 proficient HeLa SilenciX cells treated with NU7026. **E.** Clonogenic survival assays in MDA-MB-436 and MCF7 cells treated with NU7026. **F.** yH2AX immunohistochemistry in MDA-MB-436 and MCF7 cells treated with NU7026. **G.** FACS analysis in MDA-MB-436 and MCF7 cells treated with NU7026. H**.** Annexin V flow cytometric analysis in MDA-MB-436 and MCF7 cells treated with NU7026. * $p<0.05$, ** $p<0.01$.

Supplementary Figure S7: Combination index for synergism (see results section for more details). **A.** ATM inhibitor (KU55933). **B.** DNA-PKcs inhibitor (NU7441).

Supplementary Figure S8: A model for synthetic lethality in BRCA1 deficient cells using ATM or DNA-PKcs inhibitors either alone or in combination with cisplatin chemotherapy is shown here. See discussion section for details.

A

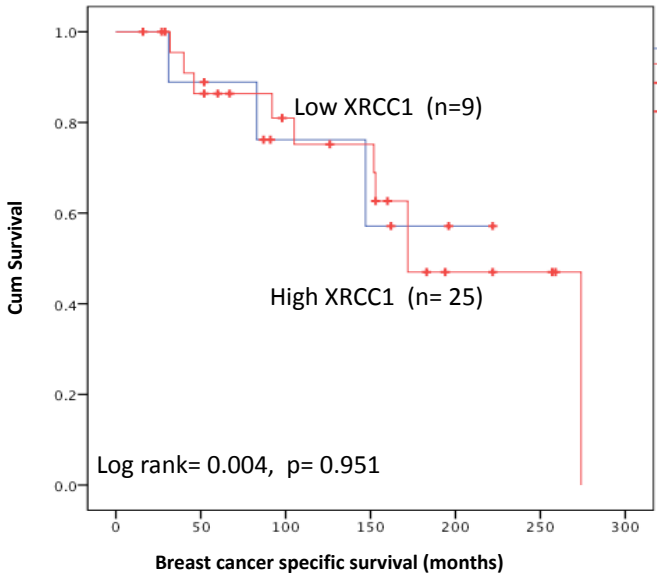

B

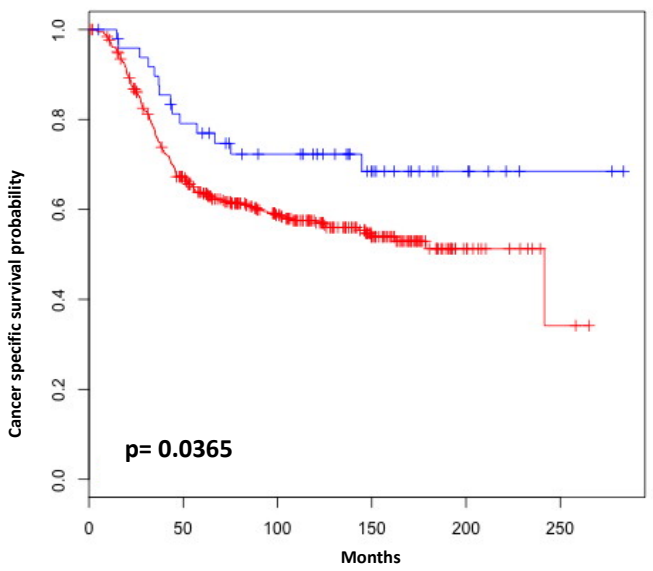

C

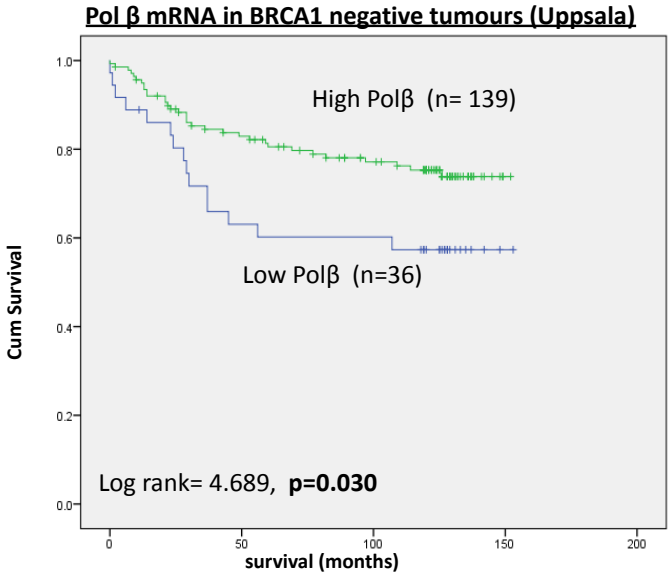

D

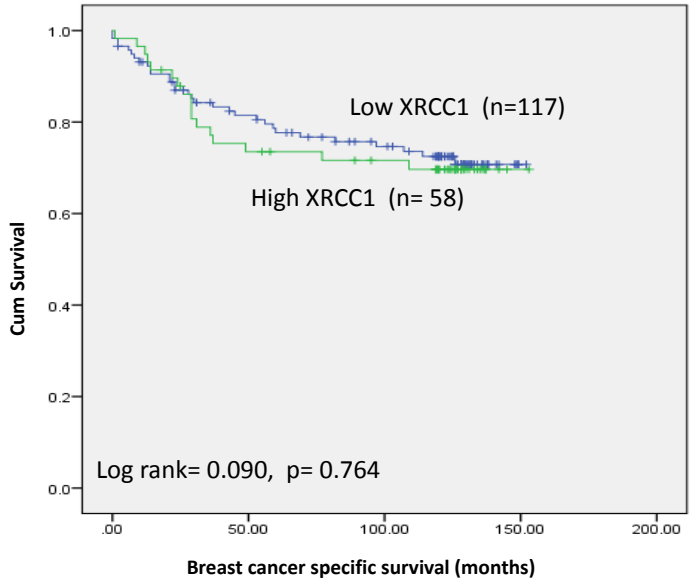

Supplementary Figure S1

A

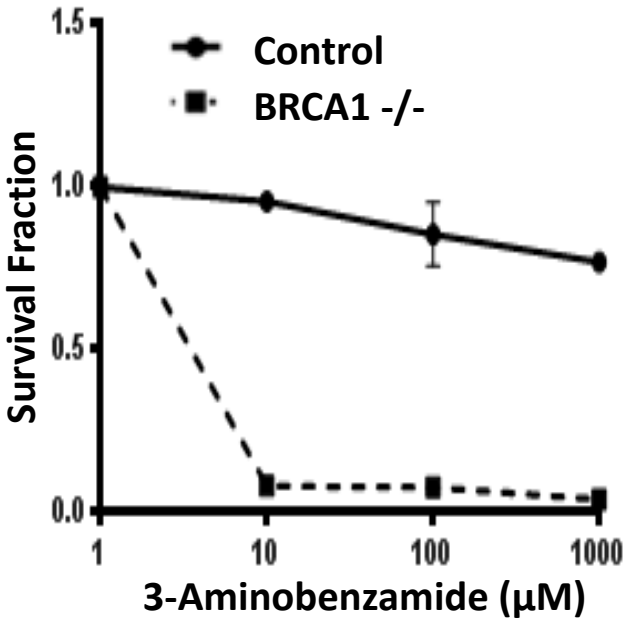

B

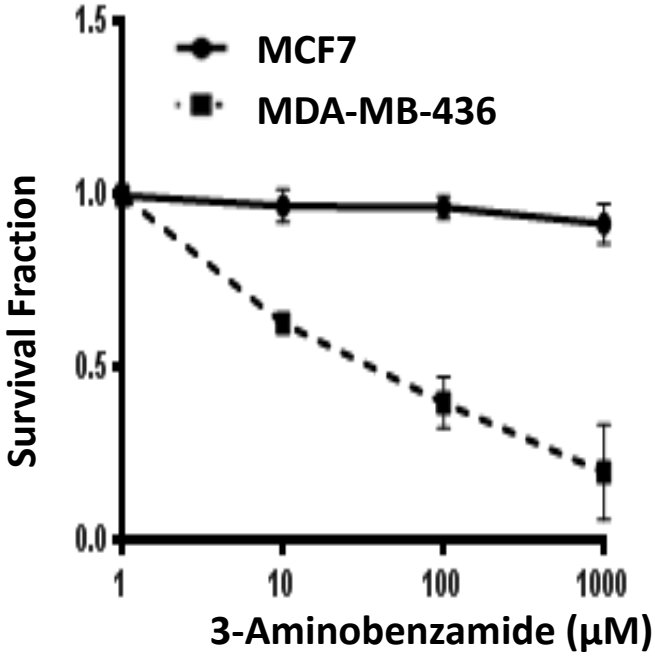

Supplementary Figure S2

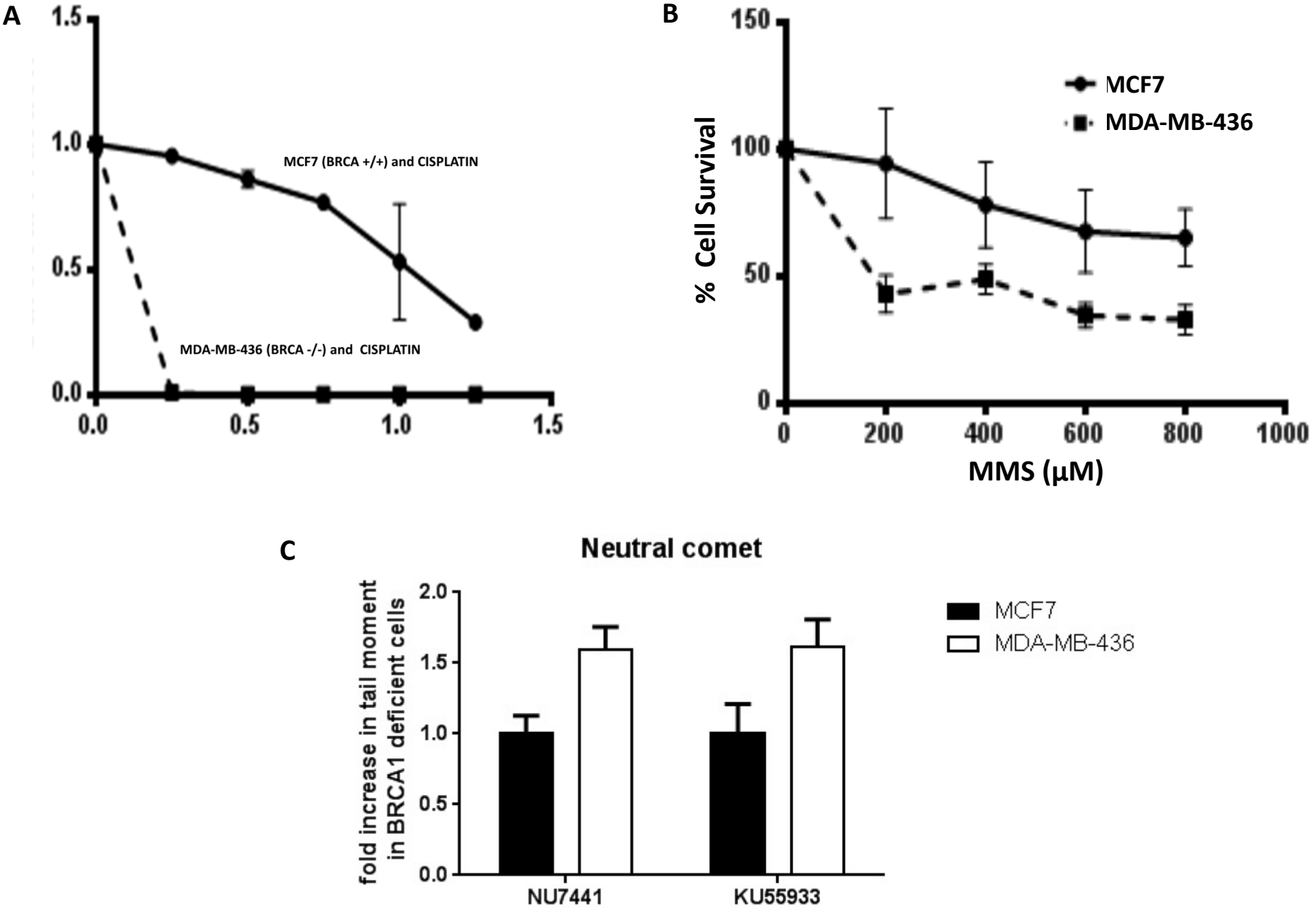

Supplementary Figure S3

A

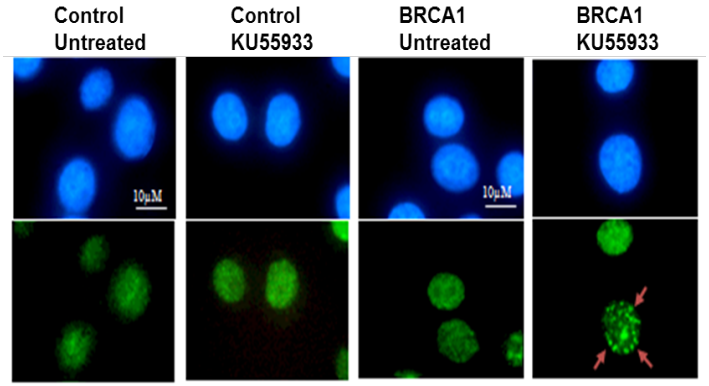

C

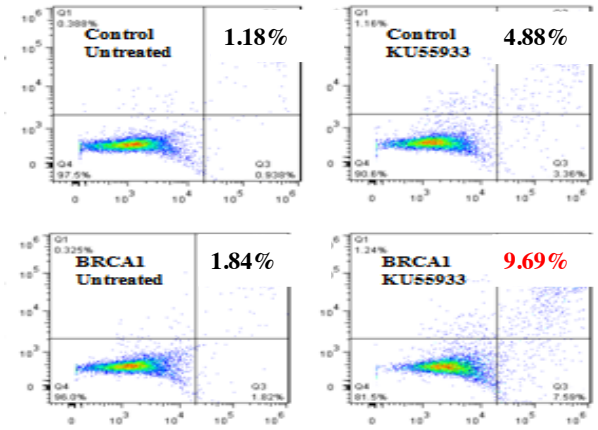

B

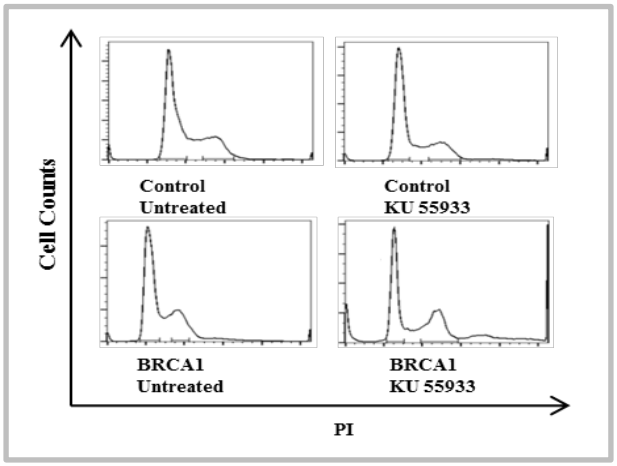

Supplementary Figure S4

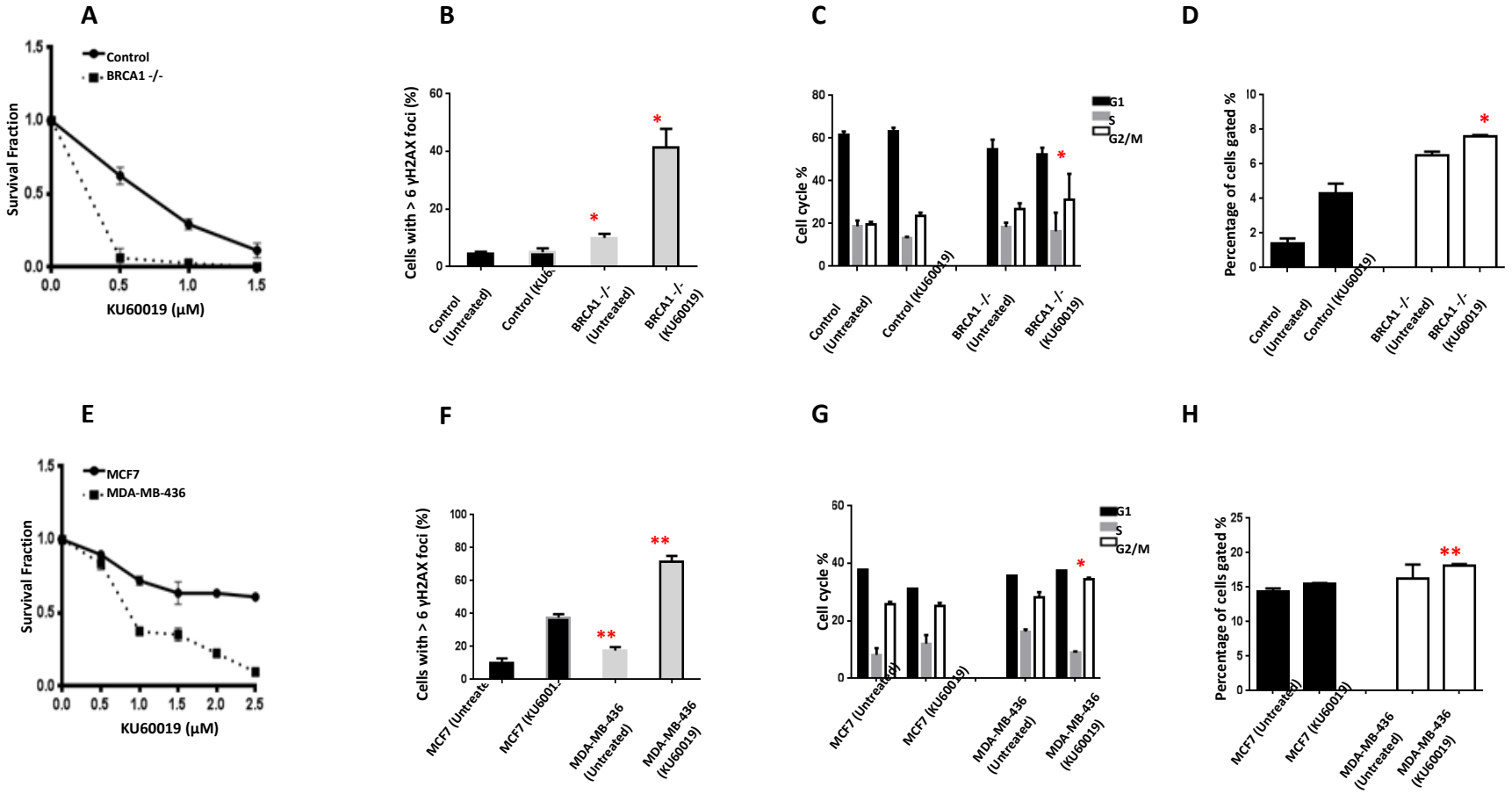

Supplementary Figure S5

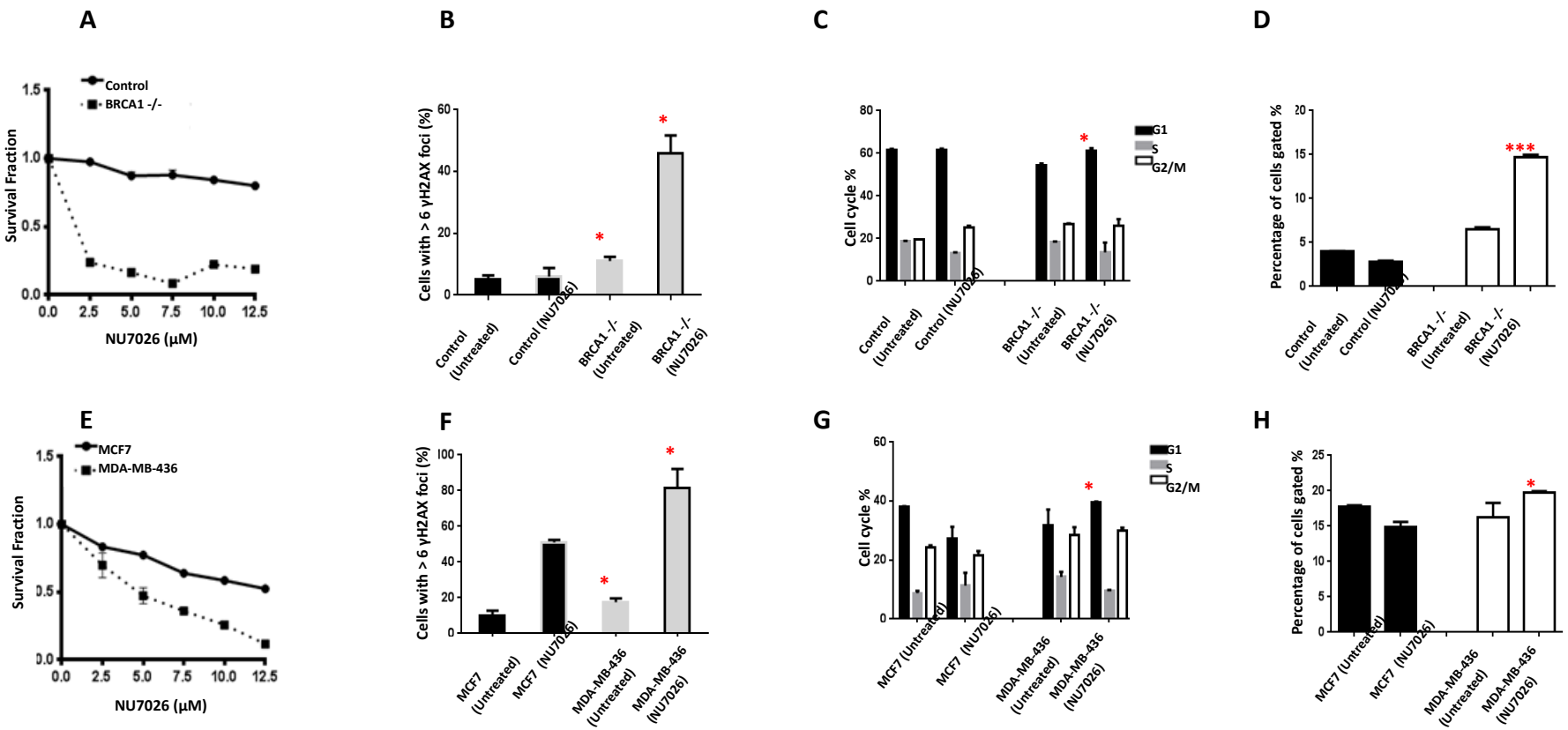

Supplementary Figure S6

A

Cell lines		KU55933 (µM;Ac)	Cisplatin (µM;Bc)	KU55933 (µM;Ae)	Cisplatin (µM;Be)	D
HeLa SilenciX®	BRCA1	5	0.1	10	1	0.6
Breast cancer	MDA-MB-436	7.5	0.1	12.5	1	0.7

B

Cell lines		NU7441 (µM;Ac)	Cisplatin (µM;Bc)	NU7441 (µM;Ae)	Cisplatin (µM;Be)	D
HeLa SilenciX®	BRCA1	0.5	0.1	1.25	1	0.5
Breast cancer	MDA-MB-436	0.75	0.1	1.5	1	0.6

Supplementary Figure S7

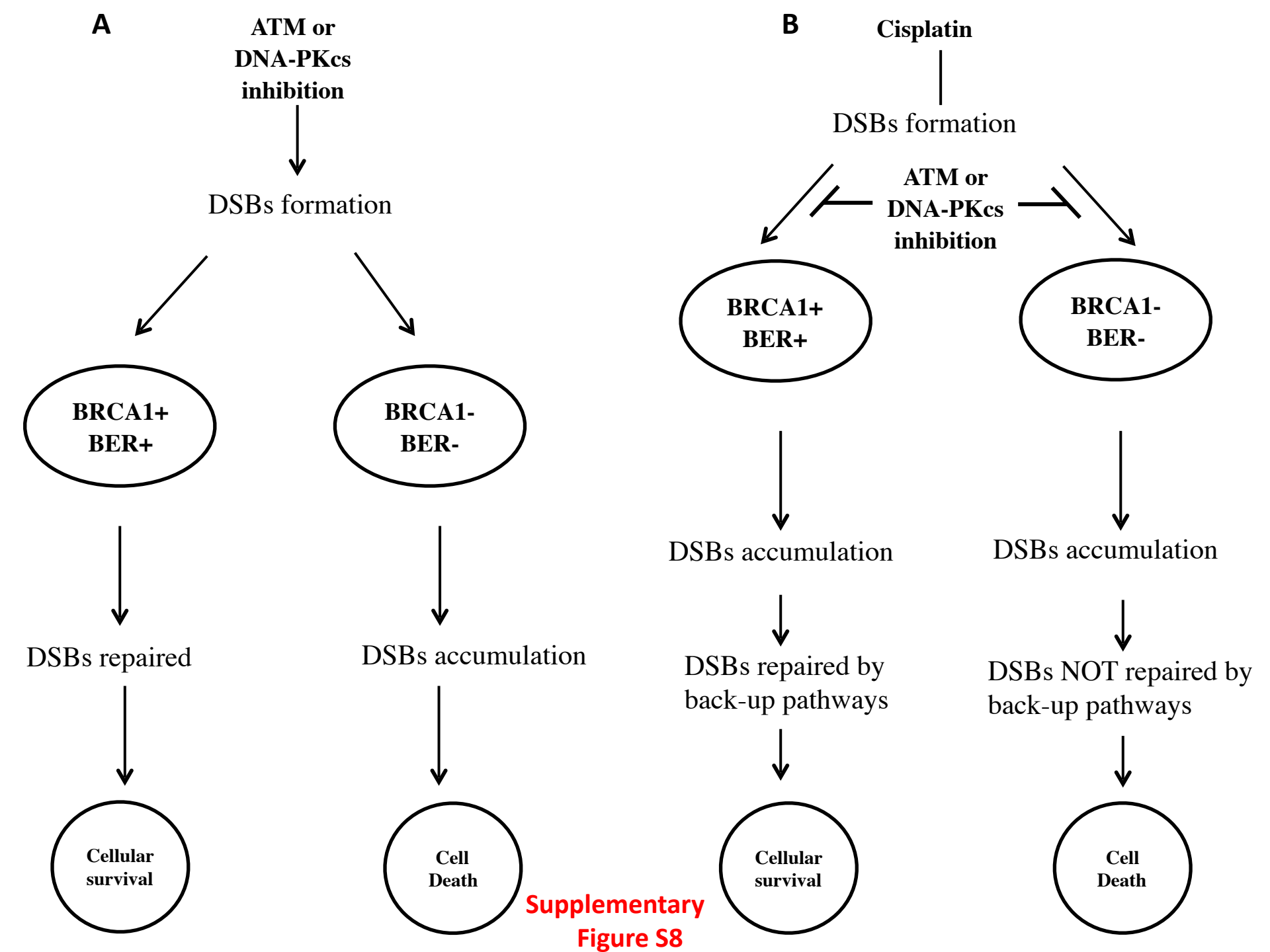

Supplementary Figure S8

Probe Id	Probe Set ID	Gene Symb	Gene Title	go biological process term	go molecul	go cellular component term
218527_at	218527_at	APTX	aprataxin	single strand break repair /// DNA	DNA bindin	chromatin /// nuclear chromatin /// nucleus /// nucleoplasm /// nucleolus /// cytoplasm
208442_s_at	208442_s_at	ATM	ataxia telangiectasia mu	cell cycle checkpoint /// DNA dam	nucleotide	chromosome, telomeric region /// nucleus /// nucleoplasm /// cytoplasm /// spindle /// cytoplasmic mem
209903_s_at	209903_s_at	ATR	ataxia telangiectasia and	cell cycle checkpoint /// DNA dam	nucleotide	XY body /// nucleus /// nucleoplasm /// chromosome /// PML body
214727_at	214727_at	BRCA2	breast cancer 2, early or	double-strand break repair via hor	protease bi	nucleus /// nucleoplasm /// nucleolus /// cytoplasm /// centrosome /// secretory granule /// BRCA2-MAGI
214816_x_at	214816_x_at	C19orf40	chromosome 19 open re	DNA repair /// response to DNA d	DNA bindin	nucleus /// nucleoplasm /// nucleolus /// intracellular membrane-bounded organelle /// Fanconi anaemia
228693_at	228693_at	CCDC50	coiled-coil domain conta	---	protein bin	cytoplasm
204093_at	204093_at	CCNH	cyclin H	regulation of cyclin-dependent pro	protein kin	nucleus /// nucleoplasm /// holo TFIIH complex /// DNA-directed RNA polymerase II, holoenzyme /// cyclin
210021_s_at	210021_s_at	CCNO	cyclin O	regulation of cyclin-dependent pro	uracil DNA	nucleus /// nucleoplasm /// nucleoplasm
204775_at	204775_at	CHAF1B	chromatin assembly fact	DNA replication /// DNA repair ///	chromatin I	nucleus /// nucleus /// nucleoplasm /// nucleolus /// cytoplasm /// cytosol /// CAF-1 complex
208619_at	208619_at	DDB1	damage-specific DNA bi	cell cycle checkpoint /// nucleotid	nucleic acic	nucleus /// nucleoplasm /// cytoplasm /// Cul4A-RING ubiquitin ligase complex /// Cul4B-RING ubiquitin lig
203409_at	203409_at	DDB2	damage-specific DNA bi	protein polyubiquitination /// nuc	DNA bindin	nucleus /// nucleoplasm /// protein complex
208382_s_at	208382_s_at	DMC1	DNA meiotic recombina	pachytene /// ovarian follicle deve	nucleotide	chromosome, telomeric region /// condensed nuclear chromosome /// nucleus /// chromosome
208955_at	208955_at	DUT	deoxyuridine triphospha	nucleobase-containing compound	dUTP dipho	nucleus /// nucleoplasm /// mitochondrion
202176_at	202176_at	ERCC3	excision repair cross-cor	cell cycle checkpoint /// nucleotid	nucleotide	core TFIIH complex /// SSL2-core TFIIH complex /// nucleus /// nucleoplasm /// holo TFIIH complex /// holo
210158_at	210158_at	ERCC4	excision repair cross-cor	meiotic mismatch repair /// resolu	single-strar	nucleotide-excision repair complex /// nucleotide-excision repair factor 1 complex /// chromosome, telome
225861_at	225861_at	FAM195A	family with sequence sir	---	protein bin	---
203678_at	203678_at	FAN1	FANCD2/FANCI-associat	double-strand break repair via hor	magnesium	nucleus
205189_s_at	205189_s_at	FANCC	Fanconi anemia, comple	myeloid cell homeostasis /// DNA	protein bin	chromatin /// nucleus /// nucleoplasm /// cytoplasm /// cytosol /// Fanconi anaemia nuclear complex
203564_at	203564_at	FANCG	Fanconi anemia, comple	cell cycle checkpoint /// phosphor	damaged D	nucleus /// nucleoplasm /// cytoplasm /// mitochondrion /// Fanconi anaemia nuclear complex
218397_at	218397_at	FANCL	Fanconi anemia, comple	DNA repair /// DNA repair /// prot	ubiquitin-p	nucleus /// nuclear envelope /// nucleoplasm /// cytoplasm /// Fanconi anaemia nuclear complex
200895_s_at	200895_s_at	FKBP4	FK506 binding protein 4	protein peptidyl-prolyl isomerizati	peptidyl-pr	intracellular /// nucleus /// nucleolus /// cytoplasm /// mitochondrion /// cytosol /// cytoskeleton /// micr
221540_x_at	221540_x_at	GTF2H2	general transcription fac	nucleotide-excision repair, DNA da	nucleic acic	core TFIIH complex /// nucleus /// nucleoplasm /// holo TFIIH complex
222104_x_at	222104_x_at	GTF2H3	general transcription fac	nucleotide-excision repair, DNA da	damaged D	core TFIIH complex /// nucleus /// nucleoplasm /// holo TFIIH complex /// holo TFIIH complex
202983_at	202983_at	HLTF	helicase-like transcriptic	ATP catabolic process /// transcrip	nucleotide	nucleus /// nucleoplasm /// nucleolus /// cytoplasm
204883_s_at	204883_s_at	HUS1	HUS1 checkpoint homol	cell cycle checkpoint /// DNA dam	protein bin	nucleus /// nucleoplasm /// nucleolus /// cytoplasm /// Golgi apparatus /// checkpoint clamp complex
209580_s_at	209580_s_at	MBD4	methyl-CpG binding dor	DNA repair /// base-excision repai	DNA bindin	chromatin /// nucleus /// nucleoplasm /// nucleolus /// cytoplasm
204880_at	204880_at	MGMT	O-6-methylguanine-DNA	DNA ligation /// DNA repair /// DN	DNA bindin	nucleus /// nucleoplasm
202520_s_at	202520_s_at	MLH1	mutL homolog 1, colon (	pachytene /// nuclear-transcribed	single-strar	condensed chromosome /// condensed nuclear chromosome /// synaptonemal complex /// male germ cel
203686_at	203686_at	MPG	N-methylpurine-DNA gly	DNA repair /// base-excision repai	DNA bindin	nucleus /// nucleoplasm
217942_at	217942_at	MRPS35	mitochondrial ribosoma	DNA damage response, detection	---	mitochondrion /// mitochondrial small ribosomal subunit /// mitochondrial small ribosomal subunit /// rib
209421_at	209421_at	MSH2	mutS homolog 2, colon	meiotic mismatch repair /// in ute	nucleotide	nuclear chromosome /// nucleus /// MutSalpha complex /// MutSbeta complex
210947_s_at	210947_s_at	MSH3	mutS homolog 3 (E. coli	meiotic mismatch repair /// DNA r	nucleotide	nuclear chromosome /// nucleus /// MutSbeta complex
221406_s_at	221406_s_at	MSH5 /// M	mutS homolog 5 (E. coli	meiotic mismatch repair /// mism	nucleotide	synaptonemal complex /// mismatch repair complex
211449_at	211449_at	MSH6	mutS homolog 6 (E. coli	meiotic mismatch repair /// meiot	nucleotide	nuclear chromosome /// nuclear chromatin /// nucleus /// chromosome /// MutSalpha complex
223112_s_at	223112_s_at	NDUFB10	NADH dehydrogenase (u	mitochondrial electron transport,	protein bin	mitochondrion /// mitochondrial inner membrane /// mitochondrial respiratory chain complex I /// mitoch
219502_at	219502_at	NEIL3	nei endonuclease VIII-lik	DNA repair /// base-excision repai	bubble DNA	intracellular /// nucleus
209731_at	209731_at	NTHL1	nth endonuclease III-like	DNA repair /// base-excision repai	DNA bindin	nucleus /// nucleoplasm /// mitochondrion
204766_s_at	204766_s_at	NUDT1	nudix (nucleoside dipho	GTP catabolic process /// purine n	RNA bindin	nucleus /// cytoplasm /// mitochondrion /// mitochondrial matrix /// cytosol
205760_s_at	205760_s_at	OGG1	8-oxoguanine DNA glycc	acute inflammatory response /// I	damaged D	nucleus /// nucleoplasm /// nucleoplasm /// nucleolus /// mitochondrion /// nuclear matrix /// nuclear sp
202239_at	202239_at	PARP4	poly (ADP-ribose) polym	DNA repair /// cellular protein mo	DNA bindin	nucleus /// cytoplasm /// spindle /// cytoskeleton /// spindle microtubule /// ribonucleoprotein complex
201202_at	201202_at	PCNA	proliferating cell nuclear	DNA damage checkpoint /// G1/S	purine-spe	nucleus /// nucleoplasm /// DNA replication factor C complex /// nucleolus /// cytoplasm /// microtubule c
219317_at	219317_at	POLI	polymerase (DNA direct	DNA replication /// DNA repair ///	DNA bindin	intracellular /// nucleus /// nucleoplasm /// intracellular membrane-bounded organelle
203103_s_at	203103_s_at	PRPF19	pre-mRNA processing fa	protein polyubiquitination /// spli	DNA bindin	ubiquitin ligase complex /// Prp19 complex /// nucleus /// nucleoplasm /// spliceosomal complex /// cytop
37793_r_at	37793_r_at	RAD51D	RAD51 homolog D (S. ce	DNA metabolic process /// DNA re	nucleotide	nucleus
203344_s_at	203344_s_at	RBBP8	retinoblastoma binding	cell cycle checkpoint /// G1/S tran	single-strar	nucleus /// transcriptional repressor complex
205091_x_at	205091_x_at	RECQL	RecQ protein-like (DNA	DNA strand renaturation /// DNA	nucleotide	nucleus /// nucleolus /// microtubule cytoskeleton
208021_s_at	208021_s_at	RFC1	replication factor C (acti	S phase of mitotic cell cycle /// mi	nucleotide	nucleus /// nucleoplasm /// DNA replication factor C complex
212696_s_at	212696_s_at	RNF4	ring finger protein 4	transcription, DNA-dependent ///	DNA bindin	nucleus /// nucleoplasm /// cytoplasm /// microtubule cytoskeleton /// PML body
203160_s_at	203160_s_at	RNF8	ring finger protein 8, E3	DNA repair /// double-strand brea	chromatin I	ubiquitin ligase complex /// chromosome, telomeric region /// nucleus /// chromosome /// midbody /// sit
201529_s_at	201529_s_at	RPA1	replication protein A1, 7	cell cycle checkpoint /// G1/S tran	nucleic acic	condensed chromosome /// condensed nuclear chromosome /// lateral element /// male germ cell nucleu
201756_at	201756_at	RPA2	replication protein A2, 3	cell cycle checkpoint /// G1/S tran	nucleic acic	nucleus /// nucleoplasm /// DNA replication factor A complex /// nucleolus /// PML body
227108_at	227108_at	STARD9	StAR-related lipid transf	microtubule-based movement ///	nucleotide	nucleus /// cytoplasm /// centriole /// cytoskeleton /// microtubule associated complex
202633_at	202633_at	TOPBP1	topoisomerase (DNA) II	DNA metabolic process /// DNA re	DNA bindin	condensed nuclear chromosome /// spindle pole /// male germ cell nucleus /// nucleus /// chromosome //
211300_s_at	211300_s_at	TP53	tumor protein p53	protein import into nucleus, trans	RNA polym	chromatin /// nuclear chromatin /// nucleus /// nucleoplasm /// nucleoplasm /// replication fork /// transc
203050_at	203050_at	TP53BP1	tumor protein p53 bindi	double-strand break repair via hor	RNA polym	chromosome, centromeric region /// kinetochore /// condensed chromosome kinetochore /// chromosom
34689_at	34689_at	TREX1	three prime repair exon	DNA metabolic process /// DNA re	nucleic acic	intracellular /// nucleus /// nuclear envelope /// cytoplasm /// endoplasmic reticulum membrane
211788_s_at	211788_s_at	TREX2	three prime repair exon	DNA metabolic process /// DNA re	magnesium	intracellular /// nucleus
201523_x_at	201523_x_at	UBE2N	ubiquitin-conjugating en	double-strand break repair via hor	nucleotide	ubiquitin ligase complex /// nucleus /// cytoplasm /// cytoplasm /// cytosol /// UBC13-MMS2 complex ///
205667_at	205667_at	WRN	Werner syndrome, RecQ	telomere maintenance /// DNA sy	nucleotide	intracellular /// nucleus /// nucleoplasm /// nucleolus /// centrosome /// MutLalpha complex
205672_at	205672_at	XPA	xeroderma pigmentosun	nucleotide-excision repair, DNA da	nucleotide	nucleus /// nucleoplasm
207598_x_at	207598_x_at	XRCC2	X-ray repair complemen	double-strand break repair via hor	DNA bindin	nucleus
216299_s_at	216299_s_at	XRCC3	X-ray repair complemen	DNA metabolic process /// DNA re	nucleotide	nucleus /// cytoplasm /// mitochondrion /// perinuclear region of cytoplasm
210812_at	210812_at	XRCC4	X-ray repair complemen	in utero embryonic development /	DNA bindin	condensed chromosome /// nucleus /// nucleus /// nucleoplasm /// cytosol /// DNA-dependent protein ki
208643_s_at	208643_s_at	XRCC5	X-ray repair complemen	telomere maintenance /// DNA re	nucleotide	nuclear telomere cap complex /// nuclear chromosome, telomeric region /// nucleus /// nucleoplasm /// c

Supplementary Table S1: Clinicopathological characteristics of whole breast cancer cohort

Variable	n*	Cases	(%)
Menopausal status	1650		
Pre-menopausal		612	(37.0)
postmenopausal		1038	(63.0)
Tumour Grade (NGS)	1650		
G1		306	(18.5)
G2		531	(32.2)
G3		813	(49.3)
Lymph node stage	1650		
Negative		1056	(64.0)
Positive (1-3 nodes)		486	(29.5)
Positive (>3 nodes)		108	(6.5)
Tumour size (cm)	1650		
T1 a + b (≤1.0)		187	(11.0)
T1 c (>1.0 -2.0)		868	(53.0)
T2 (>2.0-5)		579	(35.0)
T3 (>5)		16	(1.0)
Tumour type	1650		
IDC-NST		941	(57)
Tubular		349	(21)
ILC		160	(10)
Medullary (typical/atypical)		41	(2.5)
Others		159	(9.5)
NPI subgroups	1650		
Excellent PG(2.08-2.40)	Low risk	207	(12.5)
Good PG(2.42-3.40)		331	(20.1)
Moderate I PG(3.42 to 4.4)	High risk	488	(29.6)
Moderate II PG(4.42 to 5.4)		395	(23.9)
Poor PG(5.42 to 6.4)		170	(10.3)
Very poor PG(6.5–6.8)		59	(3.6)
Survival at 20 years	1650		

Alive and well	1055	(64.0)
Dead from disease	468	(28.4)
Dead from other causes	127	(7.6)
Adjuvant systemic therapy (AT)		
No AT	665	(42.0)
Hormone therapy (HT)	642	(41.0)
Chemotherapy	307	(20.0)
Hormone + chemotherapy	46	(3.0)

* Number of cases for which data were available.

NPI; Nottingham prognostic index, PG; prognostic group

Supplementary treatment data 1:

Patients received standard surgery (mastectomy or wide local excision) with radiotherapy. Prior to 1989, patients did not receive systemic adjuvant treatment (AT). After 1989, AT was scheduled based on prognostic and predictive factor status, including NPI, oestrogen receptor-α (ER-α) status, and menopausal status. Patients with NPI scores of <3.4 (low risk) did not receive AT. In pre-menopausal patients with NPI scores of ≥3.4 (high risk), classical Cyclophosphamide, Methotrexate, and 5-Flourouracil (CMF) chemotherapy was given; patients with ER-α positive tumours were also offered HT. Postmenopausal patients with NPI scores of ≥3.4 and ER-α positivity were offered HT, while ER-α negative patients received classical CMF chemotherapy.

Median follow up was 111 months (range 1 to 233 months). Survival data, including overall survival, disease-free survival (DFS), and development of loco-regional and distant metastases (DM), was maintained on a prospective basis. DFS was defined as the number of months from diagnosis to the occurrence of local recurrence, local lymph node (LN) relapse or DM relapse. Breast cancer specific survival (BCSS) was defined as the number of months from diagnosis to the occurrence of BC related-death. Local recurrence free survival (LRS) was defined the number of months from diagnosis to the occurrence of local recurrence. DM-free survival was defined as the number of months from diagnosis to the occurrence of DM relapse. Survival was censored if the patient was still alive at the time of analysis, lost to follow-up, or died from other causes.

Supplementary Table S2. Antigens, primary antibodies, clone, source, optimal dilution and scoring system used for each immunohistochemical marker.

Marker	Antibody	Clone	Manufacturer	Antigen retrieval	Dilution / Incubation Time	Distribution	Scoring system	Cut-offs
BRCA 1	Mouse MAb anti-BRCA1	MS 110	Calbiochem	Citrate buffer pH6 20 minutes	1:100 60 min	Nuclear	% of positive cells	<25% (negative)
Pol β	Rabbit Polyclonal	ab26343	Abcam	Citrate buffer pH6 20 minutes	1:200 60 min	Nuclear	H-score	≤100 (low)
XRCC 1	Mouse MAb anti-XRCC1	33-2-5	Thermo Scientific	Citrate buffer pH6 20 minutes	1:200	Nuclear	H-score	≤100 (low)
APE1	Rabbit polyclonal	NB100-101	Novus Biologicals	Citrate buffer pH6 20 minutes	1:500 60 min	Nuclear	H-score	≤100 (low)
SMUG 1	Goat MAb anti-SMUG1	AP08884PU-N	Acris Antibody GmbH	Citrate buffer pH6 20 minutes	1:200	Nuclear	H-score	≤35 (low)
Vimentin	Mouse MAb anti-vimentin	Vim 3B4	Dako-Cytomation	Citrate buffer pH6 20 minutes	1:250 60 min	Cytoplasm	% of positive cells	≥10% (positive)
CK18	Mouse MAb anti-Ck18	DC10	Dako-Cytomation	Citrate buffer pH6 20 minutes	1:100 60 min	Cytoplasm	% of positive cells	≥10% (positive)
ER	Mouse MAb anti-ER-α	SP1	Dako-Cytomation	Citrate buffer pH6 20 minutes	1:150 30 min	Nuclear	Allred score	≥3 (positive)
ER	Mouse MAb anti-ER-α	EP1	Dako-Cytomation	Citrate buffer pH6 20 minutes	1:80 30 min	Nuclear	% of positive cells	≥1% positive
PR	Mouse MAb anti-PR	PgR636	Dako-Cytomation	Citrate buffer pH6 20 minutes	1:125 30 min	Nuclear	% of positive cells	≥1% positive

p53	Mouse MAb anti p53	DO7	Novocastra	Citrate buffer pH6 20 minutes	1: 50 60 min	Nuclear	% of positive cells	≤20% (negative) >20% (High)
p21	Mouse MAb anti-p21	SW118	Dako-Cytomation	Citrate buffer pH6 20 minutes	1:50 60 min	Nuclear	% of positive cells	≥10% (positive)
Bax	Rabbit anti-Bax	Polyclonal	Abcam	Citrate buffer pH6 20 minutes	1:1000 60 min	Cytoplasm	% positive cells	≥10% (positive)
Bcl2	Mouse MAb anti-Bcl2	124	Dako-Cytomation	Citrate buffer pH6 20 minutes	1:100 60 min	Cytoplasm	% of positive cells	>10% (positive
TOP2A	Mouse MAb TOP2A	KiS1	Dako-Cytomation	Citrate buffer pH6 20 minutes	1:100 60 min	Nuclear	% of positive cells	>25% (positive)

All sections were pre-treated with microwave antigen retrieval using 0.1% citrate buffer (pH 6).

AR: Androgen Receptor; MAb: Monoclonal antibody; BRCA1: BC 1, ER: oestrogen receptor; PR: progesterone receptor; TOP2A: Topoisomerase II alpha; CK: cytokeratin; Bax: BCL2-associated X protein.

Supplementary Table S3. BRCA1 and DNA base excision repair protein expression in breast cancers cancers.

		BRCA1 (Negative)	**BRCA1** (Positive)	**P value**
DNA base excision repair		Number (%)	Number (%)	
Pol β	Low	276 (61.2)	278 (34.8)	**1.8×10^{-19}**
	High	175 (38.8)	521 (65.2)	
XRCC1	Low	98 (22.5)	101 (13.0)	**1.6×10^{-5}**
	High	337 (77.5)	678 (87.0)	

Supplementary Table S4. Clinicopathological significance of XRCC1 expression in BRCA1 negative tumours.

Variable	XRCC1		
	Low	High	X^2
	N (%)	N (%)	*Adjusted p value*
	A) Pathological Parameters		
Stage			
I	59 (60.2)	208 (61.7)	0.864
II	29 (29.6)	91 (27.0)	
III	10 (10.2)	38 (11.3)	
Tumour Size			
T1 a + b (≤1.0)	2 (2.1)	27 (8.2)	0.079
T1 c (>1.0 -2.0)	40 (41.7)	141 (42.9)	
T2 (>2.0-5)	52 (54.2)	146 (44.4)	
T3 (>5)	2 (2.1)	15 (4.6)	
LVI			
Negative	48 (49.0)	136 (40.6)	0.140
Positive	50 (51.0)	199 (59.4)	
Grade			
G1	3 (3.1)	9 (2.7)	0.353
G2	9 (9.2)	50 (14.8)	
G3	86 (87.8)	278 (82.5)	
Tumour Types			
IDC-NST	78 (79.6)	298 (88.7)	0.162
Tubular	7 (7.1)	9 (2.7)	
ILC	2 (2.0)	5 (1.5)	
Medullary	5 (5.1)	11 (3.3)	
Others	6 (6.1)	13 (3.9)	
Mitotic Index			
M1 (low; mitoses < 10)	7 (7.2)	34 (10.1)	0.290
M2 (medium; mitoses 10-18)	13 (13.4)	62 (18.5)	

M3 (high; mitosis >18)	77 (79.4)	239 (71.3)	
Pleomorphism			
1 (small-regular uniform)	0 (0.0)	0 (0.0)	0.480
2 (Moderate variation)	7 (7.2)	32 (9.6)	
3 (Marked variation)	90 (92.8)	303 (90.4)	
Tubule formation			
1 (>75% of definite tubule)	2 (2.1)	5 (1.5)	0.700
2 (10%-75% definite tubule)	16 (16.5)	67 (20.0)	
3 (<10% definite tubule)	79 (81.4)	263 (78.5)	
B) Aggressive phenotype			
Her2 overexpression (No)	85 (86.7)	267 (79.5)	0.106
(Yes)	13 (13.3)	69 (20.5)	
Triple negative (No)	37 (37.8)	133 (39.6)	0.744
(Yes)	61 (62.2)	203 (60.4)	
Basal like (No)	44 (81.5)	95 (76.6)	0.470
(Yes)	10 (18.5)	29 (23.4)	
Vimentin (Negative)	29 (85.3)	75 (80.6)	0.547
(Positive)	5 (14.7)	18 (19.4)	
CK18 (Negative)	38 (40.4)	146 (47.2)	0.245
(Positive)	56 (59.6)	163 (52.8)	
C) Hormonal receptors			
ER (Negative)	71 (72.4)	264 (78.3)	0.223
(Positive)	27 (27.6)	73 (21.7)	
PgR (Negative)	79 (84.0)	261 (82.1)	0.659
(Positive)	15 (16.0)	52 (17.9)	
D) DNA Repair Pathway			
APE1 (Low)	34 (79.1)	57 (56.4)	**0.010**
(High)	9 (20.9)	44 (43.6)	
SMUG1 (Low)	46 (55.4)	94 (31.4)	**0.000006**
(High)	37 (44.6)	205 (68.6)	
PolB (Low)	59 (67.8)	178 (58.7)	0.127
(High)	28 (32.2)	125 (41.3)	

TOP2A (Low)		66 (77.6)	168 (57.9)	**0.001**
	(High)	19 (22.4)	122 (42.1)	
E) Cell cycle/apoptosis regulators				
p53	(Negative)	58 (59.8)	150 (45.7)	**0.015**
	(Positive)	39 (40.2)	178 (54.3)	
Bax	(Negative)	34 (89.5)	68 (76.4)	0.090
	(Positive)	4 (10.5)	21 (23.6)	
Bcl2	(Negative)	56 (60.9)	219 (66.4)	0.328
	(Positive)	36 (39.1)	111 (33.6)	
p16	(Low)	35 (83.3)	94 (87.0)	0.557
	(High)	7 (16.7)	14 (13.0)	

Supplementary Table S5. Clinicopathological significance of pol β expression in BRCA1 negative tumours.

Variable	Pol Beta		
	Low	High	X^2
	N (%)	N (%)	*Adjusted p value*
A) Pathological Parameters			
Stage			
I	172 (62.3)	112 (64.0)	0.332
II	70 (25.4)	49 (28.0)	
III	34 (12.3)	14 (8.0)	
Tumour Size			
T1 a + b (≤1.0)	20 (7.4)	13 (7.6)	0.627
T1 c (>1.0 -2.0)	120 (44.1)	69 (40.6)	
T2 (>2.0-5)	121 (44.5)	84 (49.4)	
T3 (>5)	11 (4.0)	4 (2.4)	
LVI			
Negative	116 (42.3)	78 (44.6)	0.641
Positive	158 (57.7)	97 (55.4)	
Grade			
G1	5 (1.8)	7 (4.0)	0.331
G2	39 (14.1)	27 (15.4)	
G3	232 (84.1)	141 (80.6)	
Tumour Types			
IDC-NST	236 (86.1)	147 (84.0)	0.740
Tubular	11 (4.0)	11 (6.3)	
ILC	6 (2.2)	2 (1.1)	
Medullary	9 (3.3)	6 (3.4)	
Others	12 (4.4)	9 (5.1)	
Mitotic Index			
M1 (low; mitoses < 10)	23 (8.4)	24 (13.9)	0.184
M2 (medium; mitoses 10-18)	43 (15.7)	26 (15.0)	

M3 (high; mitosis >18)	208 (75.9)	123 (71.1)	
Pleomorphism			
1 (small-regular uniform)	2 (0.7)	0 (0.0)	0.133
2 (Moderate variation)	19 (6.9)	20 (11.6)	
3 (Marked variation)	253 (92.3)	153 (88.4)	
Tubule formation			
1 (>75% of definite tubule)	2 (0.7)	4 (2.3)	0.366
2 (10%-75% definite tubule)	54 (19.7)	33 (19.1)	
3 (<10% definite tubule)	218 (79.6)	136 (78.6)	
B) Aggressive phenotype			
Her2 overexpression (No)	225 (81.8)	140 (80.5)	0.719
(Yes)	50 (18.2)	34 (19.5)	
Triple negative (No)	101 (36.7)	75 (43.1)	0.178
(Yes)	174 (63.3)	99 (56.9)	
Basal like (No)	76 (76.8)	67 (75.3)	0.811
(Yes)	23 (23.2)	22 (24.7)	
Vimentin (Negative)	61 (89.7)	48 (81.4)	0.178
(Positive)	7 (10.3)	11 (18.6)	
CK18 (Negative)	125 (48.8)	68 (41.2)	0.126
(Positive)	131 (51.2)	97 (58.8)	
C) Hormonal receptors			
ER (Negative)	218 (79.0)	123 (70.3)	**0.036**
(Positive)	58 (21.0)	52 (29.7)	
PgR (Negative)	221 (84.4)	130 (77.4)	**0.069**
(Positive)	41 (15.6)	38 (22.6)	
D) DNA Repair Pathway			
APE1 (Low)	67 (72.0)	47 (56.0)	**0.026**
(High)	26 (28.0)	37 (44.0)	
SMUG1 (Low)	79 (34.6)	59 (41.5)	0.182
(High)	149 (65.4)	83 (58.5)	
XRCC1 (Low)	59 (24.9%)	28 (18.3)	0.127
(High)	178 (75.1)	125 (81.7)	

TOP2A (Low)		149 (64.2)	87 (58.8)	0.286
	(High)	83 (35.8)	61 (41.2)	
E) Cell cycle/apoptosis regulators				
p53	(Negative)	123 (45.6)	90 (52.6)	0.147
	(Positive)	147 (54.4)	81 (47.4)	
Bax	(Negative)	52 (77.6)	50 (84.7)	0.309
	(Positive)	15 (22.4)	9 (15.3)	
Bcl2	(Negative)	187 (70.6)	94 (55.3)	**0.001**
	(Positive)	78 (29.4)	76 (44.7)	
p16	(Low)	69 (87.3)	61 (87.1)	0.971
	(High)	10 (12.7)	9 (12.9)	

Supplementary Table S6: Clinicopathological characteristics of BRCA1 germ line mutated breast cancer cohort (N=50)

Variables	N (%)
Age (years) at diagnosis [Mean, Median (range)]	[40.66, 38.5(26-64)]
Tumour Size (cm) [Mean (range)]	[2.03 (0.4-5.2)]
T1 a + b (≤1.0)	7 (22)
T1 c (>1.0 -2.0)	22 (44)
T2 (>2.0-5)	20 (40)
T3 (>5)	1 (2)
Pathological Type	
Ductal/NST	40 (80)
Lobular/Miixed	1 (2)
Medullary (Typical/Atypical)	6 (12)
Basal	1 (2)
Spindle	1 (2)
Tubular/Mixed	1 (2)
Lymph node involvement	
No	32 (64)
LN (1-3)	15 (30)
LN (>3)	1 (2)
Unknown	2 (4)
Grade	
1	1 (2)
2	5 (10)
3	44 (88)
Stage	
1	32 (64)
2	15 (30)
3	1 (20)
Unknown	2 (4)

Vascular Invasion	
No	29 (58)
Yes	17 (34)
Unknown	4 (8)
NPI	
Excellent PG(2.08-2.40)	1 (2)
Good PG(2.42-3.40)	2 (4)
Moderate I PG(3.42 to 4.4)	19 (38)
Moderate II PG(4.42 to 5.4)	15 (30)
Poor PG(5.42 to 6.4)	9 (18)
Very poor PG(6.5–6.8)	1 (2)
Unknown	3 (6)
Oestrogen receptor (ER)	
Negative	40 (80)
Positive	9 (18)
Unknown	1 (2)
Her2	
Negative	47 (94)
Positive	2 (4)
Unknown	1 (2)
Triple Negativity	
Non TN	18 (36)
TN	31 (62)
Unknown	1 (2)
Recurrence	
No	40 (80)
Yes	10 (20)
Survival in months [Mean, Median (range)]	[122.06, 118 (9 - 274)]
Alive	36 (72)
Dead	14 (28)

Type of Surgery WLE Mastectomy	 18 (36) 32 (64)
Bilateral Cancer No Yes	 34 (68) 16 (32)
Prophylactic Mastectomy No Yes	 30 (60) 20 (40)
Prophylactic Oophorectomy No Yes	 16 (32) 34 (68)
Prophylactic Oophorectomy for Cancer No Yes	 44 (88) 6 (12)

Supplementary Table S7: Clinicopathological significance of pol β expression in germ-line BRCA1 mutated breast cancers (n=50).

Markers		**POL-B (Low)**	**POL-B (High)**	
Pathological parameters		**Number (%)**	**Number (%)**	**P value**
Tumour Size (Cm)	T1 a + b (≤1.0)	0 (0)	4 (13.8)	0.708
	T1 c (>1.0 -2.0)	2 (40)	13 (44.8)	
	T2 (>2.0-5)	3 (60)	11 (37.9)	
	T3 (>5)	0 (0)	1 (3.4)	
Histological Type	Atypical Medullary	0 (0)	4 (13.8)	0.135
	Ductal/NST	4 80)	22 (75.9)	
	Lobular	0 (0)	1 (3.4)	
	Medullary/NST	0 (0)	2 (6.9)	
	Spindle	1 (20)	0 (0)	
LN Status	Negative	4 (80)	17 (60.7)	0.409
	Positive	1 (20)	11 (39.3)	
Grade	1	1 (20)	0 (0)	0.042
	2	0 (0)	3 (10.3)	
	3	4 (80)	26 (89.7)	
Stage	1	4 (80)	17 (60.7)	0.409
	2	1 (20)	11 (33.9)	
Vascular Invasion	Absent	2 (40)	16 (59.3)	0.425
	Present	3 (60)	11 (40.7)	
ER Status	Negative	4 (80)	24 (82.8)	0.881
	Positive	1 (20)	5 (17.2)	
HeR2 Status	Negative	5 (100)	27 (93.1)	0.545
	Positive	0 (0)	2 (6.9)	

Triple Negativity	No	2 (40)	11 (37.9)	0.958
	Yes	3 (60)	18 (62.1)	
Recurrence	No	3 (60.0)	23 (79.3)	0.347
	Yes	2 (40.0)	6 (20.7)	

Supplementary Table S8: Clinicopathological significance of XRCC1 expression in germ-line BRCA1 mutated breast cancers (n=50).

Markers		**XRCC1 (Low)**	**XRCC1 (High)**	
Pathological parameters		**Number (%)**	**Number (%)**	**P value**
Tumour Size (cm)	T1 a + b (≤1.0)	2 (22.2)	3 (12)	0.824
	T1 c (>1.0 -2.0)	4 (44.4)	11 (44)	
	T2 (>2.0-5)	3 (33.3)	10 (40)	
	T3 (>5)	0 (0)	1 (4)	
Histological Type	Atypical Medullary	1 (11.1)	3 (12)	0.891
	Ductal/NST	7 (77.8)	18 (72)	
	Lobular	0 (0)	1 (4)	
	Medullary/NST	1 (11.1)	1 (4)	
	Spindle	0 (0)	1 (4)	
	Tubular/Mixed	0 (0)	1 (4)	
LN Status	Negative	8 (88.9)	14 (58.3)	0.097
	Positive	1 (11.1)	10 (41.7)	
Grade	1	0 (0)	1 (4)	0.442
	2	0 (0)	3 (12)	
	3	9 (100)	21 (84)	
Stage	1	8 (88.9)	14 (58.3)	0.097
	2	1 (11.1)	10 (41.7)	
Vascular Invasion	Absent	6 (75)	12 (52.2)	0.260
	Present	2 (25)	11 (47.8)	
ER Status	Negative	8 (88.9)	19 (76)	0.412
	Positive	1 (11.1)	6 (24)	
HeR2 Status	Negative	9 (100)	23 (92)	0.382
	Positive	0 (0)	2 (8)	

Triple Negativity	No	3 (33.3)	10 (40)	0.724
	Yes	6 (66.7)	15 (60.0)	
Recurrence	No	6 (66.7)	19 (76)	0.586
	Yes	3 (33.3)	6 (24)	

Supplementary Table S9. Patient demographics (METABRIC cohort)

Variables	N
Age at diagnosis [Median (range)]	61.8 (21.93-96.29)
Tumour size [Median (range (mm))]	23 (1- 182mm)
NPI [Median (95% CI)]	4.04 (3.99-4.09)
Survival [Median (Months, 95% Cl)]	149 (141-159)
Lymph nodes status 0 1 2 3 >3	 1012 336 170 112 316
ER status Positive Negative	 1485 437
PAM50 subtype Basal HER2 Luminal A Luminal B Normal Not classified	 322 238 714 484 188 6
<u>Adjuvant systemic therapy (AT</u>)	
No AT	290

Hormone therapy (HT)	1014
Chemotherapy	226
Hormone + chemotherapy	192

Supplementary Table S10: Clinicopathological characteristics of the Uppsala Cohort (n=249)

Variables	N (%)
Age (years) at diagnosis [Mean, Median (range)]	[62.1, 63.02 (28-93)]
Tumour Size (cm) [Mean (range)]	[2.24 (0.2-13.0)]
T1 a + b (≤1.0)	22 (8.8)
T1 c (>1.0 -2.0)	104 (41.8)
T2 (>2.0-5)	117 (47.0)
T3 (>5)	6 (2.4)
Lymph node involvement	
No	159 (66.3)
Yes	81 (33.7)
Grade	
1	68 (27.3)
2	126 (50.6)
3	55 (22.1)
Oestrogen receptor (ER)	
Negative	34 (13.9)
Positive	211 (86.1)
Recurrence	
No	160 (64.3)
Yes	89 (35.7)
Survival in months [Mean, Median (range)]	[85.7, 119 (0-153)]
Alive	160 (64.3)
Dead	89 (35.7)
Hormone therapy (Tamoxifen)	
No	183 (73.5)
Yes	66 (26.5)

Chemotherapy No Yes [Cyclophosphamide, Methotrexate, 5-Fluorouracil)	 208 (83.5) 41 (16.5)

Supplementary Table S13. QuantiTect® Primers used in RT-PCR analysis.

Gene Symbol	Source	Catalog no.
APE1	Qiagen	QT00012474
XRCC1	Qiagen	QT00016688
SMUG1	Qiagen	QT00002317
POLB	Qiagen	QT00088655
BRCA1	Qiagen	QT00039305
GAPDH	Qiagen	QT00079247

Supplementary Table S14. DNA repair mRNA expression in MDA-MB-436 compared to MCF7 cells for qPCR.

	Fold down-regulation	**P Value**
APE1	-7.02	**0.0006**
XRCC1	-15.22	**0.01**
SMUG1	-9.54	**0.001**
POLB	-2.56	**0.05**
BRCA1	-44.07	**0.002**

All significant p values are shown in bold.

Supplementary Table S15. DNA repair mRNA expression in BRCA1 knockdown cells compared to Control cells for qPCR.

	Fold down-regulation	**P Value**
APE1	-1.22	0.065
XRCC1	-4.21	**0.002619**
SMUG1	-1.60	**0.033851**
POLB	-4.53	0.0676
BRCA1	-15.80	**0.000455**

All significant p values are shown in bold.

Supplementary Table S16. DNA repair mRNA expression profiling in BRCA1 knockdown HeLa SilenciX cells compared to control HeLa SilenciX cells.

	Fold Change	P Value
BER		
APEX1	-1.06	0.856990
APEX2	1.32	**0.001814**
PARP1	-1.15	0.724495
PARP2	-1.94	0.262235
PARP3	-1.62	0.350824
POLB	-2.08	0.213085
SMUG1	-1.18	0.374608
NTHL1	-1.36	0.440362
UNG	-1.66	0.351472
FEN1	-1.04	0.759157
OGG1	-1.11	0.558876
NEIL1	-5.57	0.263241
NEIL2	1.05	0.932681
NEIL3	-1.31	0.416592
XRCC1	-2.17	0.051321
CCNO	-1.57	0.104014
LIG3	-1.92	0.271431
MUTYH	-1.84	0.201311
MPG	-1.27	0.262867
HR		
BRCA1	-3.50	**0.036557**
BRCA2	-1.24	0.239570
RAD21	-1.34	0.061085
RAD50	-1.67	0.345218
RAD51	-2.30	0.277572
RAD51B	-1.77	0.336811
RAD51C	-1.54	0.233420

RAD51D	-4.14	0.355474
RAD54L	-1.76	0.208675
RAD52	-2.05	0.347470
XRCC2	-1.50	0.220340
XRCC3	-1.63	0.370900
ATM	-1.54	0.128451
DMC1	-6.44	0.231080
MRE11A	-1.36	0.177377
NHEJ		
DNA-PKcs	-2.54	**0.000942**
XRCC4	-1.28	0.336954
XRCC5	-1.10	0.586375
XRCC6	-1.04	0.716075
XRCC6BP1	1.20	0.622443
LIG4	-1.18	0.303680
NER		
BRIP1	-1.64	0.120475
LIG1	-1.24	0.257076
ATXN3	-1.88	0.098094
RAD23A	-3.00	0.348902
RAD23B	1.17	0.693343
RPA1	-1.15	0.557166
CCNH	-1.19	0.361003
CDK7	-1.06	0.972071
DDB1	-1.00	0.789882
DDB2	-1.66	0.144235
PNKP	-1.95	0.337396
POLL	-2.92	0.333463
RPA3	-3.16	0.350940
SLK	-1.46	0.180509
ERCC1	-2.28	**0.023598**

ERCC2	-1.73	0.066389
ERCC3	-1.12	0.529309
ERCC4	-1.48	**0.006281**
ERCC5	-1.32	0.164452
ERCC6	-1.40	0.140431
ERCC8	-1.46	0.165440
XAB2	-1.33	0.338438
XPA	-1.17	0.523245
XPC	-1.59	0.285955
MMR		
POLD3	-1.64	0.141055
PMS1	-2.25	0.254384
PMS2	-1.38	0.141756
MLH1	-1.38	0.356310
MSH2	-1.18	0.599644
MLH3	-1.61	0.132913
MSH3	-1.29	0.327005
MSH4	-3.04	**0.012337**
MSH5	-2.93	0.222323
MSH6	-1.58	0.322960
TREX1	-1.16	0.605905
Others		
ATR	-1.23	0.270260
EXO1	-1.27	0.418162
MGMT	-2.62	0.224041
RAD18	-1.32	0.433195
RFC1	-1.30	0.285465
TOP3A	-1.37	0.370190
TOP3B	-1.53	0.364182

All significant p values are shown in bold.

Supplementary Table S17. DNA repair mRNA expression profiling in MDA-MB-436 compared to MCF7 cells.

	Fold Change	P Value
BER		
APEX1	-2.68	0.108045
APEX2	-2.37	0.447471
PARP1	-2.89	**0.024987**
PARP2	-2.20	**0.026338**
LIG3	-4.43	0.086662
POLB	-2.85	**0.018010**
SMUG1	-3.08	0.348467
NTHL1	-5.74	0.063845
UNG	-7.32	0.062112
FEN1	-2.71	0.401000
OGG1	-3.71	0.093199
NEIL1	-7.79	0.059311
NEIL2	-2.18	0.080271
NEIL3	-5.81	**0.049842**
XRCC1	-4.63	0.090248
CCNO	-1.85	0.056339
PARP3	-1.35	0.119678
MUTYH	-3.32	0.088049
MPG	-4.09	0.055673
HR		
BRCA1	-9.08	**0.016911**
BRCA2	-5.30	0.092852
RAD21	-3.00	**0.011678**
RAD50	-2.41	0.080741
RAD51	-5.08	**0.033865**
RAD51C	-27.35	0.089201
RAD51D	-3.91	0.092264

RAD52	-1.74	0.241065
RAD54L	-6.55	**0.027788**
RAD51B	-288.98	0.099145
XRCC2	-6.87	**0.042262**
XRCC3	-4.02	0.142791
ATM	-3.78	0.114557
DMC1	-9.53	0.126028
MRE11A	**0.049906**	-6.20
NHEJ		
DNA-PKcs	-7.06	**0.025294**
XRCC4	-5.11	**0.038131**
XRCC5	-3.84	0.102412
XRCC6	-3.30	0.078772
XRCC6BP1	-8.08	0.095138
LIG4	-4.44	0.06401
NER		
BRIP1	-48.33	0.110474
LIG1	-7.24	0.105516
ATXN3	-5.99	0.111505
RAD23A	-2.88	0.08335
RAD23B	-2.77	0.133763
RPA1	-3.28	0.077981
CCNH	-3.13	**0.043847**
CDK7	-2.93	0.099967
DDB1	-2.25	0.131174
DDB2	-10.74	0.094882
PNKP	-4.23	0.118640
POLL	-3.02	0.178876
RPA3	-3.42	**0.04816**
SLK	-2.49	0.11911
ERCC1	-2.51	**0.037378**

ERCC2	-2.46	0.068755
ERCC3	-4.61	0.057429
ERCC4	-5.68	**0.014286**
ERCC5	-1.27	0.673253
ERCC6	-3.18	**0.007035**
ERCC8	-3.64	**0.042008**
XAB2	-2.50	0.074802
XPA	-3.69	0.124376
XPC	-2.87	0.143832
MMR		
POLD3	-4.69	**0.047055**
PMS1	-3.76	0.100986
PMS2	-3.13	0.128963
MLH1	-4.47	0.071532
MSH2	-3.05	0.069132
MLH3	-4.19	0.121674
MSH3	-3.57	**0.045203**
MSH4	-1.43	0.587442
MSH5	-6.04	0.077756
MSH6	-2.81	0.064770
TREX1	-1.34	0.139725
Others		
ATR	0.088050	-6.57
EXO1	**0.038277**	-6.99
MGMT	0.123066	-3.74
RAD18	0.099833	-4.23
RFC1	0.137648	-2.14
TOP3A	0.096444	-3.61
TOP3B	0.107455	-2.51

All significant p values are shown in bold.

Probe Set ID	Gene Symb	Gene Title	go biologica	go molecula	go cellular c
210027_s_a	APEX1	APEX nuclea	DNA repair	DNA binding	intracellular
204408_at	APEX2	APEX nuclea	DNA repair	DNA binding	intracellular
218527_at	APTX	aprataxin	single stran	DNA binding	chromatin /
208442_s_a	ATM	ataxia telan	cell cycle ch	nucleotide b	chromosom
209903_s_a	ATR	ataxia telan	cell cycle ch	nucleotide b	XY body ///
205733_at	BLM	Bloom synd	regulation c	nucleotide b	nuclear chr
204531_s_a	BRCA1	breast canc	cell cycle ch	DNA binding	ubiquitin lig
214727_at	BRCA2	breast canc	double-stra	protease bir	nucleus ///
221703_at	BRIP1	BRCA1 inter	DNA damag	nucleotide b	nucleus ///
204093_at	CCNH	cyclin H	regulation c	protein kina	nucleus ///
210021_s_a	CCNO	cyclin O	regulation c	uracil DNA N	nucleus ///
209194_at	CETN2	centrin, EF-h	G2/M trans	nucleic acid	intracellular
214426_x_a	CHAF1A	chromatin a	DNA replica	chromatin b	nucleus ///
204775_at	CHAF1B	chromatin a	DNA replica	chromatin b	nucleus ///
205394_at	CHEK1	checkpoint	cell cycle ch	nucleotide b	chromosom
210416_s_a	CHEK2	checkpoint	cell cycle ch	nucleotide b	chromosom
203229_s_a	CLK2	CDC-like kin	protein pho	nucleotide b	nucleus ///
209804_at	DCLRE1A	DNA cross-li	DNA repair	hydrolase ac	nucleus ///
219490_s_a	DCLRE1B	DNA cross-li	cell cycle ch	nuclease act	chromosom
222233_s_a	DCLRE1C	DNA cross-li	telomere m	single-stran	nucleus
208619_at	DDB1	damage-spe	cell cycle ch	nucleic acid	nucleus ///
203409_at	DDB2	damage-spe	protein poly	DNA binding	nucleus ///
208382_s_a	DMC1	DNA meioti	pachytene /	nucleotide b	chromosom
208955_at	DUT	deoxyuridin	nucleobase	dUTP dipho	nucleus ///
203719_at	ERCC1	excision rep	nucleotide-	single-stran	nucleotide-
213468_at	ERCC2	excision rep	cell cycle ch	nucleotide b	SSL2-core T
202176_at	ERCC3	excision rep	cell cycle ch	nucleotide b	core TFIIH c
210158_at	ERCC4	excision rep	meiotic mis	single-stran	nucleotide-
202414_at	ERCC5	excision rep	nucleotide-	bubble DNA	nucleus ///
207347_at	ERCC6	excision rep	response to	nucleotide b	nucleus ///
205162_at	ERCC8	excision rep	protein poly	DNA helicas	nucleotide-
204603_at	EXO1	exonuclease	humoral im	DNA binding	nucleus
203678_at	FAN1	FANCD2/FA	double-stra	magnesium	nucleus
203806_s_a	FANCA	Fanconi ane	DNA repair	protein binc	nucleus ///
205189_s_a	FANCC	Fanconi ane	myeloid cel	protein binc	chromatin /
220255_at	FANCE	Fanconi ane	DNA repair	protein binc	nucleus ///
218689_at	FANCF	Fanconi ane	DNA repair	protein binc	nucleus ///
203564_at	FANCG	Fanconi ane	cell cycle ch	damaged DI	nucleus ///
213007_at	FANCI	Fanconi ane	DNA repair	DNA binding	nucleus ///
218397_at	FANCL	Fanconi ane	DNA repair	ubiquitin-pr	nucleus ///
204768_s_a	FEN1	flap structur	S phase of r	magnesium	nucleus ///
202451_at	GTF2H1	general tran	regulation c	protein kina	core TFIIH c
221540_x_a	GTF2H2	general tran	nucleotide-	nucleic acid	core TFIIH c
222104_x_a	GTF2H3	general tran	nucleotide-	damaged DI	core TFIIH c
203577_at	GTF2H4	general tran	nucleotide-	nucleotide b	core TFIIH c
213357_at	GTF2H5	general tran	DNA repair	DNA binding	core TFIIH c
205436_s_a	H2AFX	H2A histone	DNA damag	DNA binding	chromosom
202983_at	HLTF	helicase-like	ATP catabol	nucleotide b	nucleus ///
204883_s_a	HUS1	HUS1 check	cell cycle ch	protein binc	nucleus ///
202726_at	LIG1	ligase I, DNA	S phase of r	nucleotide b	nucleus ///
204123_at	LIG3	ligase III, DN	DNA replica	nucleotide b	condensed
206235_at	LIG4	ligase IV, DN	single stran	nucleotide b	condensed
209580_s_a	MBD4	methyl-CpG	DNA repair	DNA binding	chromatin /
203061_s_a	MDC1	mediator of	double-stra	protein binc	nucleus ///
204880_at	MGMT	O-6-methylg	DNA ligatio	DNA binding	nucleus ///
219396_s_a	MIR631 ///	microRNA 6	DNA repair	nucleic acid	nucleus ///
202520_s_a	MLH1	mutL homo	pachytene /	single-stran	condensed
204838_s_a	MLH3	mutL homo	ATP catabol	chromatin b	condensed
202167_s_a	MMS19	MMS19 nuc	phosphorel	transcriptio	nucleus ///
203565_s_a	MNAT1	menage a tr	regulation c	protein kina	nucleus ///
203686_at	MPG	N-methylpu	DNA repair	DNA binding	nucleus ///
205395_s_a	MRE11A	MRE11 mei	regulation c	single-stran	chromosom
209421_at	MSH2	mutS homo	meiotic mis	nucleotide b	nuclear chr
210947_s_a	MSH3	mutS homo	meiotic mis	nucleotide b	nuclear chr
210533_at	MSH4	mutS homo	meiotic mis	nucleotide b	condensed
221406_s_a	MSH5 /// M	mutS homo	meiotic mis	nucleotide b	synaptonem
211449_at	MSH6	mutS homo	meiotic mis	nucleotide b	nuclear chr
218463_s_a	MUS81	MUS81 stru	DNA metab	DNA binding	nucleus ///
218903_s_a	NABP2	nucleic acid	cell cycle ch	nucleic acid	nucleus ///
217299_s_a	NBN	nibrin	cell cycle ch	damaged DI	chromosom
219502_at	NEIL3	nei endonuc	DNA repair	bubble DNA	intracellular
219418_at	NHEJ1 /// S	nonhomolo	DNA repair	DNA binding	nucleus ///
209731_at	NTHL1	nth endonu	DNA repair	DNA binding	nucleus ///
204766_s_a	NUDT1	nudix (nucle	GTP catabo	RNA binding	nucleus ///
205760_s_a	OGG1	8-oxoguanin	acute inflan	damaged DI	nucleus ///
219530_at	PALB2	partner and	double-stra	DNA binding	nucleus ///
214086_s_a	PARP2	poly (ADP-ri	DNA repair	DNA binding	nucleus ///
209940_at	PARP3	poly (ADP-ri	DNA repair	catalytic act	nucleus ///
202239_at	PARP4	poly (ADP-ri	DNA repair	DNA binding	nucleus ///
201202_at	PCNA	proliferating	DNA damag	purine-spec	nucleus ///
202861_at	PER1	period circa	negative reg	RNA polyme	nucleus ///
213677_s_a	PMS1	PMS1 postn	ATP catabol	DNA binding	nucleus ///
209805_at	PMS2 /// PM	PMS2 postn	ATP catabol	DNA binding	nucleus ///
218961_s_a	PNKP	polynucleot	nucleotide-	nucleotide b	nucleus ///
234907_x_a	POLB	polymerase	DNA replica	DNA binding	nucleus ///
203422_at	POLD1	polymerase	S phase of r	nucleotide b	nucleotide-
201115_at	POLD2	polymerase	S phase of r	DNA binding	nucleus ///
216026_s_a	POLE	polymerase	G1/S transit	nucleotide b	nucleus ///
203366_at	POLG	polymerase	DNA metab	protease bir	mitochondr
219380_x_a	POLH	polymerase	DNA synthe	DNA binding	nucleus ///
219317_at	POLI	polymerase	DNA replica	DNA binding	intracellular
222238_s_a	POLM	polymerase	DNA repair	DNA binding	nucleus
219510_at	POLQ	polymerase	DNA replica	nucleotide b	nucleoplasm
208694_at	PRKDC	protein kina	telomere m	nucleotide b	nucleus ///
203103_s_a	PRPF19	pre-mRNA p	protein poly	DNA binding	ubiquitin lig
204053_x_a	PTEN	phosphatase	regulation c	magnesium	nucleus ///
204460_s_a	RAD1	RAD1 homo	cell cycle ch	damaged DI	nucleus ///
207405_s_a	RAD17	RAD17 hom	cell cycle ch	nucleotide b	chromosom
200608_s_a	RAD21	RAD21 hom	M phase of	protein binc	nuclear chr
201039_s_a	RAD23A	RAD23 hom	DNA repair	damaged DI	proteasome
201222_s_a	RAD23B	RAD23 hom	nucleotide-	damaged DI	proteasome
209349_at	RAD50	RAD50 hom	regulation c	single-stran	chromosom
205023_at	RAD51	RAD51 hom	double-stra	nucleotide b	nuclear chr
206066_s_a	RAD51C	RAD51 hom	DNA metab	nucleotide b	nucleus ///
37793_r_at	RAD51D	RAD51 hom	DNA metab	nucleotide b	nucleus
205647_at	RAD52	RAD52 hom	double-stra	DNA binding	nucleus ///
219494_at	RAD54B	RAD54 hom	double-stra	nucleotide b	nucleus
204558_at	RAD54L	RAD54-like (	double-stra	nucleotide b	nucleus
204828_at	RAD9A	RAD9 homo	cell cycle ch	nuclease act	nucleus ///
203344_s_a	RBBP8	retinoblasto	cell cycle ch	single-stran	nucleus ///
205091_x_a	RECQL	RecQ protei	DNA strand	nucleotide b	nucleus ///
213520_at	RECQL4	RecQ protei	DNA strand	nucleotide b	nucleus ///
221686_s_a	RECQL5	RecQ protei	DNA metab	nucleotide b	nucleus ///
218428_s_a	REV1	REV1, polyn	DNA replica	magnesium	nucleus ///
208070_s_a	REV3L	REV3-like, p	nucleobase	nucleotide b	nucleus ///
208021_s_a	RFC1	replication f	S phase of r	nucleotide b	nucleus ///
214700_x_a	RIF1	RAP1 intera	telomere m	binding /// p	chromosom
212696_s_a	RNF4	ring finger p	transcriptio	DNA binding	nucleus ///
203160_s_a	RNF8	ring finger p	DNA repair	chromatin b	ubiquitin lig
201529_s_a	RPA1	replication p	cell cycle ch	nucleic acid	condensed
201756_at	RPA2	replication p	cell cycle ch	nucleic acid	nucleus ///
209507_at	RPA3	replication p	cell cycle ch	single-stran	nucleus ///
221143_at	RPA4	replication p	DNA damag	nucleic acid	nucleus ///
202276_at	SHFM1	split hand/fo	double-stra	protein binc	proteasome
218685_s_a	SMUG1	single-stran	DNA repair	DNA binding	nucleus ///
222259_s_a	SPO11	SPO11 meio	zygotene //	DNA binding	chromosom
203743_s_a	TDG	thymine-DN	negative reg	RNA polyme	nucleus ///
219715_s_a	TDP1	tyrosyl-DNA	single stran	double-stra	nucleus ///
202266_at	TDP2	tyrosyl-DNA	DNA repair	magnesium	nucleus ///
204946_s_a	TOP3A	topoisomera	DNA topolo	nucleotide b	nucleus ///
213660_s_a	TOP3B	topoisomera	DNA topolo	nucleotide b	condensed
202633_at	TOPBP1	topoisomera	DNA metab	DNA binding	condensed
211300_s_a	TP53	tumor prote	protein imp	RNA polyme	chromatin /
203050_at	TP53BP1	tumor prote	double-stra	RNA polyme	chromosom
34689_at	TREX1	three prime	DNA metab	nucleic acid	intracellular
211788_s_a	TREX2	three prime	DNA metab	magnesium	intracellular
201899_s_a	UBE2A	ubiquitin-co	protein poly	nucleotide b	chromatin /
202333_s_a	UBE2B	ubiquitin-co	protein poly	nucleotide b	chromatin /
201523_x_a	UBE2N	ubiquitin-co	double-stra	nucleotide b	ubiquitin lig
209096_at	UBE2V2	ubiquitin-co	protein poly	protein binc	nucleus ///
202330_s_a	UNG	uracil-DNA g	DNA repair	uracil DNA N	nucleus ///
205667_at	WRN	Werner syn	telomere m	nucleotide b	intracellular
218110_at	XAB2	XPA binding	mRNA splici	protein binc	intracellular
205672_at	XPA	xeroderma p	nucleotide-	nucleotide b	nucleus ///
203655_at	XRCC1	X-ray repair	single stran	damaged DI	nucleus ///
207598_x_a	XRCC2	X-ray repair	double-stra	DNA binding	nucleus
216299_s_a	XRCC3	X-ray repair	DNA metab	nucleotide b	nucleus ///
210812_at	XRCC4	X-ray repair	in utero em	DNA binding	condensed
208643_s_a	XRCC5	X-ray repair	telomere m	nucleotide b	nuclear telo
200792_at	XRCC6	X-ray repair	telomere m	nucleotide b	nuclear telo
